IR MICROSPECTROSCOPIC IMAGING DISCRIMINATES ISOGENIC NULL WAXY FROM PARENT WHEATS WITH LIPID CLASS PROFILE SUPPORTED BY COMPOSITIONAL ANALYSES

by

LAUREN RENEE BREWER

B.S., Clemson University, 2007

A THESIS

submitted in partial fulfillment of the requirements for the degree

MASTER OF SCIENCE

Department of Grain Science and Industry
College of Agriculture

KANSAS STATE UNIVERSITY
Manhattan, Kansas

2009

Approved by:

Major Professor
David L. Wetzel

Copyright

Abstract

Isogenic waxy wheat lines differ from their non waxy (normal) parents in functionality, end use, and chemical (i.e. amylopectin/amylose, lipid) contents. Other investigations of waxy and parent wheats involved the carbohydrate and protein fractions. The goal of this work is to apply chemical images to discriminate between the waxy and parent wheats and define the contribution of contrasting lipid profiles. Recent waxy topics include current interest in plant breeding activity to develop new lines that incorporate desirable traits with advantageous success in baking and milling, and the differences needed in milling techniques for waxy versus normal wheats that may be associated with lipids. From our empirical preliminary success in sorting parent wheat kernels from waxy wheat full null specimens by nearIR chemical imaging it was anticipated that using fundamental vibrational spectra in the mid infrared would provide the chemical basis of discrimination. FT-IR microspectroscopic *in situ* probing and imaging of kernel frozen sections was applied to genetically pure, well documented isogenic breeding lines. With the use of high spatial resolution, elucidation of fundamental vibrations of mid IR provides chemical manifestation of the genetic expression that differentiates waxy wheats from their parent wheats. Comparison between numerous contiguous pixels, typically 3,000 for each type, establishes a consensus and a mean spectrum with characteristic bands for waxy and parent. Extractions with solvents of differing polarity were employed to aid in lipid extraction *in situ* and kernel extracted endosperm. Differences between kernel sections of waxy and parent are observed using FT-IR microspectroscopic imaging. However, revealing lipid class contribution to the molecular bands required infrared analysis after selective extraction. Triple mass

spectrometry of lipid molecule ions was used for compositional analyses to enhance lipid class profile distinction. A normal and waxy advanced breeding line wheat were also analyzed via the same methods. It was noted that digalactoslydyglyercides are the most abundant lipids in all samples, however the relative lipid profiles of normal wheat versus waxy wheat differ as well as tetraploid versus hexaploid. It is observed that in the endosperm of all parent wheat versus waxy wheat specimens analyzed, all waxy wheat specimens contained higher lipid content. Methods were also applied to partial waxy isogenic cultivars to determine detection limits that correspond to the degree of waxy genetic expression.

Table of Contents

List of Figures

List of Tables

Acknowledgements

Special thanks…

… to my parents (Herbert and Angela), my sister (Alisa), and **countless** friends for their assistance, support and understanding

… the Kansas State Grain Science and Industry department for an opportunity at advancement

... the Kansas Lipidomics Research Center Analytical Laboratory and its support from National Science Foundation's EPSCoR program, under grant no. EPS-0236913

... Dr. Domenico Lafriandra for supplying the unique cultivars

... Dr. Robert Graybosch for knowledge and specimens

... Dr. Shi for asking important questions during my early development stage and being a member of my committee

... Dr. Seib for references, helpful advice, and being a member of my committee

… and my advisor – “Hurray for us!”

CHAPTER 1 - Introduction

1.1.0 Current study

Through the utilization of high tech instrumentation, lipid profile classification can be achieved. Model wheat specimens were obtained and analyzed via FT-IR microspectroscopy and tandem mass spectrometry to discriminate isogenic wheat cultivars from their parent wheats. Using a six part method, isogenic cultivar were spectroscopically determined to be different (parent vs. waxy), lipids were identified spectroscopically, lipids removed with solvent to observe reduction, total extracted central endosperm lipid content analyzed, selective extraction residues analyzed, and lipid concentrations calculated.

1.2.0 Experimental samples

Two grains of importance to this study are hard wheat and durum wheat. Hard wheat is a hexaploid, i.e. AABBDD; 2n=6n= 42, used in bread making. Durum wheat is a tetraploid, i.e. AABB; 2n=2n=14, that is used in semolina production [1]. The isogenic wheat cultivars obtained for analytical study were produced by backcrossing. Backcrossing is a type of introgression for recessive traits. Through backcrossing, the desired genotype can be recovered, with no new recombination produced [2]. Mature cultivars are necessary for each wheat backcrossing, requiring this process to last several years [3]. The isogenic cultivar obtained for this study were backcrossed five times. In addition to the hexaploid, isogenic double null durum wheat cultivars

were also used in this study. [4]. The isogenic cultivars were supplied by Dr. Domenico Lafriandra of Universita Della Tuscia (Via San Camillo de Lellis, Viterbo, Italy).

1.2.1 Background on Starch

Starch is $^{2}/_{3}$ - ¾ of dry grain weight. The major portions of wheat flour are made up of storage starches, found as water insoluble granules. Storages starches of normal wheats consist of 75% amylopectin, 25% amylose, and small amounts of lipid and protein [5, 6]. Ainsworth showed evidence in the involvement of waxy protein in the production of storage starch in the waxy grains [6, 7]. Amylose and amylopectin are the polymeric chains that constitute starch. Amylose is a mixture of lightly branched, primarily linear, polymers that are not found in waxy wheat kernels [8].

It is difficult to define (individually) a starch synthase function [9]. Recently, the waxy (Wx) protein [10], involved in amylose synthesis in plants, has been identified as granule-bound starch synthase (GBSS) [11, 12, 13, 14]. GBSS binds tightly to starch granules and is also known as NDPglucose-starch glucosyltransferase, carrying the Enzyme Commission number: EC 24.1.21. The GBSS1 structural gene comprised of 11 exons interspersed by 10 introns for wheat (also rice and barley) [15].

It was once thought that the waxy locus controls the amylose synthesis in cereal endosperm, which was reported by many [3, 15]. However, Smith [16] reported that four things determine the rate of amylose synthesis: The absence of waxy protein GBSS makes them waxy, the availability of ADP-glucose and malto-oligosaccharides (2 and 3) and the physical spacing in

the matrix. GBSS can be suppressed due to cis-interaction and the wild type influence [16,17]. GBSSI transcripts are present in waxy wheat, however the translation products (of normal or differing molecular weight) are undetectable (to DNA coding) during endosperm development in the kernel [18].

Waxy kernels contain only amylopectin. Chemically, amylopectin is α (1,4) linked and α (1, 6) branched glucose units [19]. This molecule organizes into large, insoluble semicrystalline structures that make up the crystalline component in starch [9]. Amylopectin is thought to be arranged as structural lines in blockets [20]. The blockets are believed to be associated relative to each other in a various ways.

Amylopectin that is universally present in starch, is of high molecular weight, and has extreme hot water swelling capacity [18]. In considering the structure of amylopectin, all grain starches contain more 'A' type crystals than 'B' type crystals [21]. 'A' type crystals are mostly stable polymorphs and are the product of a thermodynamic process. This type is favored by short chain length, high concentration and high temperatures; descriptions that support the strength of the structure. While the B-type crystals are less stable and their production kinetically controlled [20, 22]. Normal nonwaxy kernels contain only ~5% branching, and the biosynthesis pathway and the functionality of amylopectin mostly remains to be discovered [9, 21].

When considering the three ways lipids can be associated with starch granules: non starch lipid, starch surface lipid and starch lipid, non starch lipid found in the endosperm is of greatest concern to this study. Normal wheat and waxy wheat starches also differ in the amount of lipid found in the granule. Normal wheat starches have more lipid contained in the starch granule, approximately 1% of the total kernel lipid, with 90% of that bound in the starch being

phospholipids [23]. The waxy wheat starches contain no traces of lipid inside the granule. However higher amounts of lipid are found in the endosperm of waxy wheats in comparison to that of normal endosperm [18, 24].

1.3.0 Genetic consideration

With waxy hard wheats (hexaploids) there are three null alleles – ABD; while waxy durum wheats are tetraploids, with only two null alleles, A and B, to create a full waxy specimen. The nulls in both cases are essentially amylose free [4, 25]. Amylose synthesis occurs in the pericarps, aleurone layers and embryos of waxy wheat, but not in the endosperm. Via various analytical methods, the endosperm of waxy wheat contains no detectable 56-kDa protein, which is associated with the presence of amylose [26]. Waxy null genes can be produced or bred for research using hybridization, mutagensis, and somaclomnal mutation.

Nakamura and colleagues [12] were the first to create a full waxy wheat and to separate the Wx-A1, Wx-B1 and Wx-D1 isozymes, found in hexaploidal wheat, using two dimensional gel electrophoresis. This was the first demonstration of genetic modification of wheat starch [11, 27]. The locations of the waxy alleles in the chromosomal arm were discovered as follows: Wx A1 7AS (1815 bp)– Chao 1989 [28]; Wx B1 4AL (1818 bp) – Ainsworth 1993 [6]; and Wx D1 7DS (1815 bp) – Yamamori 1994 [9], [29]. Wx-B1 was originally located at 7BS and recent discoveries reveal movement of wx-B1 from 7B to 4A [29]. Null alleles are called mutants, which occur as expected in nature, and can be characterized by the complete loss of amylose in the starch fraction [30, 31].

The three waxy loci, present in hexaploids, segregate according to Mendelian fashion [32, 33]. Chromosome segments containing the waxy loci do not carry genes giving distorted segregation. The expression is active throughout grain filling but not into the transcription of the leaves [29]. Waxy genes are not the sole control of amylose content, short arm of chromosome 4A by Araki et al 1999 detected minor effects [33].

In tetraploids, at 15k, no gel electrophoresis band indicates Durum contains the D genome [34, 35]. Friabilin is the 15k protein. This is a protein strong in soft. It is named as such because soft is more friable than hard [35, 36]. Friabilin exists in 2 major forms and is abundantly observed in waxy analysis [36].

It is possible for kernels to have 'partial waxy' mutants, lacking one or two of the three proteins available. Nakamura was the first to use the term "partial waxy". Partial waxy shows reduced amylose content in the starch [13]. In waxy, no differences are observed in the amylopectin branching frequencies or the degree of polymerization of the amylopectin chains in comparison to the parent wheats [37]. Nakamura noted that in breeding the Wx-A1 and Wx-B1 null mutations are found in abundance, while the wx-D1 null mutation is much more rare [12, 34]. Miura restates that B has the greatest effect followed by D, then A [14]. The B1 allele has a sustained deletion that appears to control the removal of the entire GBSS transcription unit [38]. Using an iodine stain (waxy showing a visual red-brown), Chakraborty [39] measured waxy durum amylose content for partial waxy durum wheats. This test also revealed that the amylose reducing effects are greatest with the presence of a null B1 allele [39]. The visual test proves coincide with double null mutants, followed by D1 and then A1 in order of most predominate

influence. The differences are not linear, suggesting action is actually in an epistatic manner [14]. With all waxy genes null, the full properties of waxy wheat type are seen.

1.3.1 Waxy kernel development vs. environment

Waxy abundance increases exponentially with the addition of nitrogen [40]. The relative abundance of transcripts will double by the increasing nitrogen supply. Also reported is the impact of environment had a slightly greater impact than genotype [4]. The regional occurrences of null waxy genes (natural mutations) also vary between different countries [4, 6, 9]. In the current study, to remove variability, the waxy samples are isogenic to their normal wheat parent, except for the nulled waxy genes. Genetically pure wheats are known not to be commercially strong [41], however this research will provide more information on the lipid chemical composition, expelling environmental affects.

1.4.0 Classical lipid studies

Lipids have been analyzed using chemical and separation techniques, such as spectroscopy and chromatography, for over a hundred years. The most basic lipid composition analytical experiment is performed using thin layer chromatography (TLC) plates [40, 42]. In traditional lipid classification methods, lipids would be extracted from their natural heterogeneous state and preparatorily analyzed via gas chromatography (GC) or liquid chromatography (LC) before mass spectrometric injection [43, 44]. Decades ago this procedure would last hours [45]. During the 90's the classical method was enhanced using supercritical fluid extraction (SFE) to reduce the process to 30 minutes, with 8 minutes for the SFE and 22 for

the mass spectrometry [46]. Relative to breadmaking fractionation, recombination and testing verified PE polar lipids as an important factor [45].

1.5.0 Current waxy research

Currently applied research on waxy wheats, is performed with x-ray diffraction, differential scanning calorimetry, and viscosity measurement [1, 4]. These empirical tests measure the influences of the ratio of amylose to amylopectin, on the functional properties. This is a molecular lipid study [47], undertaken to chemically characterize lipids present in waxy wheats that discriminate them from their normal isogenic counterparts. Knowledge of the lipid compositional and population differences between waxy wheat nulls and their corresponding parents acts as a unique model from which genetic expression can be studied.

1.6.0 New analytical technology utilized in this study

Recently, FT-IR spectroscopic imaging has emerged as an effective tool to reveal genetic expression [24, 48]. The use of biochemical and molecular techniques can determine null alleles [1, 4, 49]. Infrared microspectroscopy is utilized with the arrangement of an infrared microscope optically interfaced to an IR spectrometer. New spectroscopic technology was necessary for use of the mapping (large spectral areas collected) and imaging functions [50]. Additional capabilities of the instrument will be discussed in a later portion of the paper.

In this study, mass spectrometry is employed to assist in describing the nature of the lipids that accompany the distinction between the waxy and normal wheat parent cultivars. Studies have shown soft ionization techniques (field desorption or fast atom bombardment) will elucidate, in detail, the lipid concentrations of a biological sample [51, 52, 53]. Tandem mass

spectrometric analytical chemistry was incorporated using various methods to produce molecule ions to chemically identify the peaks, in an attempt to support the lipid differences seen in the FT-IR analyses. The methodology used in this study differs from previous lipid studies [42, 45, 46] in that prior to mass spectrometric analysis, multiple fractionations for subdivision of samples was not needed. Utilizing standards and post analysis data computation, qualitative and quantitative lipid compositional profiles were produced.

CHAPTER 2 - Experimentation

2.1.0 Wheat Specimens

Twelve samples were obtained from Dr. Domenico Lafriandra of Universita Della Tuscia (Via San Camillo de Lellis, Viterbo, Italy). The types included N11, which is a hexaploid, hard wheat, and Svevo, a tetraploid, durum wheat. The isogenic parents are references of normal wheat compared to the isogenic null kernels received. Through mutation and backcrossing [54, 55], the parent wheat produce lineage as in the diagrams found below:

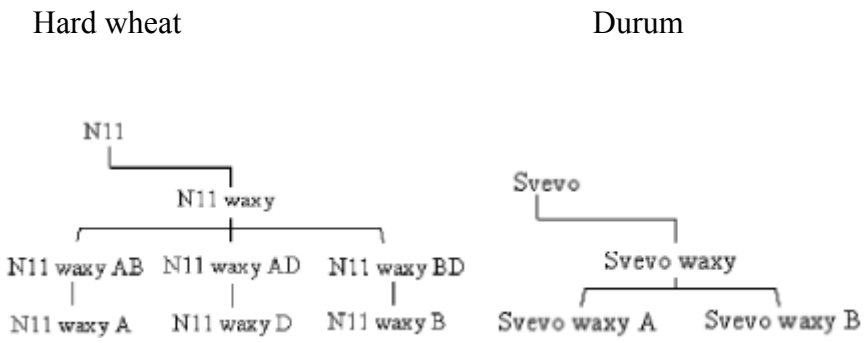

Figure 1: Flow diagram breeding representation, with no new recombination shown, of isogenic introgressive breeding.

Two advanced breeding line wheats were obtained from Dr. Robert Graybosch, USDA-ARS Plant Breeding and Genetics, University of Nebraska Lincoln. The waxy advanced breeding line sample was produced by traditional breeding methods in a field, meaning the kernels have multiple parents. Under the judgment of the wheat breeder, a relative (not isogenic)

parent is used for comparison to the advanced breeding line waxy wheat received from Dr. Graybosch for analysis.

For the total experiment, over 10,000 spectra were obtained as 14 samples were run with numerous replicates through a series of experiments. This study contained many steps for preparation and analysis, which are illustrated in the follow flow diagram:

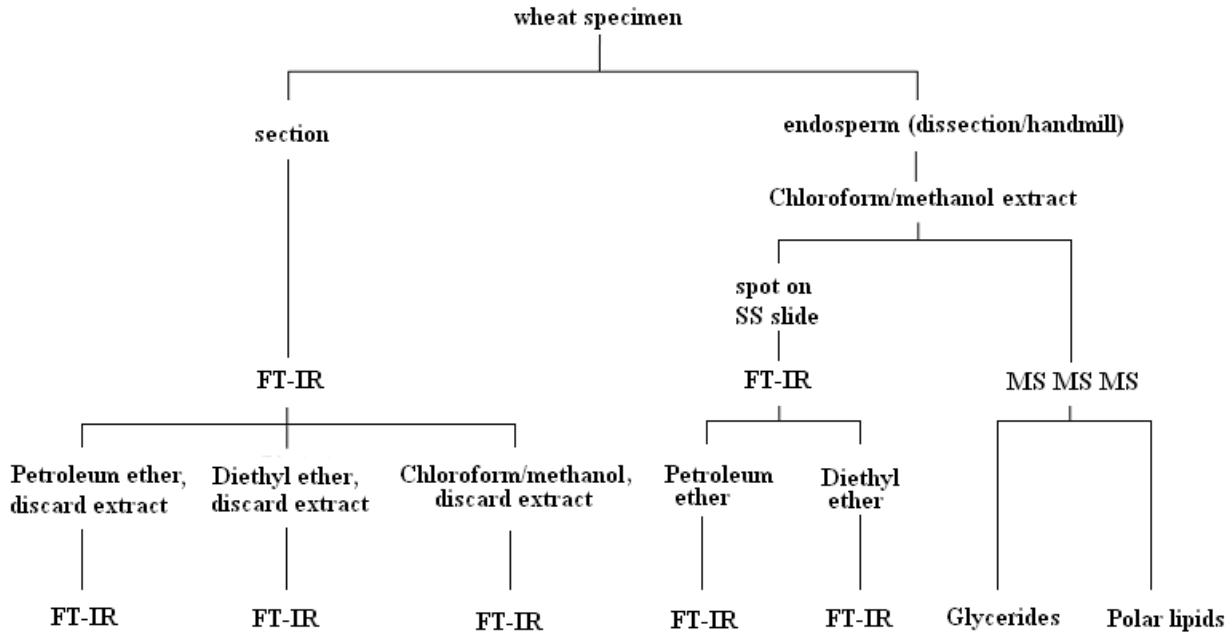

Figure 2: Experimental flow diagram displaying the six processes performed.

2.2.0 Instrumentation

2.2.1 Preliminary FT-IR microspectroscopic imaging

FT-IR microspectroscopic imaging techniques and data processing were practiced approximately two years in preceding projects. The first genetic express related project was an investigation of wheat glumes to objectively classify as "soft" or "tough" based on microspectroscopic data. Wheat selected for cultivation has a glume that is "soft" instead of "tough", because it enables mechanical threshing with efficient separation of kernel from the spikelet without damaging the kernel. Using FT-IR microspectroscopy, a chemical, objective assessment of genetic expression was developed by measuring the extent of specific lignin expression because lignification is chemical characterization accompanied with toughness [48]. (Extended summary found in **Appendix A**). Secondly, production of an objective chemically defined morphological class discrimination between hard and soft classes of wheat also provided experience in technique and sample preparation. Grain classification is subjective. In order to produce a third party method to clear disputes in grading, transverse sections of 5 μm thick wheat sections were imaged using FT-IR MCT array instrument to chemically define botanical parts within the kernel. Mapping these areas and calculating average width of the subaleurone layer combined with differing endosperm protein levels, aided in developing a method of multivariate processing and counting classified pixels to segregate hard from soft [56]. (Extended summary found in **Appendix B**).

2.2.2 Introduction to FT-IR

Vibrational spectroscopy is a technique that reveals molecular structure by using fundamental stretching and bending vibrations, or rotational motion [57]. Mid infrared and Raman spectroscopy are the basic fundamental vibrational techniques [58]. Fundamental vibrations express the vibrational motion of atoms bonded together in a molecule. The atoms within a molecule vibrate in a pattern that results in a change in dipole moment in order to absorb in the IR spectrum and produce a fundamental vibration [57, 59, 60]**.** Of the broader infrared spectrum, the mid-infrared region, from frequency 4000-500 cm^{-1} or wavelength 2.5-20 μm is explored in this study.

2.2.3 Interferometry as a way of obtaining infrared

Fourier transform infrared spectroscopy is presently the most common tool for mid-IR chemical analysis. Interferometric instruments offer several advantages over previous dispersive instruments and the superior throughput of interferometry has made infrared microspectroscopy possible and practical [61, 62]. The first is the Jaquinot advantage, that results in enhanced throughput. This is an advantage of physics, achieved because there are no slits (obstacles for the light path) and few optical components, enabling the full signal to reach the detector. Those changes facilitate high spectral resolving power and excellent wavelength reproducibility is enabled by following the modulator oscillation with a laser [60]. An additional advantage is that all radiated energy reaches the detector at one time, known as the Fellgett advantage. For an FT-

IR instrument a dispersive optical member is not needed, providing a multiplex advantage described by Fellgett [63].

The signal to noise ratio (S/N) is extremely important to FT-IR instruments. Such analytical instruments are subject to Johnson noise and their S/N is limited by the noise of the detector. The use of the liquid nitrogen cooled Mercury Cadmium Telluride (MCT) detector reduces thermal noise and increases sensitivity of the FT-IR imaging instrument [60]. The D* values plotted below illustrate the benefit of detector cooling.

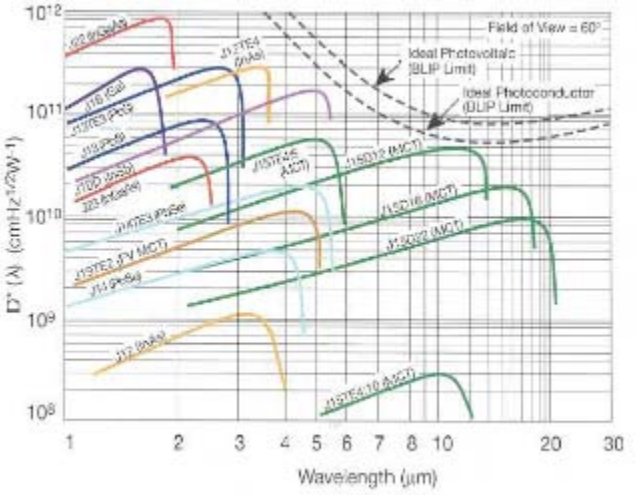

Figure 3: Graph depicting various detector sensitivity, at different wavelengths in comparison to other detectors. The liquid nitrogen cooled MCT is noted, in green, at the ideal photoconductor limit.

Fourier transform infrared spectroscopy (FT-IR) is made possible with the use of an interferometer equipped with a globar (thermal) source, mirror optics, and digital control for acquisition and computerized mathematic Fourier transformation computation [64]. In an interferometer, radiant energy hits the beam splitter and is divided into two perpendicular beams.

Beam A reflects off of a fixed mirror and beam B reflects off of a moving mirror. The speed and distance of the mirror oscillation is used in the Fourier transformation. The FT calculation is seen in $f= (2/\lambda)*v$. Where the v is the velocity of the movable mirror, λ is the wavelength and f is the frequency on the infrared spectrum [43, 59, 60]. Noted in figure 4, illustrated are the front surface optics with beams paths.

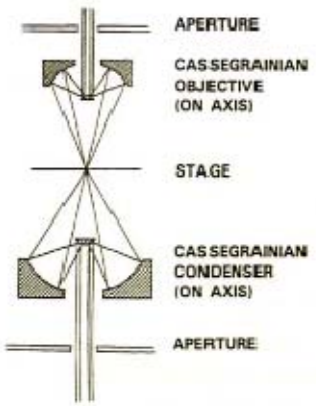

Figure 4: Sketch depicting a Cassegrainian objective and condenser, used for confocal operation with the MCT detector [63].

To generate an interferogram, a Michelson interferometer is used [59]. The speed of the mirror must remain constant and the optical frequency is a cosine function of the difference in path length between the moving and stationary mirror. At any position the measured difference is used to convert the interferogram to a spectrum [64].

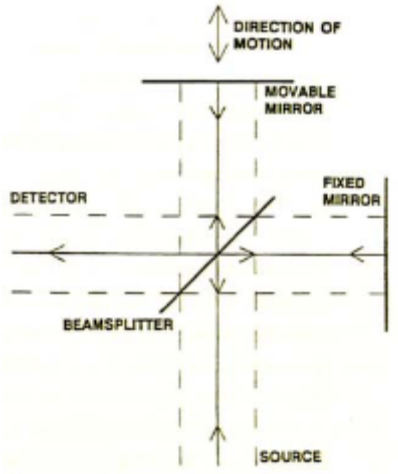

Figure 5: Diagram depicting an interferometer and the path from the beamsplitter to the two mirrors before recombination [63].

In order to produce constructive interference, the two reflected rays transfer back through the beam splitter in phase to join again into one beam [60, 63]. Detection is the next step of the process. When radiation hits the samples, molecules that exhibit changes in dipole moments, resulting from the vibration or rotation of atoms bonded together, create an electric current in the detector resulting in an interferogram, and by fourier transformation a spectrum is revealed [60, 61].

Wavelength reproduction is assured by tracking the oscillation with a parallel laser that helps avoid including inferior scans. A microscope must be optically interfaced to the spectrometer to achieve infrared microspectroscopic imaging. The infrared radiation and the visible light in the microscope, traverse the same path and with dichroic mirrors, this may be done simultaneously [63, 64].

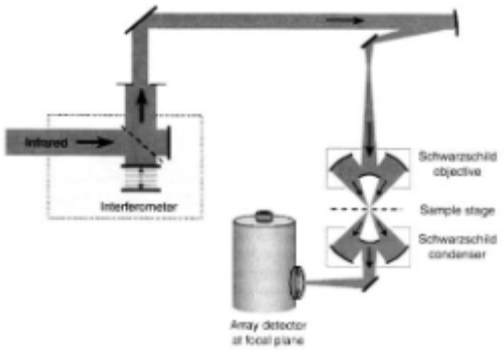

Figure 6: Diagram depicting the light path in a microspectrometer when focal plane array detection is used as in the PerkinElmer imaging system [62].

2.2.4 Mass spectrometric basis principles

Mass spectroscopy has been used for routine analysis since 1940s [65]. However the instrumentation and methods have changed, reducing the time it takes to produce and process data, improving detector sensitivity, development of ionization alternatives and improvements in resolution of mass to charge. For this study, tandem mass spectrometry was employed. By definition the method utilizes sequential multiple mass spectrometric (MS) separations [63]. The basic principle of mass spectrometry is to accelerate ions, produced in the ionization chamber and subsequently alter their path of movement in space [66]. The heavier ions will not move as far in a given time as lighter ions that are subjected to the same force in a time-of-flight system. The flight path of heavier ions accelerated to the same extent is altered less by a magnetic field. The ion population plotted for each mass/charge value constitutes the mass spectrum [66].

Molecular composition is illustrated in a mass spectrum. For this study, an Applied Biosystems API 4000 (Foster City, CA) was operated [67]. The basic set up to perform mass spectrometry can be seen as by the block diagram:

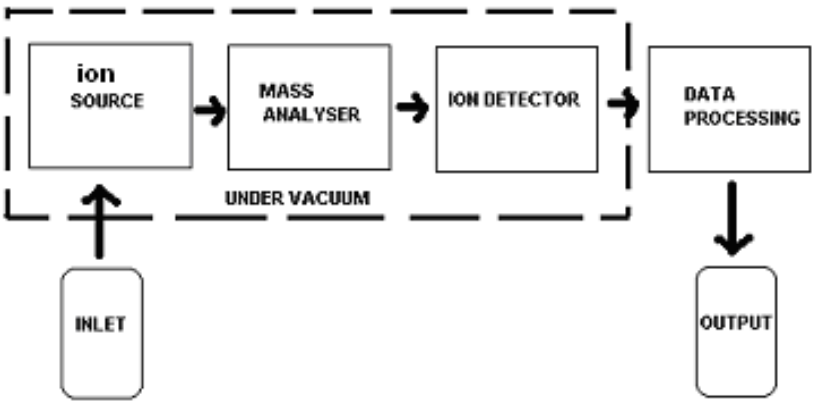

Figure 7: Sketch of mass spectrometry segments and system flow, inspired by Kiser et al. [66].

The process begins at the inlet, where the sample is presented to the ionization source after which charged molecule ions are sorted out [62]. There must be a direct inlet probe system under vaccum to avoid any open air contact with the sample [66].

In the ionization chamber the applied electron force knocks off electrons to produce charged particles. After dissociation occurs, negative ions are trapped in the electron trap (or ion trap), and the positive ions continue forward in a resonating pattern, accelerated into the analyzer alternating polarity of acceleration charges from behind and attractive forces ahead in the molecule ion path. Higher negative charges are used to attract the ion forward and positive charges from behind repelling the molecule ions along a straight trajectory. The mechanism of ionization controls what mass to charge species are produced [53]. The Applied Biosystems API

4000 operates with a patented LINAC® collision cell, under vacuum in order to preserve the sample's molecular integrity [67].

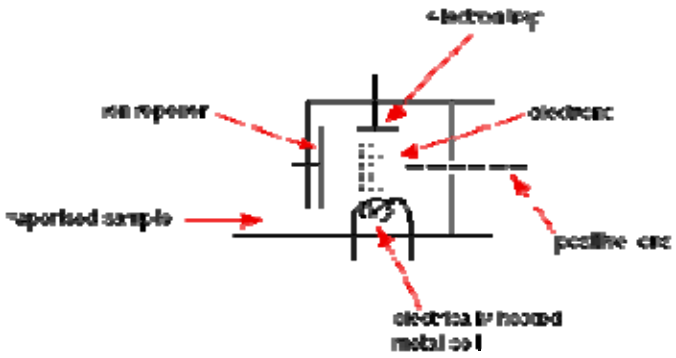

Figure 8: Diagram of the ionization chamber [reprinted from 68]

.

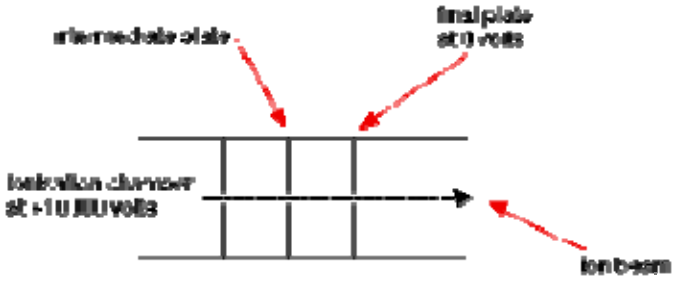

Figure 9: Model of the ion accelerator [reprinted from 68]. The ion accelerator quickly changes attractive force to pull the ions through the system with successive higher negative voltages and across the poles, towards the exit as the ions are accelerated to a constant speed (resonating) out of the ion trap [66].

Differentiation in the magnetic field deflection of the ion's straight line path is also influenced by the charge on the ions [66]. In the analyzer, the ions are deflected according to their mass to charge ratio. With those of lower mass to charge deflected to the greatest extent.

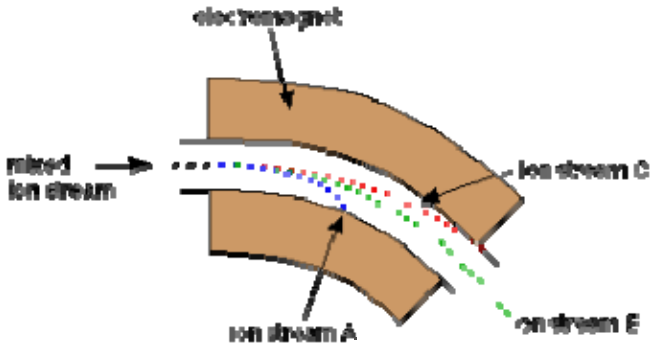

Figure 10: Diagram depicting the path of the ions, with stream A having a higher mass to charge than B, and stream B greater than C, in this example of magnetic field detection [reprinted from 68].

The Applied Biosystems API 4000 is a tandem in space instrument with triple quadrapole units. The quadrapole units are lined up for forward geometry that provides better separation, more sensitivity and enables the preselected molecule or fragmented ions to be detected [65]. Forward geometry promotes the molecule ions to resonate, whereas resonation promotes organization prior to ejection from the system. The first quadrapole is a mass filter to provide the first stage of mass separation in the instrument [67]. The 2nd and 3rd quadrapole units further separate the newly sorted ions, by separation into ions of different masses. In the 3rd quadrapole as ions leave the region, they are metered out by mass to charge to be measured and produce a spectrum. Changes in voltage between the exit lens and the auxiliary voltage increase are used to adjust resolution and sensitivity. Altering the voltage from the auxiliary voltage determines what mass to charge ion molecule will exit the system at a given time [67, 68].

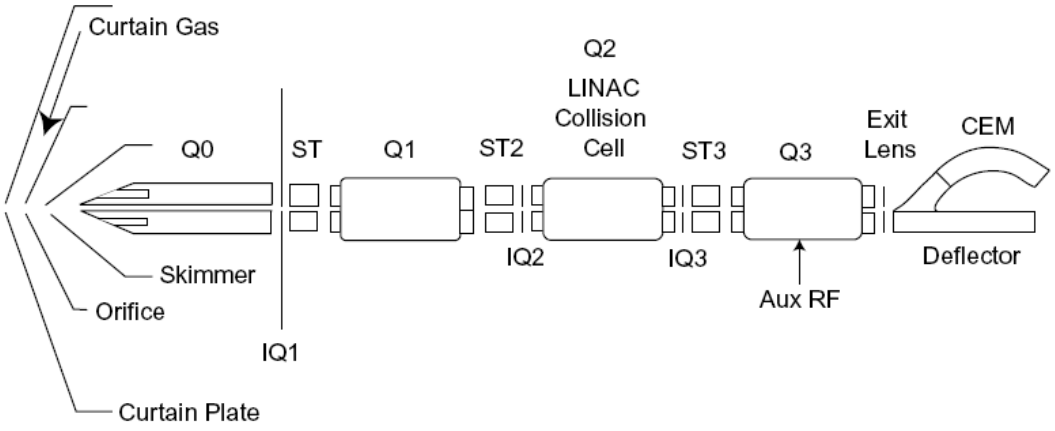

Figure 11: Applied Biosystems API 4000 [reprinted from 67]

The detector measures the number of ions with a particular mass/charge ratio [66]. The ions are separated in space to specific areas in the detector according to the deflection experienced (diagram below). Alternatively, by cycling the magnetic influence with difference in time, mass to charge ions will exit to impinge on the detector through an opening in between two plates.

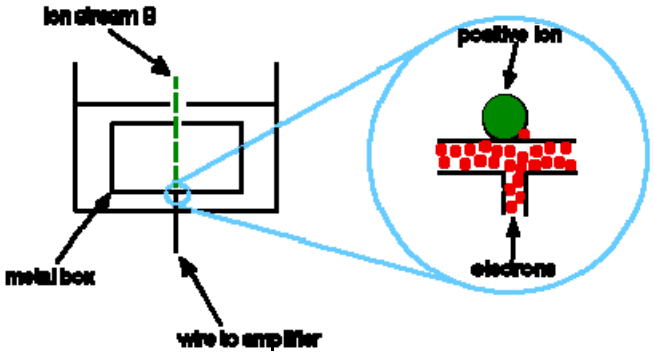

Figure 12: Diagram of passage way of ions between two plates for detection [reprinted from 66].

2.2.5 Specific equipment operated for isogenic waxy wheat lipid study

A Perkin-Elmer® (Shelton, CT) Spectrum™ Spotlight™ IR microscope optically interfaced to a SpectrumOne™ spectrometer was used to obtain the spectra. The nominal pixel size for all mapping procedures is 6.25 x 6.25 μm. The aperture size selected for individual spectrum collection was 25 x 25 μm. The instrument was equipped with a liquid nitrogen cooled mercury cadmium telluride (MCT) detector, and was operated from 4000-800 cm^{-1}.

After finding bands in the infrared spectrum that appear to differentiate the isogenic waxy wheat from the parent normal wheat, identification of the contributing lipid groups was needed. This was not possible from *in situ* FT-IR microspectroscopy of the section alone, each absorption band had a large number of contributing substances. Selective extraction studies that involved infrared were subsequently employed to identify lipid classes.

Previous studies have shown that soft ionization techniques (field desorption or fast atom bombardment) will allow mass spectrometric analysis to describe the individual lipid class representation of a biological sample [52, 53, 65]. An Applied Biosystems API 4000 tandem mass spectrometry analytical instrument was incorporated into the procedure in an attempt to support the lipid differences seen in the FT-IR analyses. The MS methods were run as neutral loss, where the instrument was programmed to scan for molecule ions of specific mass to charge ratios that were accelerated after ionization. The voltage of the instrument was set at 5500 V, injection speed was 100μl/s, and the temperature was 100°C.

2.3.0 Procedure

2.3.1 Microtome sample preparation

Approximately 5-10 kernels, of each specimen, were soaked in deionized water (18 hours at refrigeration temperature) to toughen the bran and soften the endosperm before microtoming. All kernels were refrigerated until use in order to avoid germination prior to sectioning. The germ end of each kernel was cut off, prior to mounting, to avoid sampling the germ portion of the kernel and to effectively mount specimens onto an aluminum sample holder with OCT (Optimal Cutting Temperature) tissue freezing medium, (Electron Microscopy Sciences, Fort Washingtion, PA). Cryogenically prepared frozen sections 4-6 μm thick were thaw mounted onto 13 x 1 mm BaF_2 windows for analysis in transmission, that allow for thicker sample preparation than in reflection absorption with an IR reflecting glass. Rectangular false color imaging and numerical maps (example available in **Appendix C**) obtained in transmission mode resulted in 500-1500 pixels per section of the central endosperm of a kernel, using a PerkinElmer Spotlight 300 FT-IR microspectroscopic imaging instrument described in another section (PerkinElmer, Waltham, MA). The data was processed with the Spotlight acquisition software furnished with the microspectrometer and Omnic, distributed by Thermo Fisher Scientific Inc., Waltham, MA. SpecAlign from the Cartwright Group of Oxford University, Oxford, Oxfordshire, Great Britain was also used. Within the three programs, calculations were performed and spectra were baseline corrected, normalized and subtracted, however no smoothing was employed or necessary.

2.3.2 Selective extraction from microtomed sections

After the afore mentioned microtomed samples were analyzed using FT-IR microscopic imaging, lipids were selectively extracted from the same sections with solvents of varying polarity. The solvents included petroleum ether, diethyl ether, and a (2:1) chloroform methanol mixture. Each section, previously thaw mounted on a BaF_2 window, was placed in a Pyrex Petri dish (Corning Incorporated, Corning, NY), submerged in 27-30 mL of solvent, covered with a watchglass, and allowed to stand overnight in the dark under a hood. On the following day any evaporated solvent was replenished. The assembly containing the wheat section and solvent was placed on an orbital shaker (Fisher Scientific model 361). The shaker was operated for 60 minutes, at 150 rotations per minute in an orbital diameter of 1.5 inches. Each section mounted on a BaF_2 window was removed from submersion and rinsed with fresh solvent that was allowed to evaporate.

The sections of each specimen were reanalyzed via FT-IR microspectroscopic imaging to reveal lipid removed and the data was processed as previously described. Because lipids are contained within more than the surface layer of a 4-6 μm slice, submersion in excess solvent and orbital oscillation was necessary in the process. From oscillation, a few samples, less than 10%, were lost. The selectively extracted specimens were rinsed with fresh solvent to avoid residual extracted lipids remaining on the surface. Presumably, approximately 50% of the extractable lipids were removed from the substrate tissue with this procedure.

2.3.3 Isolation of endosperm and total lipid extraction

Total endosperm lipid extraction was needed for the two remaining experiments. With 40 kernels for each extraction set (some set produced in duplicate, triplicate, and sets replicated to five), over 900 kernels were debranned by hand under a low power microscope and germ portion of the kernel removed with a razor blade. This was required because there are no methods to effectively mill under 100 g of wheat into flour. The debranning weights were monitored and recorded carefully to ensure that all of the bran and subaleurone layer had been removed. Calculated from multiple 40 kernel sets by weighing at various points in the process, it was recorded that 618.8 - 677.9 mg of endosperm remained to be ground after debranning the kernel and removing the germ end during this portion of the experiment.

In order to make the particle size comparable to flour, the debranned kernels were ground on a Burr mill (Falling Number AB Type 3303 grinder, S-12611, Stockholm, Sweden). The ground endosperm particle size was further reduced with a mortar and pestle, to pass through a 100 mesh sieve. A 0.2 ± 0.003 g portion of each endosperm fraction was weighed into a separate screw cap 11 mL test tube.

The samples were extracted according to the chloroform methanol lipid extraction procedure developed by the Kansas State University Lipidomic research center (KLRC) [52] as recommended by the KLRC to remove at least 95% of lipids present, not contained in the starch granules. The procedure, as written, is found in **Appendix D**.

For each 0.2 g of sample used, 0.7 mL of HPLC grade H_2O was added to a 17 mL screw cap test tube in order to bring the sample into a aqueous phase, and mixed with 1 mL chloroform and 2 mL methanol in a vortex mixer. One mL chloroform and 1 mL of HPLC grade water H_2O

was added to the screw cap test tube, mixed via shaking and centrifuged for 8 minutes. The lower layer containing lipid and $CHCl_3$ was removed via a disposable pipet and saved in a clean screw cap test tube to collect all combined removed lower layers for each sample type.

In the endosperm extraction tube, 1 mL of chloroform was added to each screw cap test tube before centrifuging for another 8 minutes. This process was repeated two more times. After 0.5 mL of 1M KCl to the test tube containing the combined removed lower layers, they were vigorously shaken, and the mixture was centrifuged for 4 minutes. After discarding the top aqueous layer which was removed with a disposable pipet, 0.5 mL HPLC grade H_2O was added to the combined layers the test tube was vigorously shaken, and the mixture was centrifuged for 4 minutes. Once again, the top layer was removed and discarded. This procedure was repeated for each 0.2 g endosperm fraction. The chloroform extracts were evaporated from the test tubes under nitrogen gas for a minimum of 60 minutes. One mL fresh chloroform was added to the dried samples before storage in a -80C freezer until preparation for injection.

2.3.4 Spectra from selective extraction from total lipid specimen

Stainless steel plates cut to dimensions of a microscope (1 in x 3 in) slide, were spotted with approximately 2 μL of each chloroform methanol extract, after coming to room temperature from storage in a -80C freezer. Each spot was deposited on a separate plate with a sterile BD Ultra Fine 328431 0.3 mL diabetic syringe (BD, Franklin Lakes, NJ) that had a 120 gauge needle to produce a small spot. The solvent of the deposited spots evaporated before storing the spotted stainless steel plates in closed containers protected from light and air (O_2), until analysis. The total extract residue whole spots were imaged via the focal plane array optics of the FT-IR

microspectrometer to provide multiple spectra from the center of each. The focal plane array microspectroscopic analyses were performed in the reflection absorption mode.

Following the spectroscopic analysis for each of the total extracts, fractionation was carried out using selective extraction solvents. Under a hood, a slow stream of petroleum ether was delivered from a sterile 0.3 mL diabetic syringe on one total lipid extract spot. On a replicate of the total lipid spot, diethyl ether was delivered in a slow stream via the same method. Each selective solvent extract ran down the slightly tilted plate while evaporation took place under the hood. When evaporation was complete, the plates were stored in closed containers, out of the light and air, for not more than 4 hours prior to analysis via microspectroscopy in a reflection absorption mode. These spectra were compared for lipid classification.

2.3.5 Preparation of total lipid extracts for mass spectrometry

Using the chloroform methanol total endosperm extraction described earlier, 134 vials were prepared for autosampling. Three sets of vials were prepared, each receiving a different reference standard, one for phospholipids, glycolipids or glycerols [47, 52, 53, 69, 70] at a measured amount. For mass spectrometry the polar lipids and glycolipids were analyzed together in the sample vials because their masses do not obstruct one another as a standard. The standard for triacylglycerides is also used for diacylglycerol and triacylglycerol molecule ion references because the triacylglycerides are essentially diacylglycerides with another covalently bonded fatty acid, or head group [69], the molecule ion lost after ionization as described in lipidomic terms. The contents of the specimen vials are listed in the following table:

Sample #	dry weight	Total volume	Sample added (nl)	Polar lipid* (µl)	Glycolipid (µl)	Triglyceride (µl)	Chloroform/ methyl acetate (µl)
1	0.200 g	1.00	0.05	6	3	1	310
2	0.400 g	1.00	0.025	6	3	1	335
3	0.400 g	1.00	0.025	None	None	None	335

Table 1: Recipe for contents of the mass spectrometry specimen vials.

Each vial contained the indicated respective sample, dissolved in a mixture of chloroform and methyl acetate. In addition to that, each of the three vials was spiked with a reference standard of the indicated amount, except for vials run as MS positive/MS negative, which contain no standard; as seen on line 3. Replicates ranged from 2-5 each different sample.

* The polar lipid standard contained molecule ion references for phospholipids, monogalactosyldiglycerides and digalactosyldiglycerides

2.3.6 Mass spectrometry operational parameters

Following each mass spectrometry sample, blanks were included in the injection sequence that contained only chloroform and methyl acetate. Twenty-nine of 134 vials were blanks incorporated to cleanse the MS system before introducing a new sample. The samples were run in two 25 hour periods on an Applied Biosystems 4000, tandem mass spectrometry analytical instrument a method to collect all molecule ions formed.

Molecule ions were produced and the mass spectrometry methods were run to discover the neutral loss lipids. A neutral loss molecule ion is a fraction of the total lipid molecule that is broken off via soft ionization, i.e. a diacylglycerol 273 neutral ion scan was run for a neutral loss

of 273 mass to charge, from diglycerides lipids that weight approximately 830-930 m/e before ionization. For this text, the number of the method is the mass to charge ratio of a fatty acid lost from a lipid molecule.

CHAPTER 3 - Results and Discussion

Two sets of isogenic wheat cultivar genetic families were obtained and lipids analyzed via multiple analytical chemical methods as noted in Figure 1. As reported in this section, the results are assembled by specimen, rather than by process. Part1: N11, a hexaploid, hard wheat, with lipid discrimination of isogenic partial waxy wheats, in order to determine detection limits that corresponds to the degree of waxy genetic expression. Part 2: Svevo, a tetraploid, durum wheat, along with its isogenic partial waxy cultivar. Part 3: In addition, the advanced breeding line wheat cultivar (waxy and nonwaxy) samples Arapahoe, the close parent wheat, and Nx05m4499_1, a near isogenic waxy wheat were run.

3.1.0 N11 – hexaploid model, hard wheat

3.1.1 Initial in situ microspectroscopic probing of central endosperm

Seventy-one wheat kernel specimens were sectioned and spectra collected from the central endosperm of each for comparison. For each cultivar examined, c.a. 3500 spectra were

recorded for the N11 triple null and repeated for the parent wheat. A consensus from the comparison revealed that the parent spectroscopically differs from the waxy null for the isogenic hexaploid family. The following spectra resulted:

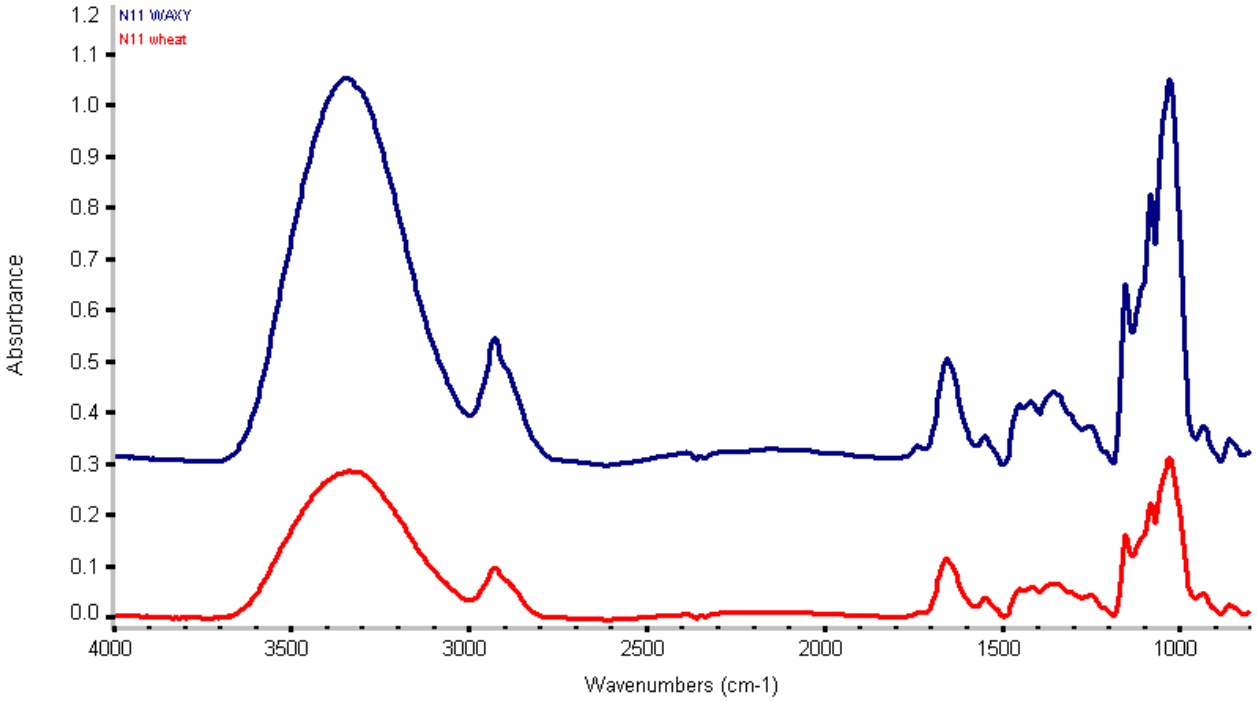

Figure 13: Differing central endosperm spectra collected from N11 waxy (top) and N11 parent (bottom).

Using the imaging system previously described, large central endosperm areas were mapped from which an average spectrum would represent the type, waxy wheat vs. parent wheat central endosperm. The spectra were normalized to the 1550 cm^{-1}, amide II [71] band and averaged, prior subtraction. Spectral subtraction was employed in which the parent spectrum was subtracted from that of the waxy null to determine what bands would represent differences between the two. Bands of interest included 1740 cm^{-1}, a classical carbonyl band of lipid, 1469 cm^{-1} that illustrates a CH bend, and 1250 cm^{-1} noted as a P=O phospholipid band [63]. Not

shown in the current subtraction are 1158 cm^{-1}, 1085 cm^{-1}, and 1024 cm^{-1} all of which remain after the subtraction and represent carbohydrate presumably due to glycolipids.

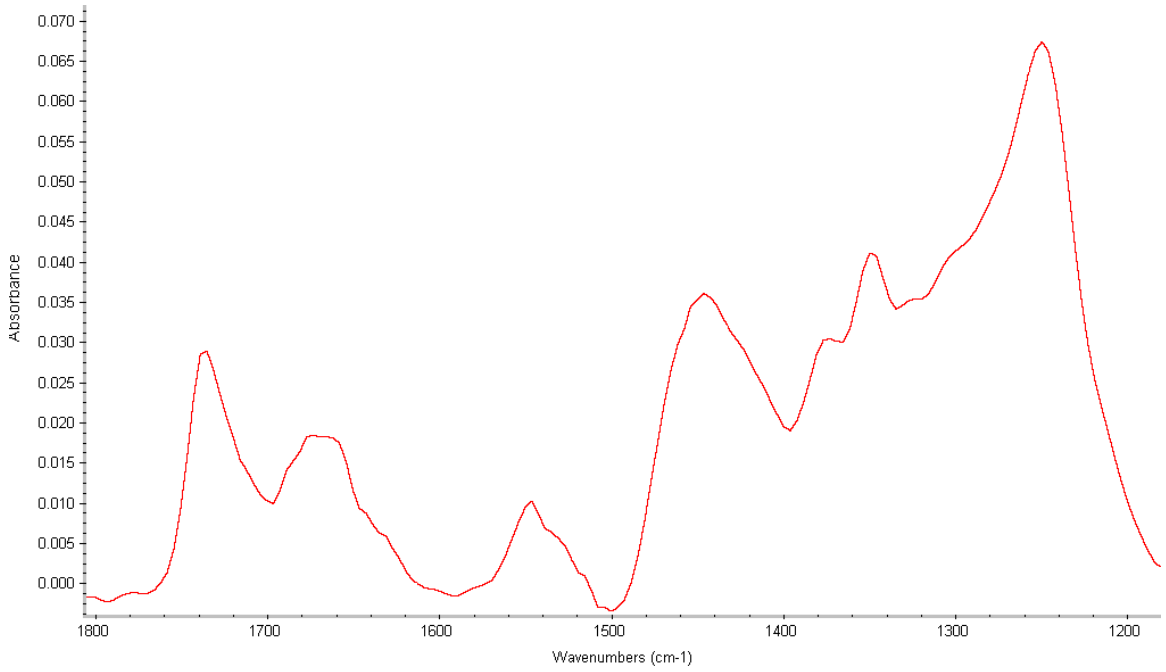

Figure 14: N11 waxy average spectrum minus the average parent spectrum shown resulted when the parent spectrum was scaled to 1.19. Note the prominent residual peaks include: 1740 cm^{-1}, 1469 cm^{-1}, and 1250 cm^{-1}.

Subtracting the parent spectrum from that of the waxy null spectrum, a difference between the two central endosperm regions is evident. And those bands in the waxy nulls that differed from the parents were noted. In the fingerprint region, there were broad bands resulting from the vibrational contributions of multiple species and functional groups. In this instance, spectral resolution was not the limiting factor; the spectrometer is capable of operation at a higher resolution.

In nature, heterogeneity is not unusual. Collecting individual spectra and mapping of a large spectral population did not answer if the lipid is evenly dispersed throughout the central

endosperm. In a separate subsequent study, large areas of central endosperm were mapped and compared in band area ratio maps greater than 1000 μm^2. The first question is whether more lipid is present in the waxy samples versus the parent wheats. Figure 15 shows the distribution of 1740 cm^{-1}/1025 cm^{-1} ratios for N11 waxy null (left) and the parent (right). The difference in mean ratios for these two maps is 11% at the lowest point, doubling in 1740 cm^{-1}/1025 cm^{-1} band area ratio in some area. This difference is illustrated by producing a false color image map using FT-IR microspectroscopic imaging of 1740 cm^{-1}, indicative of lipid, to show waxy has more lipid compared to its isogenic parent wild wheat.

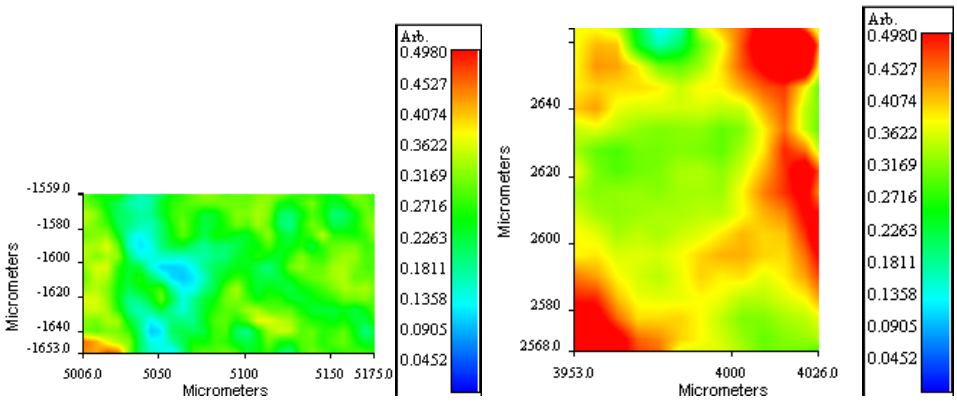

Figure 15: N11 waxy map (right) and N11 parent wheat (left) at 1740 cm^{-1} ratioed relative to the 1025 cm^{-1} band area. In this false color representative figure, numerical scale defining the ratio of 1740 cm^{-1} are found to the right of each map and set to the same scale.

This difference was in agreement with our previous near-IR imaging results [24] that exhibited a higher amount of less well defined lipid in waxy isogenic kernels than in the non waxy parent wheat kernels.

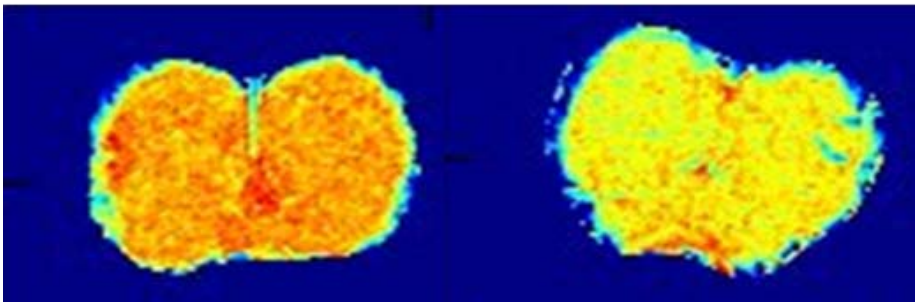

Figure 16: Near infrared imaging false color representation elucidating lipid at 2310 nm combination band. The waxy section is on the left, the isogenic parent section is on the right. Warm colors (reds) represent the strong presence of (carbonyl) lipid. (reprinted from [24]).

3.1.2 Selective in situ lipid extraction from individual sections

Microtomed wheat sections were reanalyzed to monitor selective reduction of nonpolar lipids, glycolipids and phospholipids after extraction with petroleum ether, diethyl ether, and chloroform/methanol, respectively. These solvents represented increasing polarities, respectively.

Whereas the carbohydrate band is a large portion of a central endosperm spectrum, carbohydrate absorption bands are unaffected during the lipid extraction. Therefore locally baseline adjusted carbonyl (1740 cm^{-1}) peak areas were ratioed to a representative carbohydrate band (1025 cm^{-1}) to avoid the influence of varying thickness. A ratio of the desired change-indicating band and representative band from the carbohydrate region [71] at 1025 cm^{-1}, will remain as a constant ratio throughout all of the *in situ* experiments.

There are trace amounts of lipid in the central endosperm of normal wheat. No consistent changes in the spectra were observed with the *in situ* extracted parent N11 wheat. Therefore,

only maps with a significant change from solvent extractions are displayed. Subsequent to mapping, functional group maps were produced for presumed to be distinguishing bands from spectral subtraction of the initial experiment. N11 wheat at the band ratio 947 cm^{-1}/1025 cm^{-1}, had no reduction before and after extraction via petroleum ether and diethyl ether on the same area in the central endosperm. However, the resulting 947 cm^{-1} functional group map of the N11 waxy (false color image map, on the same scale) after sequential extraction with petroleum ether and diethyl ether indicates that the lipid at the highest point of concentration nearly 38% reduction after extraction. In the range of around 900 cm^{-1}, ester bands are found on the spectrum. According to Colthup [43], additional ester bond activity can be seen in the fingerprint region down to 700 cm^{-1} (900-700 cm^{-1}). However the use of the BaF_2 windows, does not allow measurement of absorption lower than 800 cm^{-1}. Also, noted by Colthup in the range around the 947 cm^{-1} band are =C-H and $=CH_2$ bending vibrations.

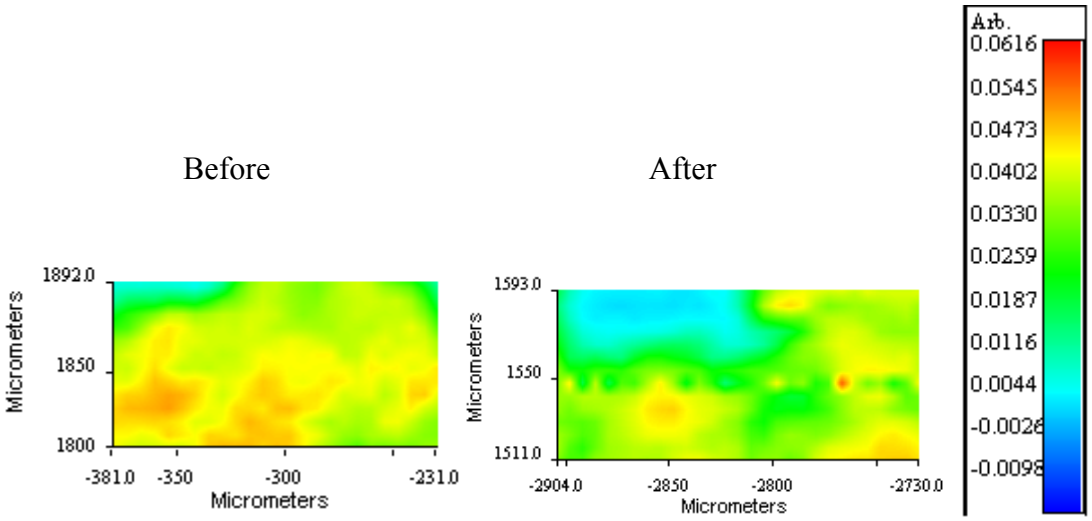

Figure 17: N11 waxy 947 cm^{-1}/1025 cm^{-1} band ratio image showing before extraction (left) and after petroleum ether and diethyl ether extraction (right). The scale to the extreme right applied to both images

Functional group 1469 cm^{-1}/1025 cm^{-1} image maps of the N11 null, obtained after a diethyl ether extraction resulted in 23% reduction of the band from those maps before extraction. In contrast, the N11 parent wheat showed no change with extraction. The 1469 cm^{-1} band is caused by a CH_3 deformation, CH bending vibrations associated with the hydrocarbon fatty acid chain indicative of lipid presence. If higher CH bending vibrations at the 1469 cm^{-1} accompany the carbonyl at 1740 cm^{-1}, then they are accounted for as part of the fatty acid chains that are part of the triglycerides fraction.

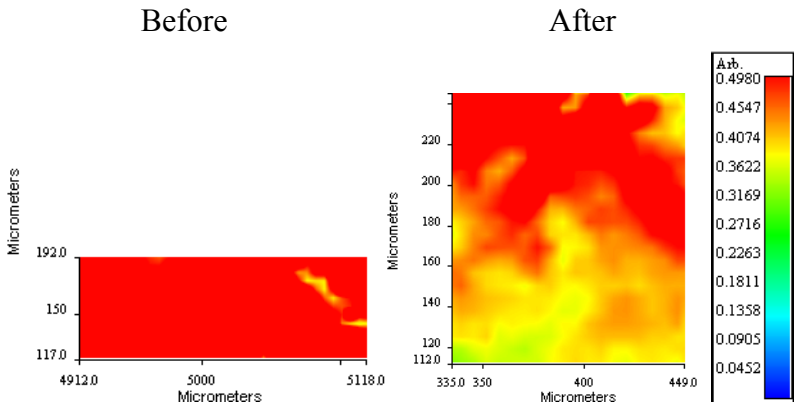

Figure 18: N11 waxy shows the 1469 cm^{-1}/1025 cm^{-1} band ratio images, before (left) and (right) post petroleum ether and diethyl ether extraction. The scale to the extreme right applied to both images. In the after extraction image, a greater area was surveyed in order to assure that the original area surveyed before extraction was included in the after extraction analysis.

In the 1469 cm^{-1} functional group map, after chloroform/methanol extraction, the N11 parent cultivar exhibited no reduction when ratioed to the 1025 cm^{-1} band. The 1469 cm^{-1}/1025 cm^{-1} band ratio image of N11 waxy reduction via chloroform/methanol extraction has 26% reduction after extraction.

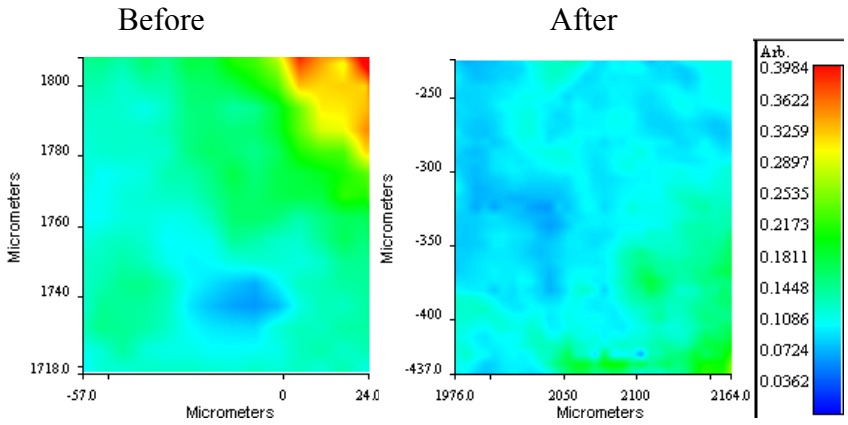

Figure 19: N11 waxy 1469 cm^{-1}/1025 cm^{-1} band ratio image before (left) and after extraction (right) chloroform extraction. The scale to the extreme right accounts for both images. In the after image, a greater area was surveyed in order to assure the originally surveyed area was included in the after extraction analysis.

At the 1740 cm^{-1} band there is a strong absorbance of the ester carbonyl. The stretching vibrations present are C=O (saturated aldehyde) and C=O (saturated ketone). The N11 waxy 1740 cm^{-1} functional group map image before and after chloroform methanol extraction provides at minimum a 24% (maximum of 50%) numerical band ratio reduction in the spectra of the false color image.

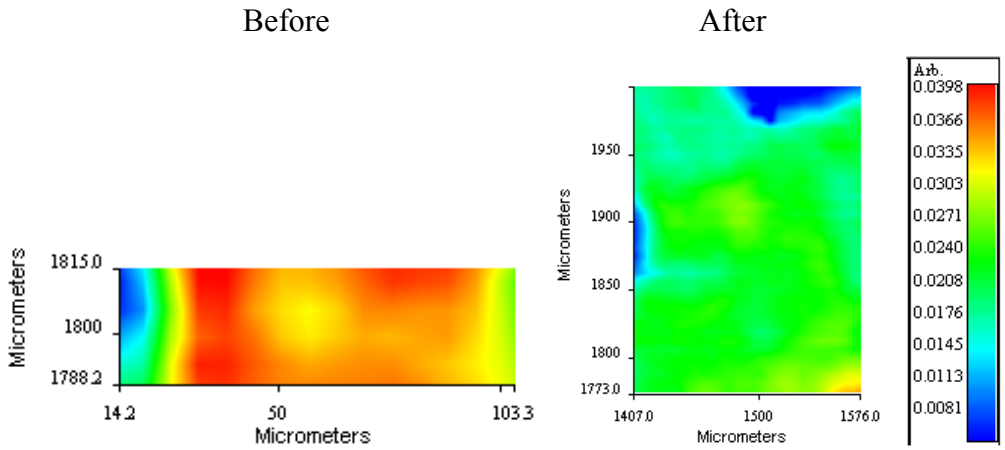

Figure 20: N11 waxy, before (left) and after chloroform/methanol extraction (right), 1740 cm^{-1}/1025 cm^{-1} band ratio image. The scale to the extreme right accounts for both images.

The band found at 2930 cm^{-1} is in the group frequency region of a spectrum and also often indicative of lipid. Reduction of this band by extraction was inconsistently less in comparison to the 1740 cm^{-1} or the 1469 cm^{-1}. These results were expected because the 2930 cm^{-1} band is very prominent. Even with a high-powered extraction step, this band would still be present.

In transmission, infrared radiation penetrates through a specimen and can identify lipid that could not be completely removed from the samples. A high pressure extraction may have yielded greater reduction, however this was regarded as impractical. It is assumed that the lipid class identification would be enhanced by examining the spectrum of the total extract isolated from the finely divided endosperm, rather than that extracted from the *in situ* tissue sections.

In the results following, using the mean value and the maximum and minimum, from the *in situ* endosperm mapping census, the average difference before and after extraction was plotted against the average band area ratio. Those band ratios were collected for each pair of sections and the following graphs resulted for wavelengths of importance to lipids. Figure 21 shows a bar graph of representative data, N11 waxy (black) and N11 parent (white), illustrating more lipid quantitatively found in the waxy specimens than in the parent. While figure 22 illustrates the reduction of lipid after eluding lipids from *in situ* slices with extraction solvents of differing polarities. Lipid reduction was observed in respect to the original numerical data collected before extraction. Figure 23 is a histogram, representing more than 1000 spectra, illustrating populations found at various numerical 1740/1025 cm^{-1} band area ratios. With ten data sets seen

in the graph, triglycerides reduction is seen in 60% of cases, while there is 100% occurrence of reduction for glycolipids and phospholipids.

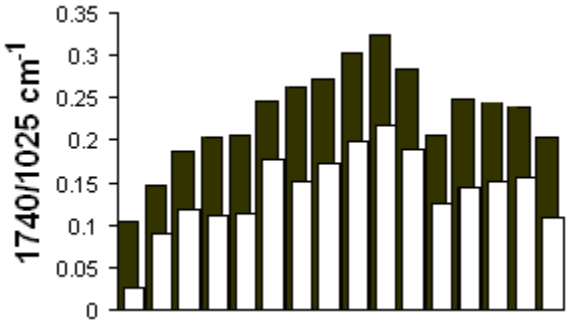

Figure 21: Bar graph of typical N11 waxy (black) and N11 parent wheat (white) maps illustrated as 1740 cm^{-1} ratioed relative to the 1025 cm^{-1} band area. Each bar represents one sample set, including multiple mapped central endosperm areas.

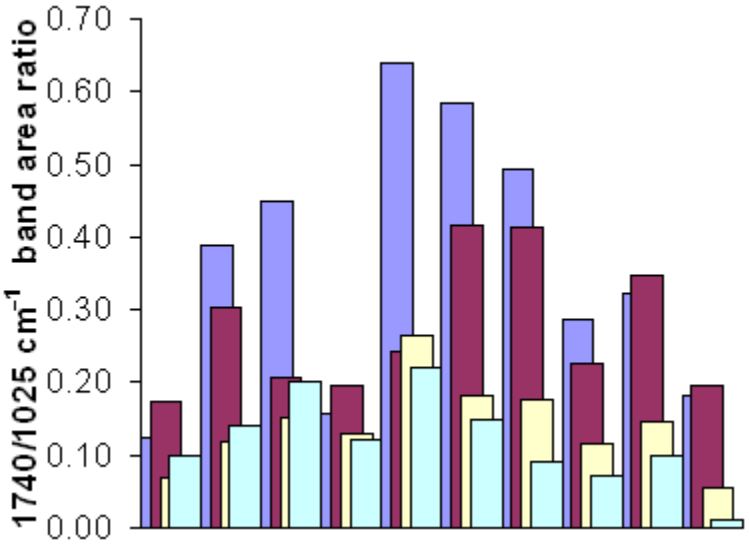

Figure 22: Typical N11 numerical calculation from data represented in the false color images, illuminating the changes before and after in situ lipid extraction. Starting from the back, is the N11 untreated in blue, in the yellow are the diethyl ether after extraction results, petroleum ether after extraction is found in maroon and $CHCl_3$/MeOH,

chloroform/methanol, is the teal bar denoted in the front of the graph, illustrating the most reduction in lipid. Each bar in the graph represents a typical data set.

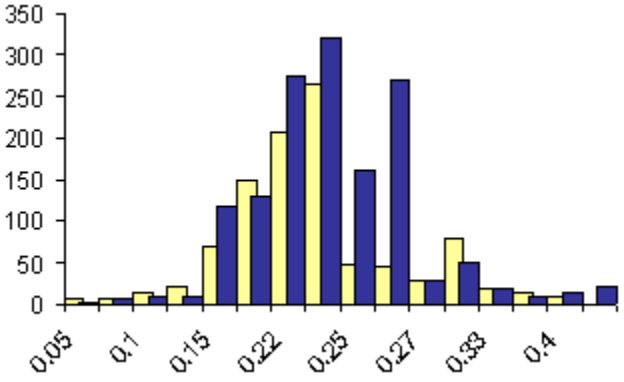

Figure 23: Histogram of N11 waxy (blue) and N11 wheat (yellow) reporting a population of 1000 spectra on the y axis and band area ratio of 1740/1025 cm^{-1} on the x axis.

3.1.3 Total Lipid Extract fractionated with selective solvent

Initially, multiple spots of total extract were mapped using the 16 detector linear array to check for separation that was due to diffusion. Spectra were collected and well as photomicrographs, and false color images produced.

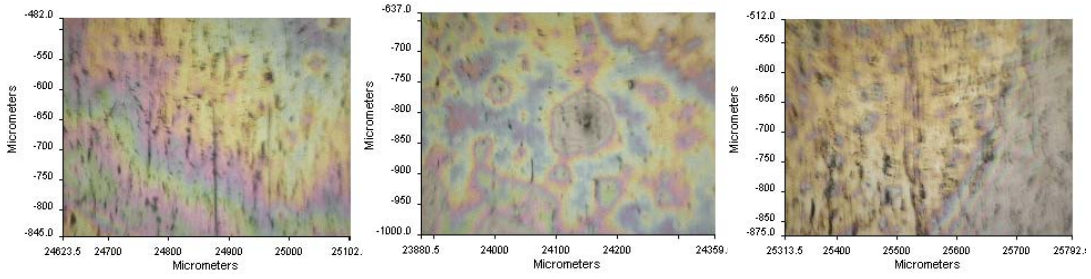

Figure 24: Photomicrographs of the extract spots on the plates. Areas represented from left to right: edge, middle, center of an extract spot on stainless steel.

Examining the spectra with the photomicrograph, it was determined that the separation occurring on the stainless steel is due to diffusion mass transfer. Large, foreign (not lipid) particles, that did not travel with the solvent, due to mass. The foreign particles were spectroscopically identified as having lignin, with a band at 1508 cm^{-1} if the particle was dust, and had 1025 cm^{-1} bands, if it was identified as a starch contaminant.

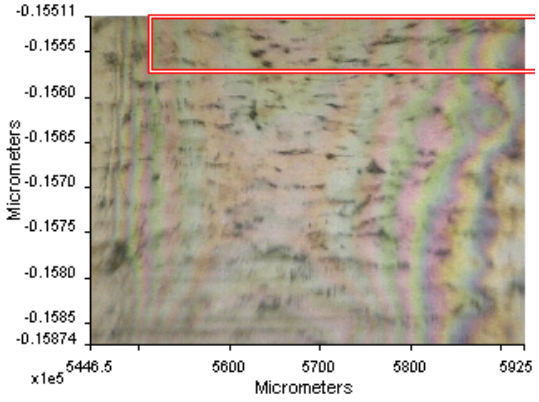

Figure 25A: An extraction spot dried on stainless steel. The spot was mapped from edge to center to observe any physical or chemical separations that could, but did not, occur on the stainless steel plate.

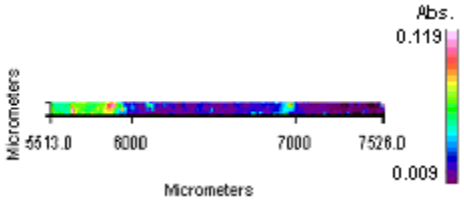

Figure 25B: The corresponding false color image map, representing 1740 cm^{-1} of the photomicrograph found in figure 25A steel plate.

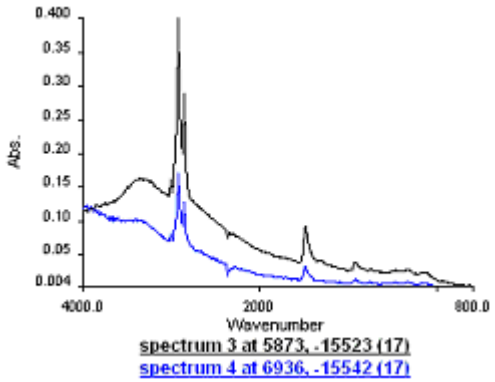

Figure 25C: Spectra taken from two seemingly "opposing" points in the mapped area. Proving there is no chemical separation of the extract spot occurring on the stainless steel.

Subsequently, the spots were sampled for multiple point spectra only, no longer mapping across and throughout the spots. After pure extraction spectra were collected from each sample, using two different spots of the same material, petroleum ether and diethyl ether (via separate rinses) removed polarity selective lipids. Those residue streams were analyzed to see what bands would be carried away using different polarities, process flow illustrated in figure 26A.

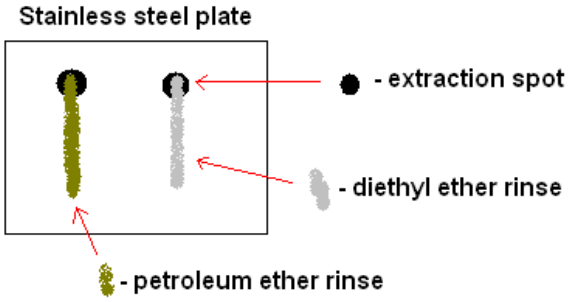

Figure 26A: Diagram representation of the selective extraction method. The black spots represent where spectra were previously collected as an unaltered reference before being rinsed with solvent. The rinses (green and gray), not the extraction spots, were analyzed for polarity selective lipids.

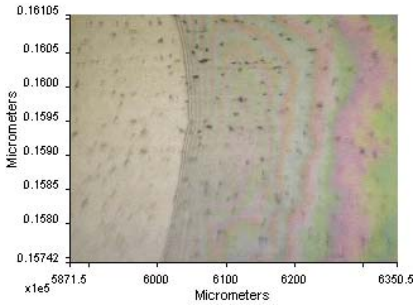

Figure 26B: Photomicrograph of a solvent rinse of an extract spot. From the rinses, streams washed away lipids with the same polarities as the solvent.

Microspectroscopic *in situ* analysis alone did not explain lipid classification based on polarity. However, the treatment of total lipid extract with solvents of more select polarity, provides added supporting lipid classification data. It is noted from the middle spectrum that the petroleum ether extracted the CH stretching bands at 2927 cm^{-1}, 2855 cm^{-1}, and the CH bending absorption at 1469 cm^{-1}. Also the carbonyl band at 1740 cm^{-1} was present in the fractional extract. Unsaturated hydrocarbon groups were also extracted as evidenced by the appearance of the 3015 cm^{-1} band. Presumably, this nonpolar fraction included most of the triglycerides present. While diethyl ether extracted substances with absorption band 2964 cm^{-1}, 1254 cm^{-1}, 1096 cm^{-1}, and 1014 cm^{-1}. In the diethyl ether fraction the 1254 cm^{-1} band reveals the P=O vibration of phospholipids and the 1090 cm^{-1} and 1014 cm^{-1} in the carbohydrate region indicate presence of the conjugated form as glycolipid. Subsequent mass spectrometric data obtained from the total extracts potentially provides speciation within these lipid classes. In the waxy kernel, more lipid is available in the endosperm. It was noted that a larger amount of lipid was carried in the waxy specimen extracting rinses resulting in bands of greater magnitude than those observed in spots extracted from the parent wheat.

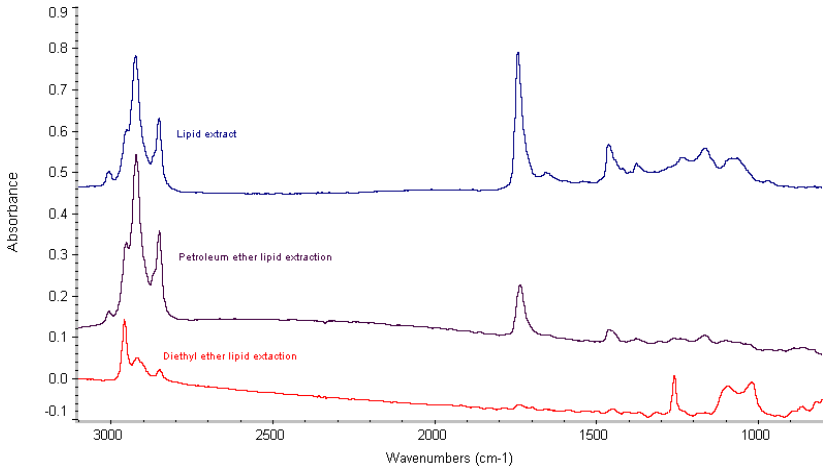

Figure 27: Spectra fractionated from waxy total extract spots on polished stainless steel. The total lipid extract (top) is a reference for comparison to petroleum ether (middle) and diethyl ether (bottom) selective extracts.

3.1.4 Mass spectrometry applied to total lipid extract

Mass spectrometry was performed on multiple lipid extracts testing for glycerides (digalactosyldiglycerides, monogalactosyldiglycerides, triglycerides, and diglycerides) and phospholipids. In this study, polar lipids include all digalactosyldiglycerides, monogalactosyldiglycerides, and phospholipids, under the methods of KLRC, while the triglycerides, and diglycerides were analyzed separately as neutral lipids. Nonimpact results have been removed from the text for readability (full results **Appendix E**). Results cited were run on samples along with quantitative standards and mathematically manipulated to remove the standard from the numerical results.

Diglycerides are easily analyzed by soft ionization because their fatty acids are covalently bonded with ester linkages. To separate the two during detection, the removal of one fatty acid chain is identified in mass spectrometric analysis, and due to molecular weight it is also

discriminated from the triglycerides. The diglycerides determined from a 0.400g sample of N11 waxy wheat were 9.09 nmol/L, as compared to the 5.18 nmol/L found in the normal wheat samples. The most prominent diacylglycerol in waxy wheat, $C_{37}H_{72}O_5N$, had a molecule ion mass to charge ratio of 610.5. These are seen in the spectra of the MS positive scans (figure 29). Both MS positive and MS negative (figure 30) scans were run, since lipid research on waxy wheats has not been reported previously and it was not certain what specific lipids the instrument should meter in the specimens. The nonpolar diglycerides MS negative scan provided little information and therefore will not be discussed. The most prominent diglycerides had mass/charge of 610, 610.5, 634.5, 636.5, and 638.6 mass/charge. Corresponding only to fatty acid groups of diglycerides.

The diglyceride results lead towards N11 waxy wheats having more short (273) and long (301) fatty acid chains, with few medium chains, compared to the N11 parent. The shorter chains are exemplified in the chart found in figure 32 by a shift to the left in the MS spectrum.

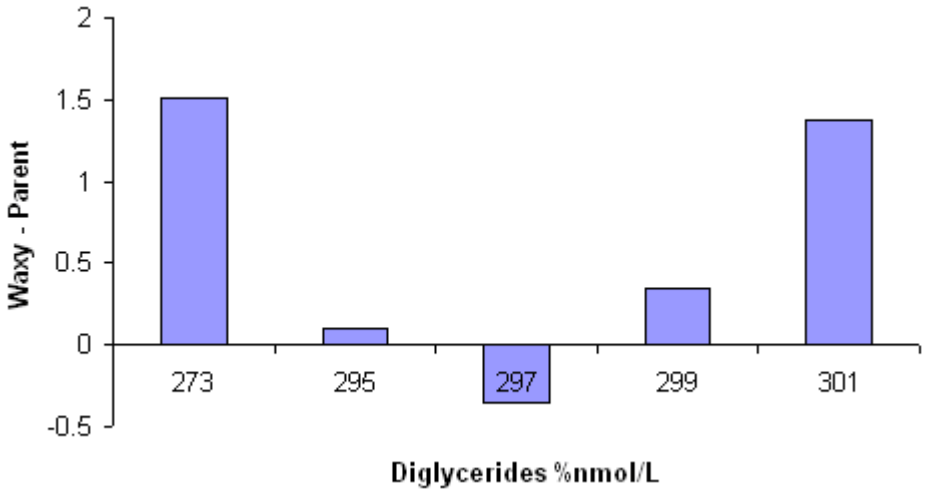

Figure 28: Summary of the diglycerides mass spectrometric analysis calculated as %nmol/L. The substrate parent results were subtracted from the waxy to provide the difference found on the y axis.

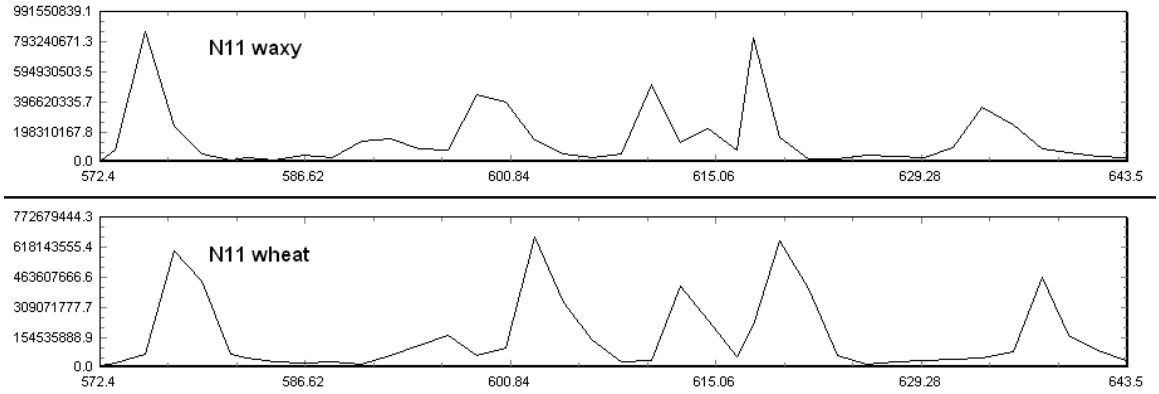

Figure 29: N11 MS positive mass spectrometric fractionation scan of N11 waxy and N11 wheat. The bins of the spectra have been adjusted and the spectra have been baseline corrected and normalized to the largest individual mass/charge peak.

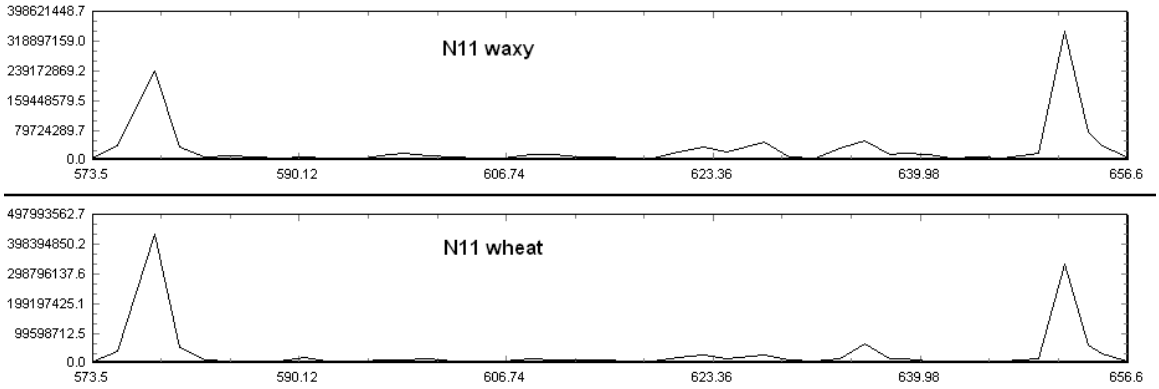

Figure 30: N11 MS negative mass spectrometric fractionation scan of N11 waxy and N11 wheat. The bins of the spectra have been adjusted and the spectra have been baseline corrected and normalized to the largest peak.

The soft ionization technique resulted in only removed one fatty acid head group from the end of triglycerides present in the sample. Triglycerides have three fatty acid chains covalently bonded. The mass spectrometer detector only scans for one fatty acid head group and because of the weight of the molecule after ionization it is categorized as a triglyceride. The full results have been deleted from the text for readability (additional numerical data available in **Appendix F**). Triglycerides determined from a 0.400g sample of N11 waxy wheat endosperm was 6.91 nmol/L, as compared to the 4.58 nmol/L found in the normal wheat samples. The N11 parent wheat had significantly more triglycerides with a fatty acid in the 273 mass/charge scan, however N11 waxy host predominately fatty acid chains detected in the 301-molecule ion scan. It is speculated that N11 has longer fatty acid chains, perhaps by 2 CH_2, since 28 is the molecule weight of 2 CH_2 and the difference in 301-273 is 28.

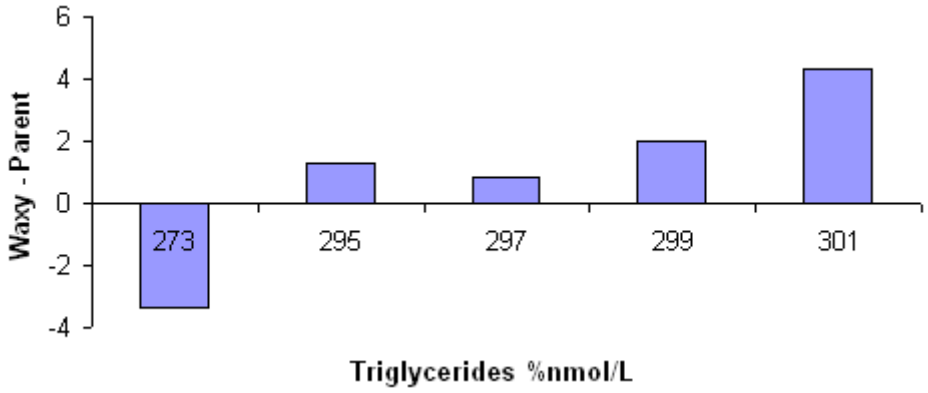

Figure 31: Summary of triglycerides mass spectrometric analysis calculated as %nmol/L. The substrate parent results were subtracted from the waxy to provide the difference found on the y axis.

The most prominent mass to charge ratios found in the triglyceride results had a mass to charge ratio of 848.8, 870.8, 872.8, 874.8, and 900.8, which overlap in the

digalactosyldiglycerides mass to charge range. The prominent mass to charge ratios represent $C_{53}H_{102}O_6N$, $C_{55}H_{100}O_6N$, $C_{55}H_{102}O_6N$, $C_{55}H_{104}O_6N$ and $C_{57}H_{106}O_6N$, respectively. The mass to charge ratio of 848.8 is seen in both the MS positive and negative scans (figures 32 and 33). While the prominent triglyceride, $C_{55}H_{106}O_6N$, had a molecule ion mass/charge 876.8. In the diglycerides and triglycerides results, a downward shift occurred in the spectra denoting the high occurrence of fatty acid chains with low mass to charge. It is speculated that the triglyceride shift maybe "diluted", but not annihilated due to the higher molecular weight of a triglyceride, in respect to a diglyceride. More results from a greater population of samples are need to make that conclusion. It is also possible that the shift is a factor is occurring not evident to the types of analysis used in this experiment.

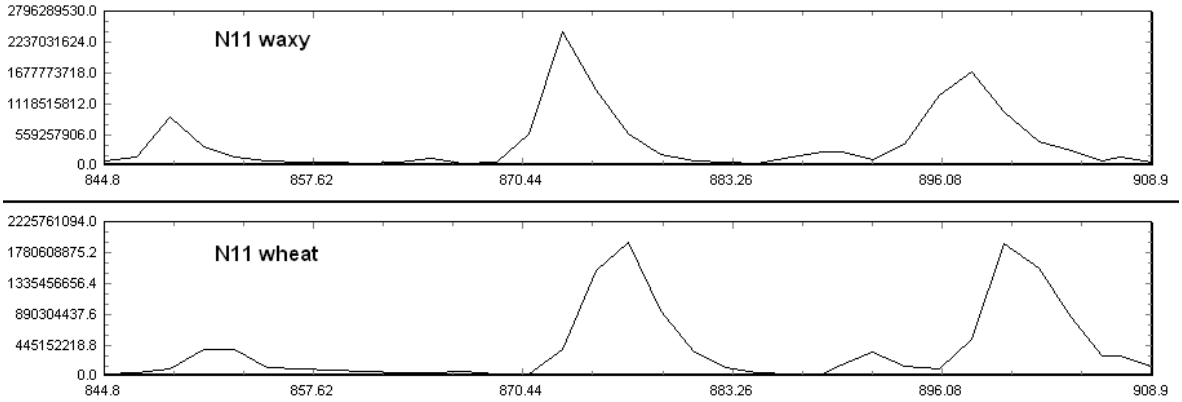

Figure 32: N11 variety MS positive mass spectrometric fractionation scan of N11 waxy and N11 wheat. The bins of the spectra have been adjusted and the spectra have been baseline corrected and normalized to the largest peak.

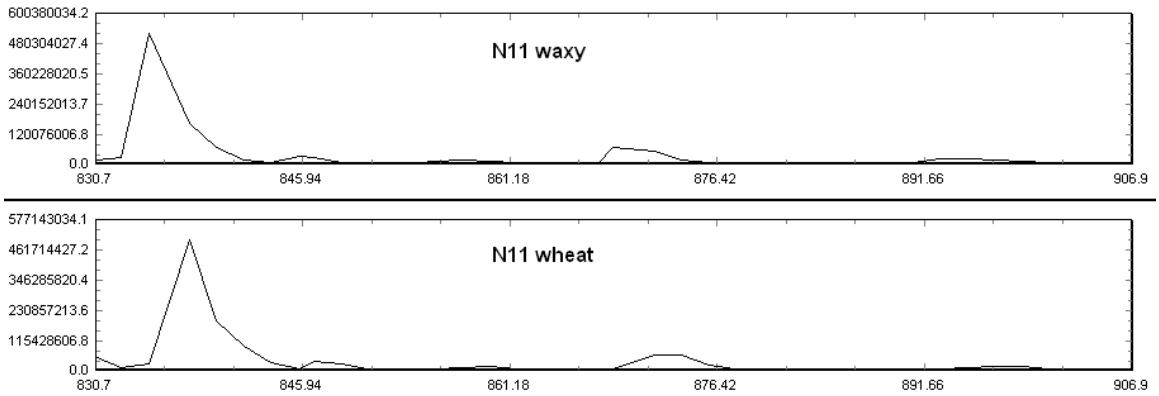

Figure 33: N11 variety MS negative mass spectrometric fractionation scan of N11 waxy and N11 wheat. The bins of the spectra have been adjusted and the spectra have been baseline corrected and normalized to the largest peak.

The following table contains a collection of glycerides results. The coefficient of variation reported, because standard deviation depends on the units that are used. N11 waxy wheat shows an increase in diglycerides and triglycerides when going from the normal parent to the waxy.

Diglycerides and Triglycerides (nmol/L)			
	Mean	Range	CV (%)
N11 wheat	1.43	0.36	17.48
N11 waxy	2.29	0.34	10.48

Table 2: Summary of diglycerides and triglycerides in nmol/L with mean, range and coefficient of variation reported.

The neutral lipids resulting from fractionation during the ionization process were digalactosyldiglycerides (DGDG) and monogalactosyldiglycerides (MGDG). While the phospholipids included: phosphatidylcholine (PC), phosphatidylethanolamine (PE), phosphatidylinositol (PI), phosphatidic acid (PA), phosphatidylserine (PS), phosphatidylglycerol (PG), lysophosphatidylcholine (LPC), lysophosphatidylethanolamine (LPE), and lysophosphatidylglycerol (LPG) to be discussed in later sections. The phosphatidylcholine (PC) results, would not provide reliability between samples, therefore that group was excluded from discussion.

The table results are provided below and list only the impactive results, other results have been removed from the list for readability (full results available in **Appendix G**). Widely known in the grain industry, digalactosyldiglycerides and monogalactosyldiglycerides are the most prominent lipids found in wheat. The most prominent digalactosyldiglyceride observed in the N11 variety was 36:4, $C_{51}H_{92}O_{15}N$. Figure 34 illustrates that waxy wheat contains more polar lipid than the parent wheat. However, in some categories, the parent wheat contains more of a certain lipid, such as monogalactosyldiglycerides (36:4), phosphatidylserine (40:2), phosphatidylinositol (34:2), and lysophosphatidylethanolamine (18:2). The

lysophosphatidylglycerol (18:3), lysophosphatidylethanolamine (18:2) and phosphatidylinositol (34:2) were not prominent in the samples, however for all of those, the normal parent endosperm contained more than the waxy samples. Waxy wheat central endosperm, total polar lipids, determined from a 0.400g sample, were analyzed at 5.01 nmol/L compared to normal wheat with only 3.22 nmol/L. The polar lipids results were reported in the same style as the diglycerides and triglycerides.

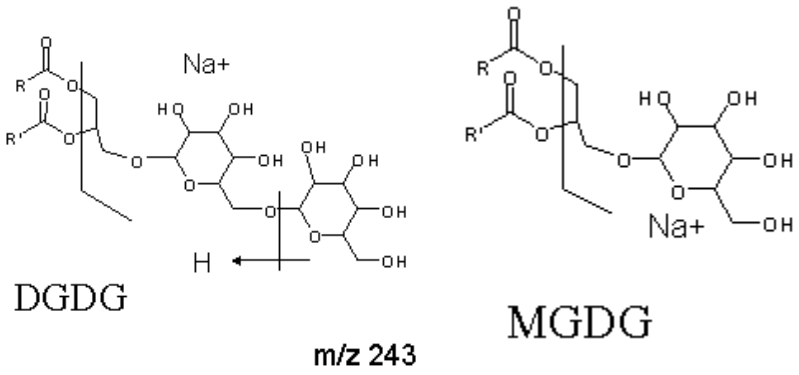

Figure 34: Chemical formula of the most abundant lipids found in wheat, digalactosyldiglycerides (DGDG) and monogalactosyldiglycerides (MGDG) [from 53].

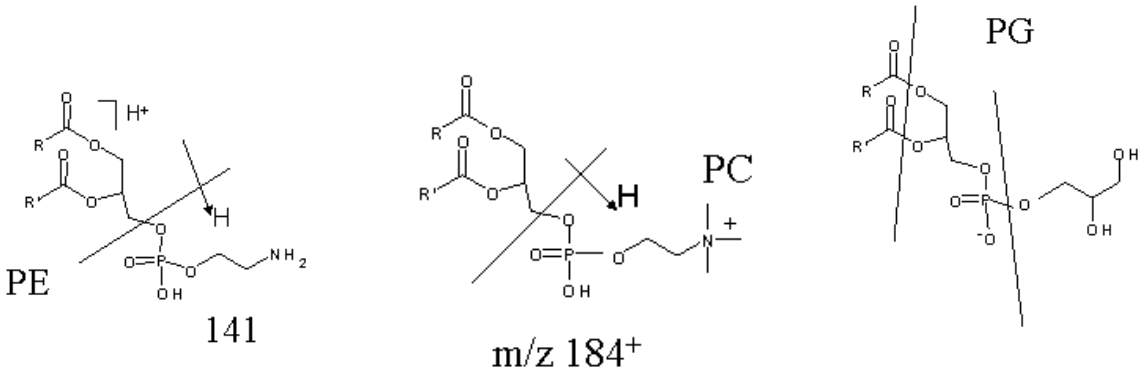

Figure 35: Chemical structure of phosphatidylethanolamine (PE), phosphatidylcholine (PC), and phosphatidylglycerol (PG). The lysophosphatidylethanolamine chemical structure is not drawn out because it is the same as phosphatidylethanolamine, however with only one lipid head group [from 53].

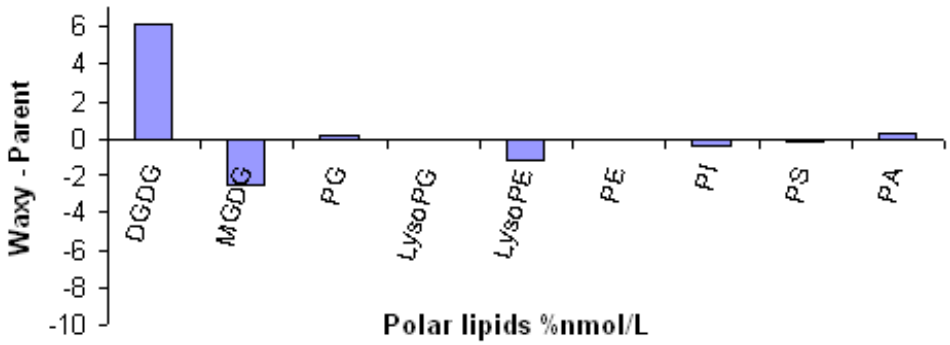

Figure 36: Summary of the polar lipid mass spectrometric analysis calculated as %nmol/L. The substrate parent results were subtracted from the waxy to provide the difference found on the y axis.

Total Polar Lipid (nmol/L)			
	Mean	Range	CV (%)
N11 wheat	3.12	1.07	24.36
N11 waxy	5.01	0.53	7.58

Table 3: Summary of total polar lipids in nmol/L with mean, range and coefficient of variation reported.

3.2.0 Isogenic partial waxy

The isogenic partial waxy specimens provided corresponding results to the N11 normal parent and waxy wheat endosperms. For one of three double nulls possible, genetic expression

results would appear as though the specimen being analyzed was a N11 full waxy sample, instead of a partial waxy. This was true for N11 AB. However, all other partial waxy specimens (N11 BD, N11 AD - the remaining double nulls and all single nulls) would show diminished band concentration for bands of interest or nothing at all.

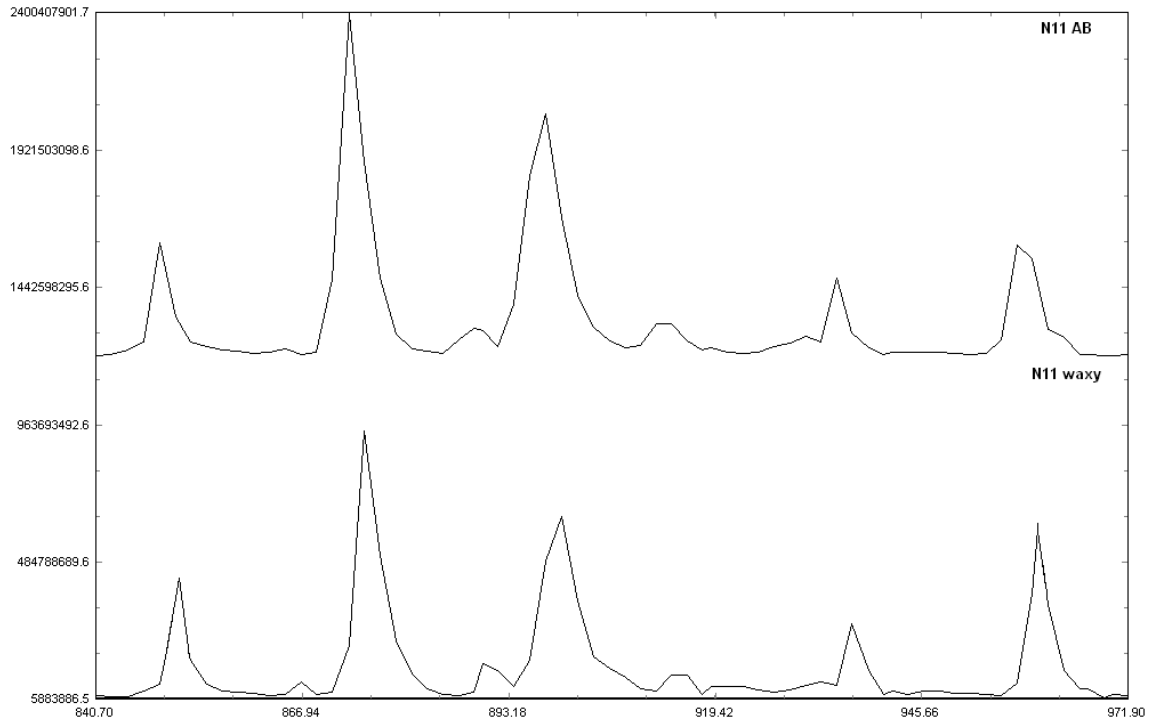

Figure 37: Mass spectra depicting N11 AB versus N11 waxy. The spectra are similar accept for elevated molecule ions at mass to charge ratios 848.9 and 958.8, found in the digalactosyldiglycerides mass to charge range.

N11 is a hexaploid with AABBDD alleles; it has three double nulls and three single nulls. When the double null containing allele B is present, the cultivar contains more lipid in the central endosperm than with alleles A and/or D present. An observation made by researchers [4, 18] of the B allele increasing the occurrence of lipid in the waxy kernel is supported by the results of this study. These results are also consistent with previous NIR imaging observations [24].

3.2.1 N11 partial waxy in situ microspectroscopic probing of central endosperm

All N11 double null subtractions were comparable to that produced by N11 triple null. Subtraction of an average N11 waxy double null spectrum minus a parent spectrum did not recover any unexpected, prominent residual bands. The bands found were the carbonyl (1740 cm^{-1}) and CH bend (1469 cm^{-1}). The previously noted carbohydrate contribution found at1158 cm^{-1}, 1085 cm^{-1}, and 1024 cm^{-1}, were not recovered from the spectral subtraction. Via *in situ* microspectroscopic probing of central endosperm, no consistent differences could be measured to separate the parent wheat spectra from those of the single nulls found in the central endosperm.

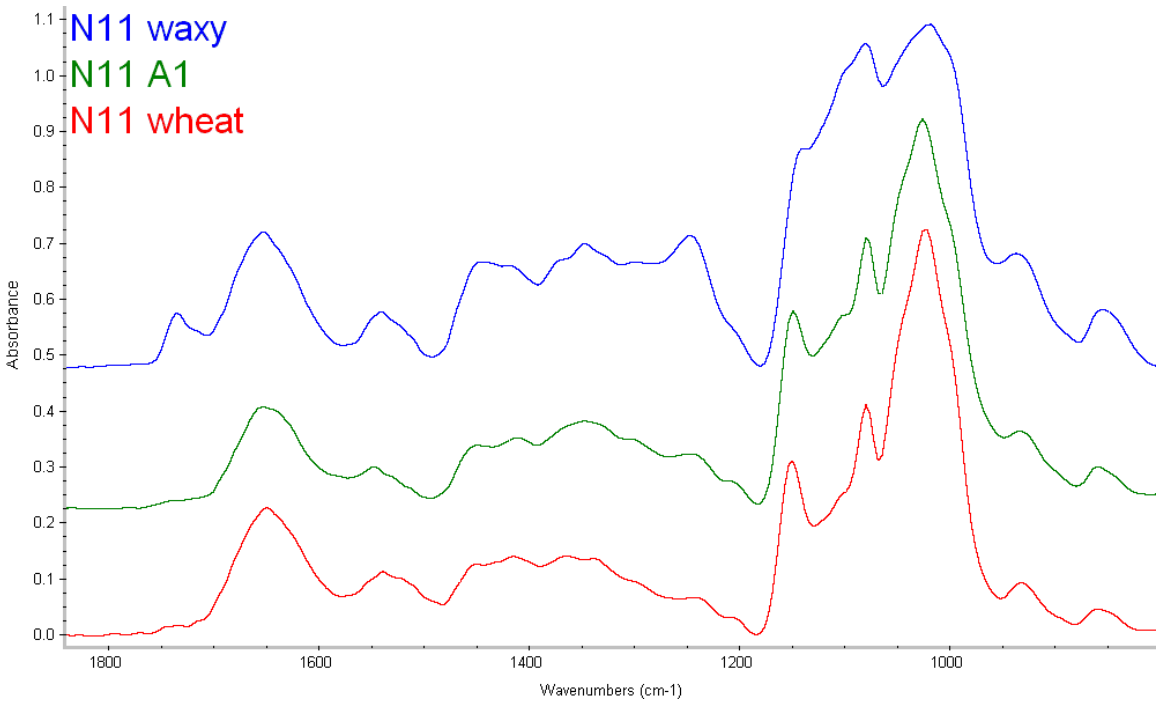

Figure 38: Central endosperm spectra showing differences between N11 waxy (top), N11 A (middle) and N11 parent (bottom).

N11 AB was in agreement with the results reported earlier of the full waxy sample. The two specimens differ in molecule ions of mass to charge ratios 848.9 and 958.8, speculated to be

a derivative of digalactosyldiglycerides. The earlier study with near infrared imaging, performed on isogenic waxy wheats [24], showed N11 AB could be discriminated from parent (normal) wheat spectroscopically via near infrared imaging. With AB being the only partial waxy discriminated in the mid infrared study as well, it is extremely interesting that N11 AB genetic expression is detectable via these analytical methods, and that N11 BD and N11 AD do not exhibit any tendency in that direction.

3.2.2 N11 partial waxy selective in situ lipid extraction from individual sections

No results will be reported on the extractions of partial waxy samples. Waxy wheat contains lipid in the endosperm, and parent (normal) wheat contains little lipid in the central endosperm. Because some reduction was seen in the N11 wheat samples in the previous results, the partial waxy *in situ* lipid exaction results were within the same range as the nonwaxy parent, assuming these differences will be in conjunction with the previous results after extraction.

3.2.3 N11 partial waxy mass spectrometry applied to total lipid extract

For the partial waxy samples an increase in lipid was observed, however that increase was not consistent within the lipid class or within the cultivar, only that the nmol/L were increased for all the partial waxy samples, including an observable difference between normal parent wheat spectra from that of the single null spectra. There is a decrease in molecule ions of 896.9 mass to charge in all partial waxys, in retrospect to the parent wheat. Also, there is an increase of 480.4 mass to charge in the partial waxy cultivar, a molecule ion found in the lysophosphatidylethanolamine (18:1) scan.

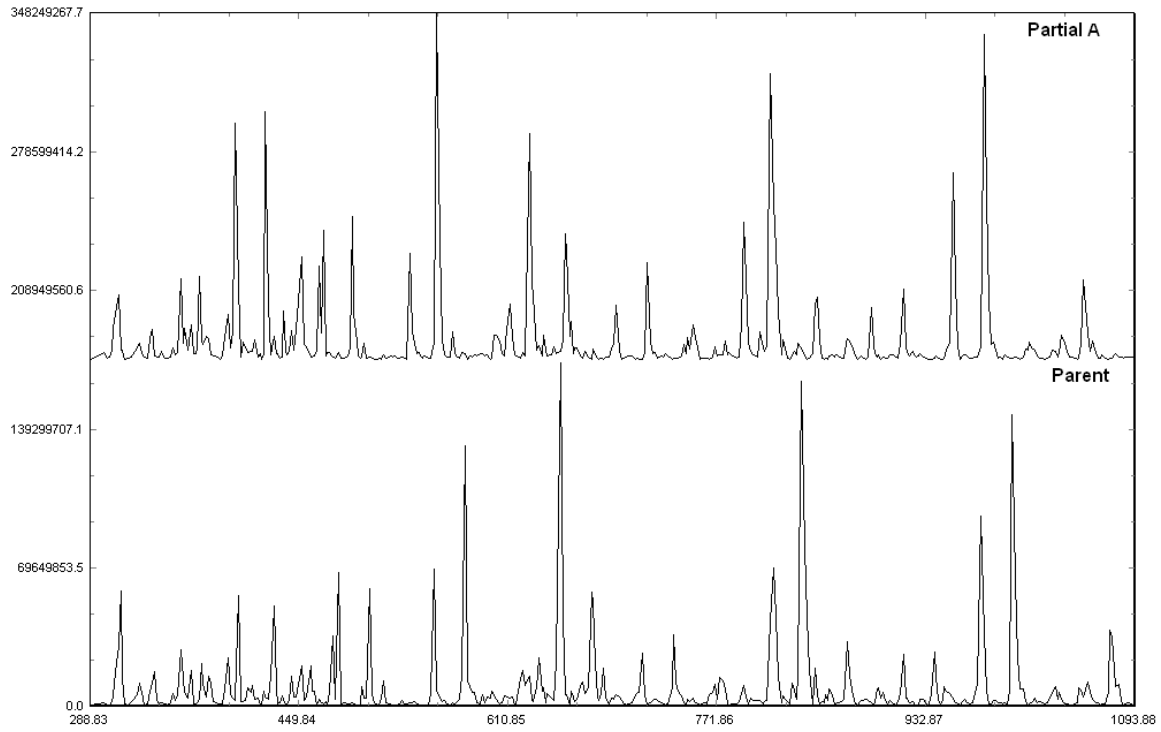

Figure 39: Partial waxy, single null A exhibiting a mass to charge spectral shift to the left, as seen in the full waxy samples. This is true for all single null wheats of N11 cultivar.

3.2.4 N11 partial waxy total lipid extract fractionated with selective solvent

The results were consistent with the previous experiments conducted on parent and triple null – N11 waxy. Though the specimens agreed with the prior results, the selective extracts of the double nulls of N11 and the single nulls of N11 did not provide a significant difference to distinguish the samples from each other (i.e. N11 A from N11 B from N11 AB) or the full null samples. Differentiation at that level may be possible. Experimental variation in the amount of sample analyzed on polished stainless steel and variation in the concentration found in the solvent rinse may have clouded this result.

3.3.0 Svevo – tetraploid, durum wheat

Using the same methods as with the N11 isogenic normal wheat and waxy wheat, a tetraploid, Svevo (produced under the same methods and grown in the same location as the N11 line [54, 55]) was studied to reveal the spectroscopic difference between Svevo waxy versus Svevo normal parent wheats. A consensus from the comparison revealed the normal parent wheat is spectroscopically different versus the full null waxy wheat for the isogenic tetraploid family. In the Svevo waxy versus parent central endosperm samples, differences could be seen at 1740 cm^{-1} a classical lipid band and 1250 cm^{-1} assigned a P=O for the phospholipids present. In addition, bands were still present at 1150 cm^{-1} and 1085 cm^{-1}, both carbohydrates, speculated to be in excess amylopectin. Finally 947 cm^{-1} was distinguished as C=O ester, bending vibration.

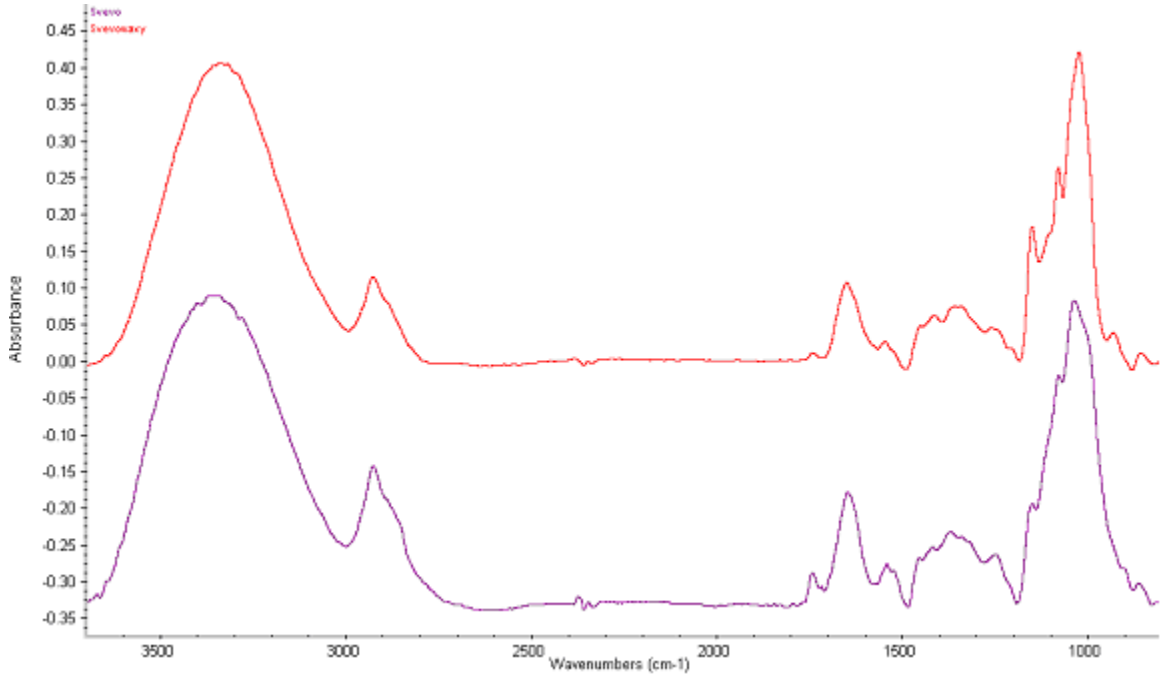

Figure 40: Svevo waxy (top) and Svevo parent (bottom) spectra collected from differing central endosperm specimens.

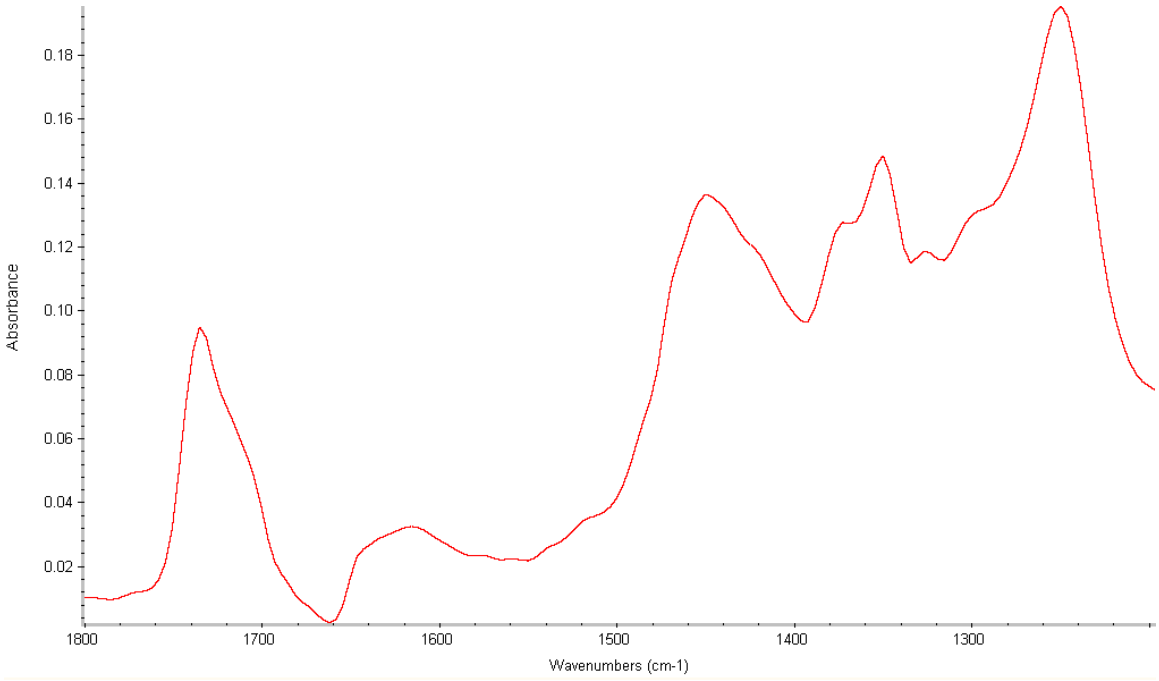

Figure 41: Subtraction of Svevo waxy versus parent samples. Differences could be seen at 1740 cm^{-1}, 1250 cm^{-1}, 1150 cm^{-1}, 1085 cm^{-1}, and 947 cm^{-1}. The amide I differences were seen, and not discussed in this experiment. The subtraction was calculated at 1.94:1 due to sample thickness variation.

After a consensus of spectra for Svevo normal parent and Svevo waxy central endosperm suggested a difference occurred in the tetraploid, the experiment with the isogenic Svevo samples continued as with the N11 variety.

3.2.1 Selective in situ lipid extraction from individual sections

Svevo provided comparable results, with approximately 49 slices analyzed, however it was observed that the intensity of the lipid present seemed to be detectably higher than that of the N11 variety when comparing the false color images produced from mapping spectra. This theory is enforced in later results, i.e. mass spectrometric data.

In situ selective lipid extraction from individual sections of the durum isogenic Svevo line reported reductions of discriminating lipid bands. Svevo parent, 1469 cm^{-1} band area, remained constant, before extraction to after extraction, while the same band of the Svevo waxy sample was reduced by nearly 20%. Notably, Svevo parent wheat and Svevo waxy, before extraction to after extraction at the 1740 cm^{-1} band area ratio area, were both reduced by 20%. The Svevo normal parent and Svevo waxy, before and after extraction, both exhibit no reduction at a 2930 cm^{-1} band area ratio.

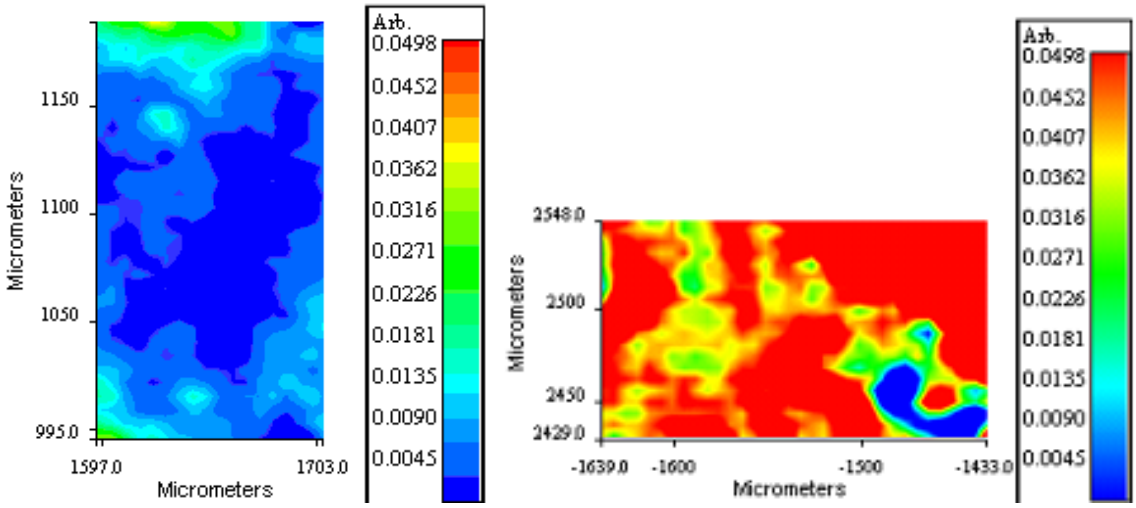

Figure 42: Svevo parent (left) versus Svevo waxy (right) 1740 cm^{-1}/1025 cm^{-1}band ratio images.

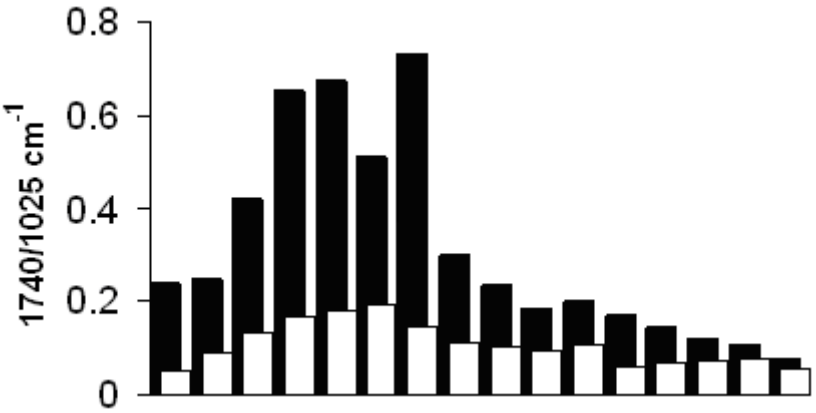

Figure 43: Bar graph of typical Svevo waxy (black) and Svevo parent wheat (white) maps illustrated as 1740 cm^{-1} ratioed relative to the 1025 cm^{-1} band area. Each bar represents one sample set, including multiple mapped central endosperm areas.

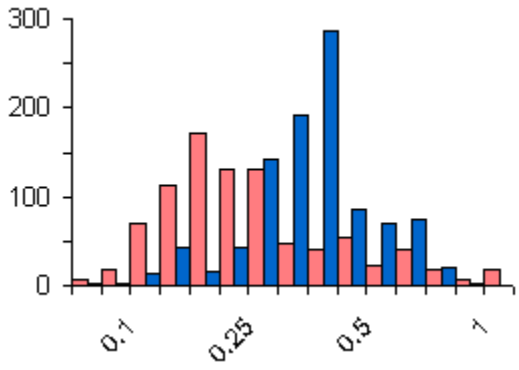

Figure 44: Histogram of a typical Svevo parent (pink) and Svevo waxy (blue) numerical data set illustrating a 1740 cm^{-1}/1025 cm^{-1} band area ratio. The histogram acts as a numerical representation of a population of over 1000 spectra collected from false color imaging.

3.3.2 Total Lipid Extract fractionated with selective solvent

The Svevo waxy and parent wheat selective extraction spots on stainless steel, proved to behave as the N11 waxy and normal parent. The same bands occur in the fractionated rinses of the tetraploid as in the hexaploid. It is concluded that the selective solvents of differing polarities will remove bands from the original total lipid extraction spectrum, and that the tetraploid and hexaploid share those common lipids.

3.3.3 Mass spectrometry applied to total lipid extract

Results of MS analysis are provided in comparison to the previous N11 experiment. Diglycerides, triglycerides, and polar (noted in this research as digalactosyldiglycerides, monogalactosyldiglycerides, and phospholipids) lipids are reported below and list only the impactive results, other results have been removed from the text for readability (results available for viewing at **Appendix E-G**). The most prominent diacylglycerol, $C_{37}H_{72}O_5N$, was a molecule ion at 610.5 mass/charge; observed as the same most prominent molecule ion of the N11 hexaploid. Svevo waxy (in total) has more diglycerides and triglycerides (11.54 nmol/L and 5.85 nmol/L determined from a 0.400g endosperm sample, respectively) than the Svevo parent (6.56 nmol/L and 5.84 nmol/L determined from a 0.400g endosperm sample, respectively). Note no difference seen between the diglycerides of Svevo waxy and normal parent at the neutral loss fatty acid scan performed at mass to charge 273, however a significant difference is seen at 295 mass to charge. Neutral scan methods 273 and 295 have a difference in neutral loss fatty acid composition of less than two carbons.

The most prominent triglyceride fraction was $C_{55}H_{106}O_6N$, found at molecular mass 876.8, a mass to charge also found in the digalactosyldiglycerides MS scan. Svevo (maroon) and N11 (blue) line results are shown together for readability. Triglycerides composition, results seen in figure 46, illustrate the waxy durum wheat has significantly less triglycerides than diglycerides, figure 45. Also, note the Svevo normal parent central endosperm contains a higher concentration of triglycerides than the Svevo waxy.

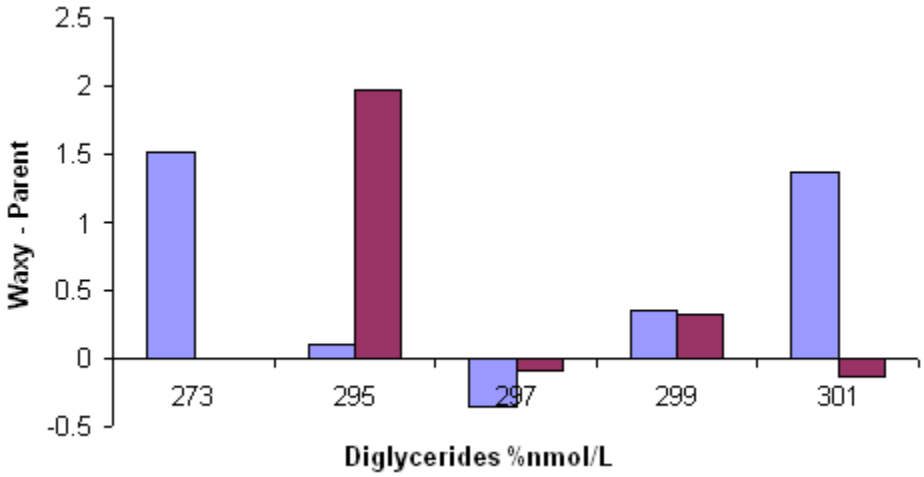

Figure 45: Summary of diglycerides mass spectrometric analysis calculated as %nmol/L. The N11 (blue) cultivar results are shown with the Svevo (maroon) cultivar results, in order to compare and contrast. The substrate parent results were subtracted from the waxy to provide the difference found on the y axis.

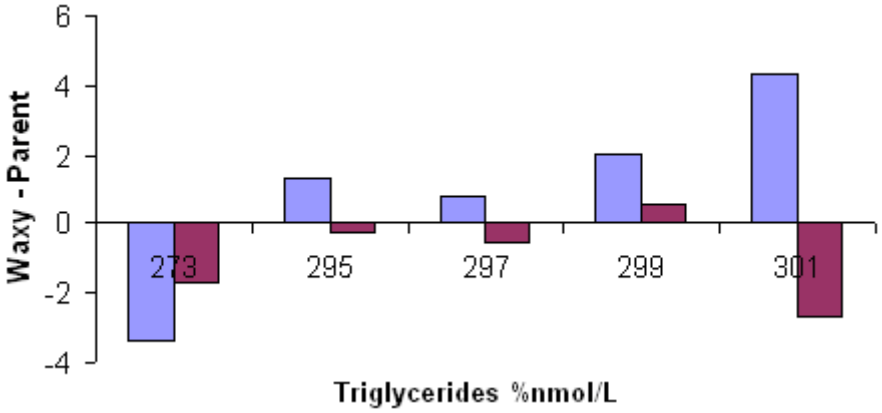

Figure 46: Summary of triglycerides mass spectrometric analysis calculated as %nmol/L. The N11 (blue) cultivar results are shown with the Svevo (maroon) cultivar results, in order to compare and contrast. The substrate parent results were subtracted from the waxy to provide the difference found on the y axis.

Svevo waxy digalactosyldiglycerides (the most abundant lipid found in wheat) are less concentrated than in the Svevo normal parent, even though both specimens contain majority digalactosyldiglycerides. The most prominent digalactosyldiglyceride observed in the Svevo

variety was 36:4, $C_{51}H_{92}O_{15}N$. That said, Svevo waxy compared to N11 waxy are opposites in concentration of digalactosyldiglycerides. The lysophosphatidylglycerol, lysophosphatidylethanolamine, and phosphatidylethanolamine were not prominent in the samples, however for all of those, in both parents, N11 and Svevo, the normal parent central endosperm samples contained more lysophosphatidylglycerol (18:3), lysophosphatidylethanolamine (16:0) and phosphatidylethanolamine (36:4) than the waxy samples. Noted strongly in Figure 47, phosphatidic acid is extremely abundant in the Svevo waxy samples (phosphatidic acid 36:4) in comparison to all samples analyzed in this experiment.

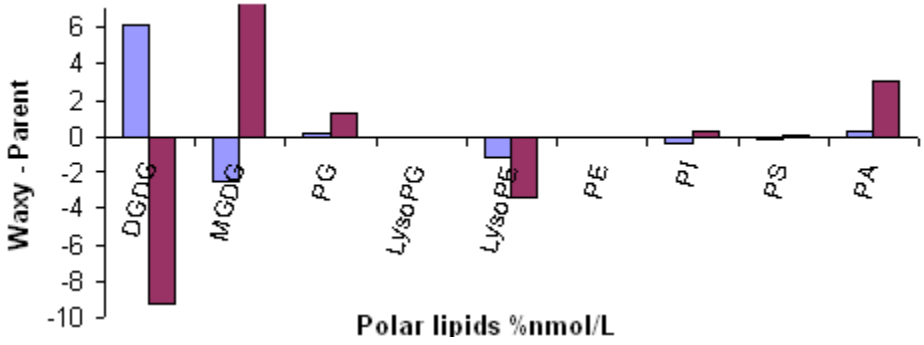

Figure 47: Summary of the polar lipid mass spectrometric analysis calculated from %nmol/L. The N11 (blue) cultivar results are shown with the Svevo (maroon) cultivar results, in order to compare and contrast. The parent results acted as a substrate and were subtracted from the waxy to provide the difference found on the y axis.

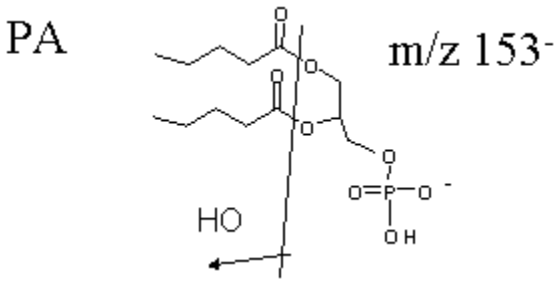

Figure 48: Chemical structure of phosphatidic acid. Phosphatidic acid is found in Svevo waxy to a greater extent than all other specimens studied [from 53].

3.3.4 Svevo partial waxy

Portions of the experimental method were run on Svevo partial waxy cultivar, including initial spectral collection, total lipid extract fractionated with selective solvent, and mass spectrometry applied to total lipid extract. No measurable differences that consistently separated the parent wheat from Svevo single null could be found via these methods.

However, after an examination of total lipid extract fractionated with selective solvent for Svevo partial waxy specimens, the results were consistent with the previous experiments conducted on parent and Svevo double null waxy. Though the specimens agreed with the prior results, the selective extracts of single nulls of Svevo did not provide a significant difference to distinguish the samples from each other (i.e. Svevo A from Svevo B) or the full null samples. This may be due to variation in amount analyzed during analytical data collection and variation in the concentration found in the solvent rinse.

3.4.0 Advanced breeding line wheat samples

The method developed was applied on nonisogenic, advanced breeding line samples. These samples were not run in conjunction with the N11 and Svevo isogenic varieties because the advanced breeding line specimens are only genetically related and were not grown in the same location, under the same conditions. As with the isogenic central endosperm specimens analyzed, using 16 slices, the advanced breeding line waxy samples Nx05m4499_1 (waxy) had an observable increase in lipid, compared to the normal relative parent Arapahoe. A spectral subtraction of Nx05m4499_1 and Arapahoe was produced to enhance lipid differences.

Numerical calculation from data represented in the false color images, illuminating the difference in 1740 cm^{-1} between advanced breeding line specimens Nx05m4499_1 (waxy) vs. Arapahoe (parent). Figure 52 represents a population of approximately 1200 spectra to compare the differences seen in normal parent vs. waxy central endosperm.

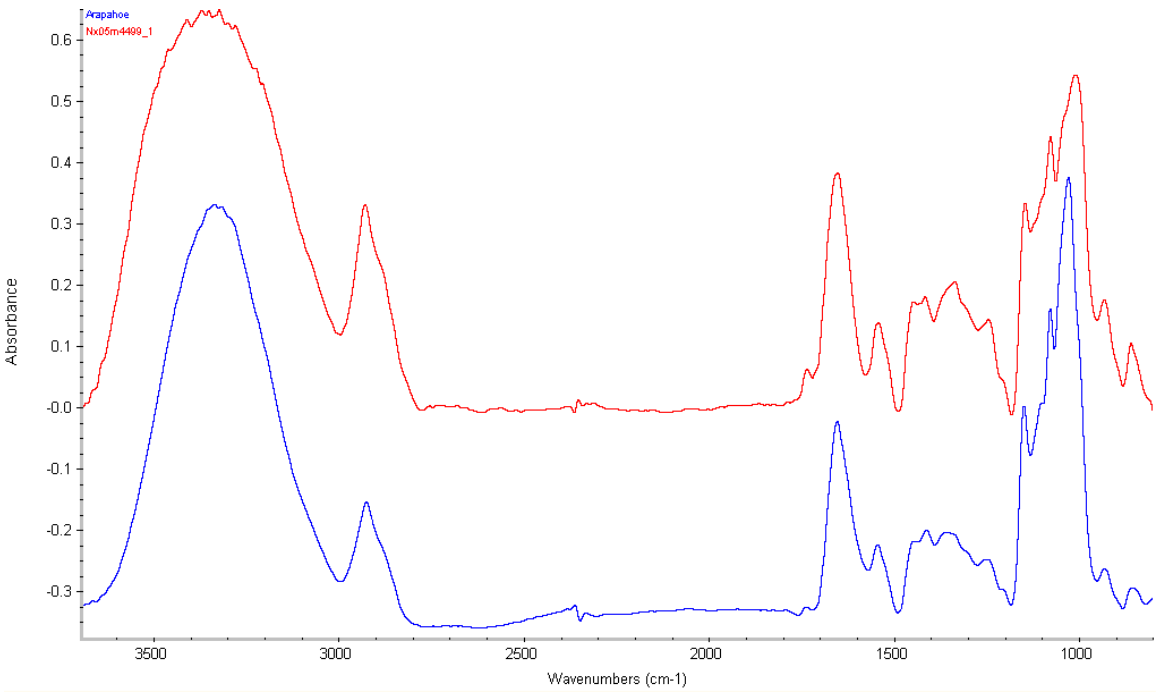

Figure 49: Central endosperm spectra of advanced breeding line samples obtained from Graybosch waxy NX05m4499_1 (top) and parent Arapahoe (bottom).

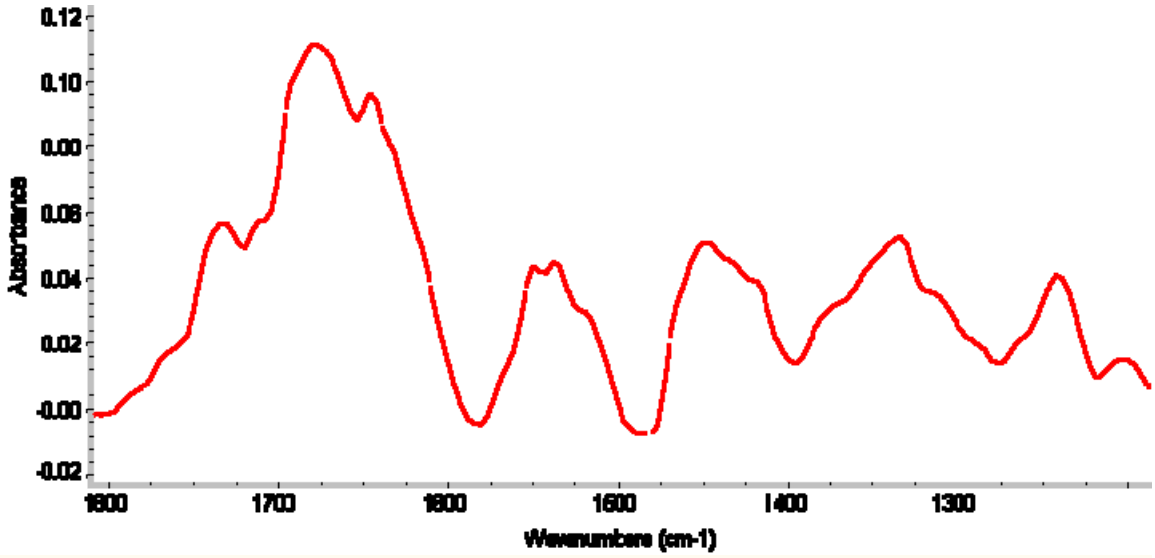

Figure 50: Central endosperm spectral subtraction of parent Arapahoe subtracted from waxy Nx05m4499_1. The subtraction is performed at 0.97:1

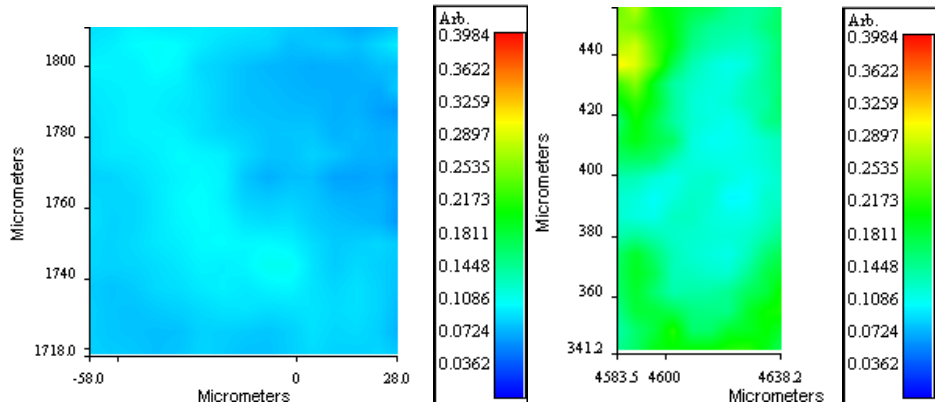

Figure 51: Arapahoe (left) versus Nx05m4499_1 (right) 1740 cm^{-1}/1025 cm^{-1} band ratio images.

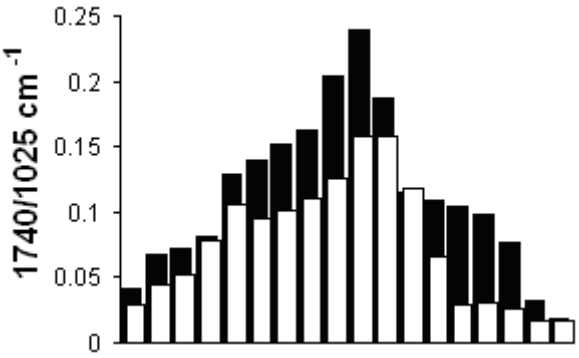

Figure 52: Bar graph of typical Nx05m4499_1, waxy, (black) and Arapahoe, parent, wheat (white) maps illustrated as 1740 cm^{-1} ratioed relative to the 1025 cm^{-1} band area. Each bar represents one sample set, including multiple mapped central endosperm areas.

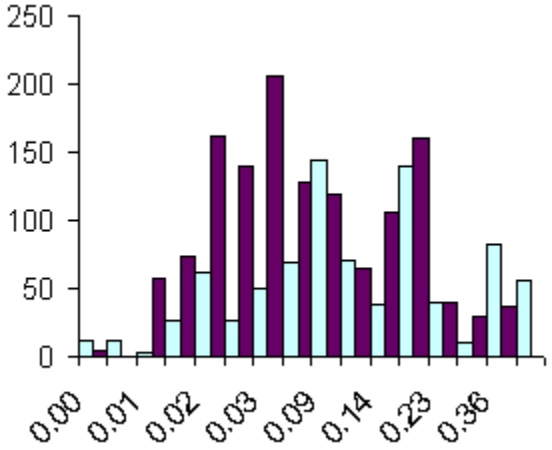

Figure 53: Histogram comparing Arapahoe (purple) and Nx05m4499_1 (teal) 1740 cm^{-1}/1025 cm^{-1} band ratio numerical data sets illustrating a population of 3000 spectra from false color imaging.

3.4.1 Selective in situ lipid extraction from individual sections

The false color imaging results from this experiment were difficult to compare, because of vast differences in whole kernel moisture and kernel quality for the relative advanced breeding

line wheat. Many seeds were damaged via insects, weather, etc. Also because the parent and waxy advanced breeding line samples were grown in different locations under differing conditions, the *in situ* false color imaging measurements are not reliable enough to comparable to each other, let alone to the model isogenic hexaploid or tetraploid.

In the *in situ* extraction, as seen in false color images and spectra, the Arapahoe specimens extracted with chloroform always calculated to have a higher amount of the lipid than the unaltered specimen, for all wavelengths examined. The calculated coefficient of variation for this analysis was extremely low, showing that the similarity of the mean to the samples was not very strong.

3.4.2 Total Lipid Extract fractionated with selective solvent

The advanced breeding line samples, Svevo line, and N11 line (including waxy and parent for every specimen) all revealed the same bands during selective extraction implying the specimens share those common lipids, in differing concentrations. A notable difference is that the spectra from the advanced breeding line wheats on polished stainless steel had a greater adsorption for relatively the same volume than that of the Svevo specimens, followed by the absorption of N11 specimens.

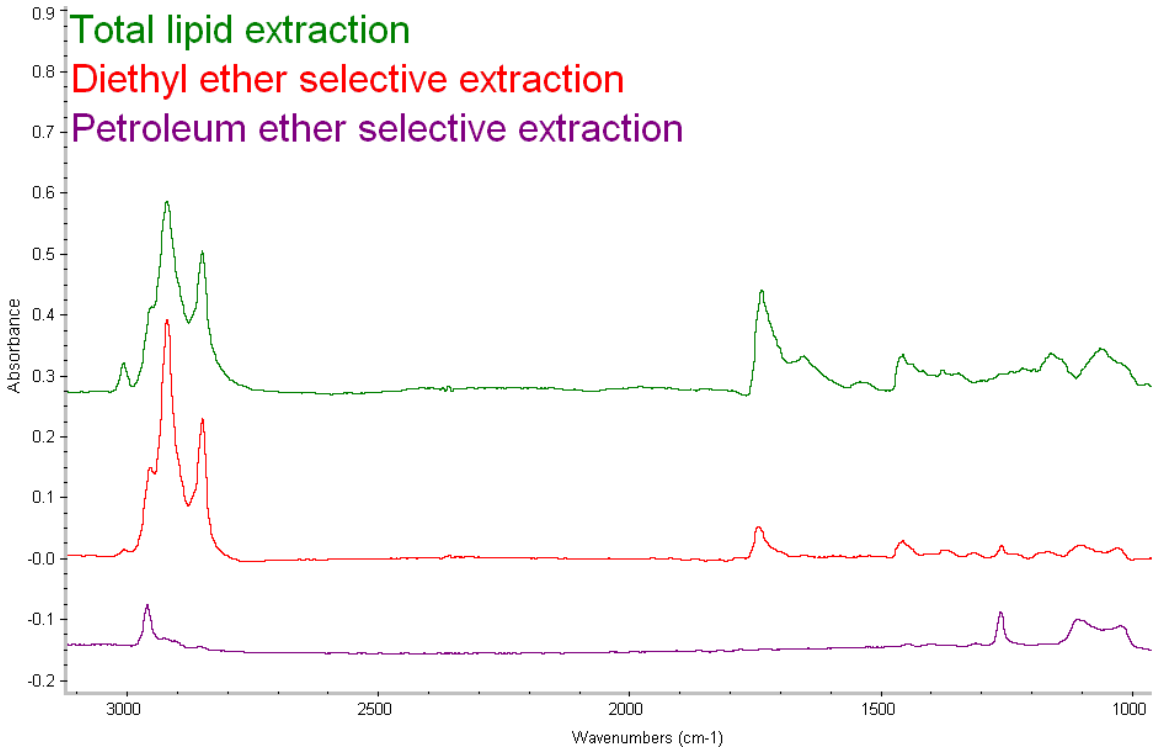

Figure 54: Nx05m4499_1 selective extraction. A large amount of lipid was carried in the rinses resulting in greater bands than seen in the parent wheat extracted spots.

3.4.3 Mass spectrometry applied to total lipid extract

This experiment was run under the same methods as the N11 and Svevo specimens. Nx05m4499_1 was analyzed to have 4.67 nmol/L diglycerides determined from a 0.400g endosperm sample. The majority of Nx05m4499_1 diglycerides were found in the 273 scan. The diglycerides of Nx05m4499_1 possess more short chain fatty acids than Arapahoe (2.82 nmol/L diglycerides determined from a 0.400g endosperm sample), whose fatty acid chains mainly have a mass to charge of 301. The advanced breeding line wheats are hard wheats, hexaploids, however the results of mass spectrometry, show the advanced breeding line wheats behaving as

the tetraploid, Svevo, results by the Nx05m4499_1 (waxy specimen) containing more triglycerides than the relative normal wheat specimen, Arapahoe. In the analysis triglycerides of Nx05m4499_1 were determined at 4.95 nmol/L while Arapahoe reported 3.75 nmol/L triglycerides determined from a 0.400g endosperm sample.

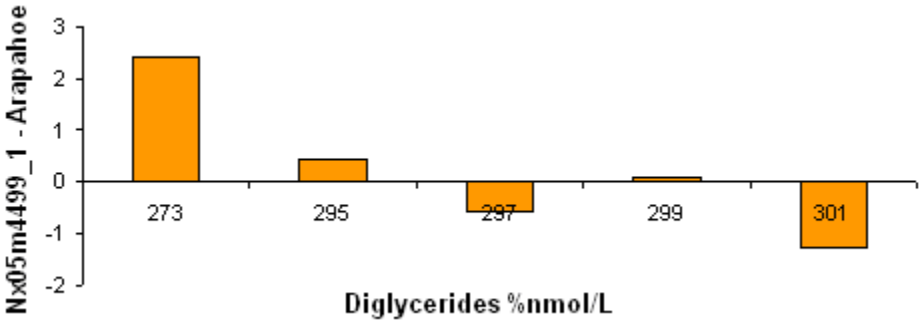

Figure 55: Summary of diglycerides mass spectrometric analysis. The x axis is the neutral molecule ion mass to charge scan in % nmol/L. The substrate parent results were subtracted from the waxy to provide the difference found on the y axis. (i.e. Nx05m4499_1 minus Arapahoe).

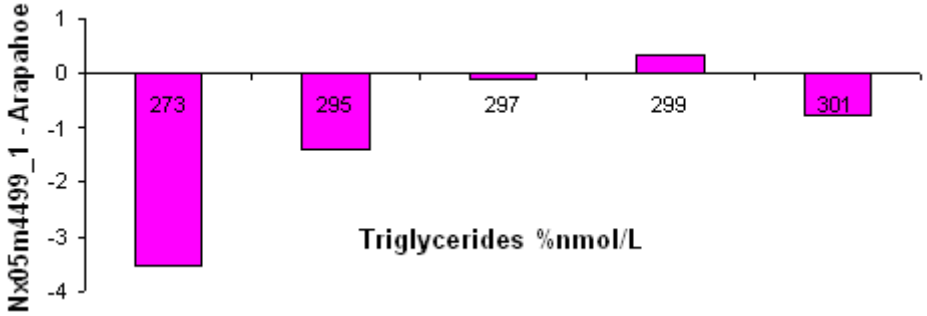

Figure 56: Summary of triglycerides mass spectrometric analysis. The x axis is the neutral molecule ion mass to charge scan in % nmol/L. The substrate parent results were subtracted from the waxy to provide the difference found on the y axis. (i.e. Nx05m4499_1 minus Arapahoe).

The advanced breeding line wheats are hard wheats, hexaploids, however the results of mass spectrometry, following the trend seen earlier, show the advanced breeding line wheat MS results behaving as the tetraploid's MS results. The Nx05m4499_1 (waxy specimen) contained more monogalactosyldiglycerides than digalactosyldiglycerides, in comparison to the relative parent specimen, Arapahoe. While Arapahoe, the parent normal wheat, had the more digalactosyldiglycerides at 36:4. The prominence of digalactosyldiglycerides (36:4) over monogalactosyldiglycerides (36:4) may not be due to the ploidity of the specimen, but perhaps environment or another factor not examined in this research. Many lipid classes present in the isogenic lipid profiles, show no observable differences between Nx05m4499_1 and Arapahoe as noted in figure 54. The total polar lipid (nmol/L) summary, found below, has an extremely low coefficient of variation, showing that the similarity of the mean to the samples was not very strong.

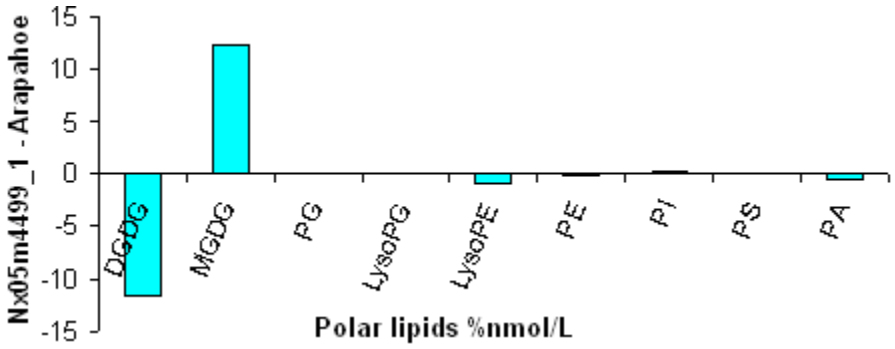

Figure 57: Summary of advanced breeding line wheat, polar lipid mass spectrometric analysis. The substrate parent results were subtracted from the waxy to provide the difference found on the y axis (i.e. Nx05m4499_1 minus Arapahoe).

Total Polar Lipid (nmol/L)			
	Mean	Range	CV (%)
Arapahoe	2.10	0.21	0.75
Nx05m4499_1	4.37	0 .43	2.32

Table 4: Summary of total polar lipid in nmol/L with mean, range and coefficient of variation reported.

CHAPTER 4 - Summary

Over 130 slices were produced for *in situ* microspectroscopic imaging to compare numerous contiguous pixels. Tens of thousands of spectra support the conclusion that a spectroscopic difference is observed between parent and waxy cultivar of the varieties analyzed (isogenic hard wheat, isogenic durum, and advanced breeding line relative wheats). Approximately, nine hundred kernels were hand milled to produce replicate total lipid extracts for FT-IR analysis and mass spectrometry. Both FT-IR analysis of extracts and mass spectrometry results support the conclusion that the total amount of both mildly and distinctly polar (digalactosyldiglycerides, monogalactosyldiglycerides, and phospholipids) lipids found in waxy are elevated, compared to the normal wheat for the hexaploid, tetraploid, and the advanced breeding line waxy specimens tested. Also, it was observed that all three specimen sets have different lipid class profiles and differing molecular compositions.

4.1.0 N11 genetic expression

In situ selective lipid extraction from individual sections of the isogenic N11 line was reported as resulting discriminating band reductions. The chloroform/methanol extraction as anticipated proved to be the most polar lipid removing solvent system, as the strongest lipid removal method. After extraction the N11 parent 1469 cm^{-1} band remained constant while for the N11 waxy sample, the CH bending absorption was reduced 26% after extraction in the most concentrated region. The N11 normal wheat, before and after extraction had no reduction for

either the 1740 cm^{-1} band or the 2930 cm^{-1} band area ratio. While the 1740 cm^{-1} band area ratio of N11 waxy before extraction was reduced by 50% in the most concentration region after extraction, there was no reduction of the 2930 cm^{-1} band area ratio via the same extraction.

The total lipid extract fractionated with selective solvent experiment results remained constant throughout the entire study, regardless of specimen analyzed. This consistency reinforces the band assignments that were made. Lipid class profiling was achieved. For all specimens analyzed, the petroleum ether rinse extracted hydrocarbon chains, the CH stretching evident by bands at 2927 cm^{-1}, 2855 cm^{-1}, and the CH bending absorption at 1469 cm^{-1}. Also the carbonyl band at 1740 cm^{-1} was present in the petroleum ether fractional extract. Unsaturated hydrocarbon groups, found in the nonpolar fraction, were also extracted as evidenced by the appearance of the 3015 cm^{-1} band. Diethyl ether extracted substances with absorption bands 2964 cm^{-1}, 1254 cm^{-1}, 1096 cm^{-1}, and 1014 cm^{-1}. In the diethyl ether fraction the 1254 cm^{-1} band reveals the P=O vibration of phospholipids and the 1090 cm^{-1} and 1014 cm^{-1} in the carbohydrate region indicate presence of the conjugated form as glycolipid.

Data from the partial waxy mutants displayed differing results for double null waxy wheat, exhibiting AB as a dominant combination, detectable via FT-IR microspectroscopy and mass spectrometry. In comparing the parent data to that of mutants missing the B gene there was an increase in lipid levels. Strong compositional influence from the inactive B allele was expected [32] and observed.

N11 waxy yielded a prominent diacylglycerol molecule ion with a mass to charge ratio of 610.5 and is majorly composed of long chain triglycerides. N11 waxy contains mainly diglycerides with fatty acid groups at 273 and 301, in comparison to the parent. The prominent lipid groups in the N11 normal wheat are monogalactosyldiglycerides (36:2) and

lysophosphatidylethanolamine (18:2). In addition, N11 normal wheat has more digalactosyldiglycerides than the N11 waxy.

4.2.0 Svevo genetic expression

In situ selective lipid extraction from individual sections of the durum isogenic Svevo line was reported in the same manner. The Svevo waxy was reduced by 20% from before extraction to after extraction. While the Svevo normal wheat and waxy wheat exhibited the same results before extraction to after extraction at the 1740 cm^{-1} band area ratio area reducing by approximately 20%. No reduction, for either specimen, was seen in a 2930 cm^{-1} band area ratio image.

Mass spectrometry of N11 waxy and Svevo waxy wheats total lipid extracts yielded the same prominent diacylglycerol molecule ion with a mass to charge ratio of 610.5. Both, N11 waxy and Svevo waxy contain primarily long chain triglycerides. Digalactosyldiglycerides (36:4) occur in a greater quantity in the Svevo waxy than in the Svevo normal wheat lipid profile. Svevo waxy has more monogalactosyldiglycerides (36:4) that the Svevo normal wheat. This distinction is completely opposite of what was found with the N11 isogenic line.

The Svevo waxy contains more diglycerides (predominantly as short chain fatty acids) than the Svevo normal wheat. While Svevo normal wheat consistently has more triglycerides than the Svevo waxy. Lastly, phosphatidic acid (36:4) was extremely abundant in the Svevo waxy sample.

4.3.0 Advanced breeding line genetic expression

Lipid profiles were produced for each specimen, providing quantitative and qualitative information on lipids shared in differing proportions to one another. The use of isogenic specimens removed the variables (i.e. maturation, environment, etc) that can sometimes overpower the genetic effects [4]. The Nx05m4499_1 and Arapahoe analyses provided the opportunity to test the method on wheat produced for eventual commerce, under normal field conditions. The advanced breeding line wheats were grown in different locations and under differing conditions; the Nx05m4499_1 and Arapahoe specimens were not expected to provide the same corresponding results. Results for the advanced breeding line wheats were similar to those of the tetraploid, Svevo, even though the advanced breeding line wheats selected for analysis are hexaploid, hard wheat.

4.4.0 Closing remarks

In all cases the model hexaploid, model tetraploid and advanced breeding line wheat, waxy specimens had a distinctly higher lipid content compared to their parent specimens. Availability of unique specimens of high genetic purity provided the opportunity to develop a model for exploration of lipid genetic expression via various molecular techniques. Use of a well documented model, intended to be used as a baseline in any corresponding study, held environmental and genetic variation to a constant minimum. Infrared microspectroscopy *in situ* readily discriminated waxy versus parent, while the broad distinction is seen in the total lipid content, the profile of lipid classes, and molecular composition within different classes provide the detail.

For future work, testing isogenic parent and waxy flours, not only central endosperm fractions, may provide a larger database. This was not an original intent of the project, only a speculated avenue of exploration. The low levels of bran contamination may point out additional lipid profile differentiation between isogenic waxy versus parent. Secondly, perhaps a stronger extraction could be employed to remove the lipids from inside the *in situ* specimen to provide a higher yield of lipid extract during *in situ* selective extraction. If slices of the kernel were extracted separately and the material captured, perhaps the classes of lipid would differ at kernel portion close to the germ, in comparison to the lipid classes, prominently around the kernel crease. For another project extension, hundreds of N11 parent, double null, single null and triple null would need to be obtained, endosperm and lipids individually extracted, and analyzed via FT-IR microspectroscopy and mass spectrometry. These spectra could be run statistically, for example in a multiple linear regression, to observe if any bands or peaks are predominately influential in an attempt to better explain the genetic expression exhibited in the single nulls.

References

1. R. N.Chibbar and M. Chakraborty. Specialty grains for foods and feeds, 2004, Ch 6, pgs.143-166.
2. S. Singh and G. S. Sethi. Expression of 17 rye (Secale cereal. L.) traits in a range of durum wheat (triticum durum Desf.) and bread wheat (T. aestivum L.) genetic backgrounds. *Euphytica.* 60:37-44,1992.
3. G. Boggini, M Cattaneo, C. Paganoni, and P. Vaccino. Genetic variation for waxy proteins and starch properties in Italian wheat germplasm. *Euphytica.* 119: 1-2 (113-116) 2001.
4. R. A. Graybosch. Waxy wheats: Origin, properties, and prospects. *Trend Food Sci.* 9:135-142, 1998.
5. S. Rama and B. Misha. Biochemical basis and molecular genetics of processing and nutritional quality traits of wheat. *J. Plant Biochem & Biotechn*. 17: 2 (111-126) 2008.
6. C. Ainsworth, J. Clark and J. Balsdon. Expression, organisation and structure of the genes encoding the waxy protein (granule-bound starch synthase) in wheat. *Plant Mol. Biol.* 22: 67-82, 1993.
7. K. Denyer, C. M. Hylton, C. F. Jenner, and A. M. Smith. Identification of multiple isoforms of soluble and granule-bound starch synthase in developing wheat endosperm. *Planta.* 196:256-265, 1995.
8. T. Yasui, J. Matsuki, T. Saski, and M. Yamamori. Amylose and lipid contents, amylopectin structure and gelatinization properties of waxy wheat (Triticum aesticum) starch. *J. Cereal Sci.* 24: 131-137, 1996.
9. A. M. Myers, M. K. Morell, M. G. James, and S. G. Ball. Recent progress toward understand biosynthesis of the amylopectin crystal. *Plant Physiol.* 122: 989-997, 2000.

10. C. S. Echt and D. Schwartz. Evidence for the inclusion of controlling elements within the structural gene at the waxy locus in maize. *Genetics.* 99: 275-284, 1981.
11. T. Nakamura, M. Yamamori, H Hirano and S. Hidaka.. Decrease of waxy (Wx) protein in two common wheat cultivars with low amylose content. Plant Breeding, September 1993b, vol. 111, no. 2, p. 99-105.
12. M. Yamaori, T. Nakamura, T. R. Endo, and T. Hagamine. Waxy protein deficiency and chromosomal location of coding genes in common wheat. *Theor. Appl. Genet.* 89: 179-184, 1994.
13. T. Nakamura, M. Yamamorim, and T.R. Endo. Waxy Protein deficiency and Chromosomal Location of Coding Genes in Common. *Theor. Appl. Genet*. 89: 2-3 (179-184) 1994.
14. H. Miura, S. Tanii, T.Nakamura, and N Watanabe, Genetic control of amylose content in wheat endosperm starch and differential effects of three Wx genes. *Theor. Appl.Gentic*. 89: 276-280, 1994
15. T. Demeke, P. Hucl, and R. N. Chibbar. Frequent Absence of GBSS 1 B Isoprotein in Endosperm Starch Of Canadian Wheat Cultivars. *Starch – Stärke*. 56: 8 (339 – 347) 2004.
16. A. M. Smith, K Denyer, and C. Martin. The synthesis of the starch granule. Annu. Rev. Plany. *Physicol Plant Mol Biol* .48: 67-87, 1997.
17. T. M. Giersch, J-M. Wu, L. Duncan, Z. Xiaochun, and J. Chin. Detection of mutations in the 7A allele of wheat (Triticum aestivum) granule-bound starch synthase (Wx-7A) with a monoclonal antibody produced by targeted peptide immunization. *J Cereal Sci.* 45:2 (162-171) 2007.
18. T. Nakamura, M. Yamamorim, H. Hiranoh, S. Hidaka, and T. Nagamine. Production of waxy (amylose-free) wheats. *Mol. & Gen Genet*. 248: 3 (253-259) 1995.
19. M. Bhattcharya, S. Erazo, D. C. Doehlert, M.S. Mcmullen. Staling of bread as affected by waxy wheat flour blends. *Cereal Chem*. 57:178-182, 1980

20. H. A. M. Wickramasinghe and H. Miura. Gene dosage effect of the wheat Wx alleles and their intersection on amylose synthesis in the endosperm. *Euphytica* 132:3 (303-310) 2003.
21. D. J. Manners. Recent developments in our understanding of amylopectin structure. *Carbohydr. Polym*., 11: 87-112, 1989.
22. M. J. Gidley, I. C. M. Dea, G. Eggleston and E. R. Morris. Structure and gelation of rhizobium capsular polysaccharide. *Carbohydr. Res.* 161: 291-304, 1987.
23. M. Kugimiya and J. W. Donovan. Calorimetric determination of the amylose content of starches based on formation and melting of the amylose-lysolecithin complex. *J. Food Sci.* 46: 765-771, 1981.
24. H. Dogan, V. W. Smail, and D. L.Wetzel. "Discrimination of Isogenic Wheat by InSb Focal Plane Array Chemical Imaging", *Vibr. Spectrosc*. 48:2 (189-195) 2008.
25. J. Murai, T. Taira, and D. Ohta. Isolation and characterization of the three Waxy genes encoding the granule-bound starch synthase in hexaploid wheat. *Gene*. 234: 1 (71-79) 1999.
26. N. Fujita and T. Taira. A 56-kDa protein is a novel granule-bound starch synthase existing in the pericarps, aleurone layers, and embryos of immature seed. in diploid wheat (Triticum monococcum L.). *Planta*. 207: 125-132,1998.
27. T. Nakamura, M. Yamamori, H. Hirano and S. Hidaka. Identification of three Wx proteins in wheat (Triticum aestivum L.). *Biochemical Genetic*. 31:1-2 (75-86) 1993.
28. S. Chao, P.J. Sharp, A. J. Worland, E.J. Warham, R.M.D. Koebar, and M. D. Gale. RFLP-based genetiic maps of wheat homoeologous group 7 chromosomes. *Theor Appl. Genet*. 78: 495-504, 1989.
29. W. Kim, J.W. Johnson, R.A. Graybosch, and C.S. Gaines. The Physicochemical properties and end use quality of wheat starch as a function of waxy protein alleles. *J. Cereal Sci*. 37:195-204, 2003.
30. R. Mishra, R. S. Baenziger, and W. K. Russell. Crossover interactions for grain yield in multienvironmental trials of winter wheat. *Crop Sci*. 46: 3 (1291-1298) 2006.

31. J. R. Clark, M. Robertson I, and C. C. Ainsworth. Nucleotide sequence of a wheat (Triticum aestivum L.) cDNA clone encoding the waxy protein. *Plant Molecular Biol.* 17: 957, 1991.

32. X. Shan, S. R. Clayshulte, S. D. Haley, and P. F. Byrne. Variation for glutenin and waxy alleles in the US hard winter wheat germplasm. *J. Cereal Sci.* 45: 199-208, 2007.

33. H. Miura, E. Araki, and S. Tarui. Amylose synthesis capacity of the three Wx genes of wheat cv. Chinese Spring. *Euphytica*. 108: 91–95, 1999.

34. R. A. Graybosch, C. J. Peterson, L. E. Hansen, S. Rahman, A. Hill, and J. H. Skerritt. Identification and Characterization of U.S. Wheats Carrying Null Alleles at the wx Loci. *Cereal Chem.* 75: 1 (162-165) 1998.

35. Communication to the editor. A starch granule protein associated with endosperm softness in wheat. *Cereal Chem.* 63:4 (379-380) 1986.

36. C. F. Morris. Puroindolines: the molecular genetic basis of wheat grain hardness. *Plant Mol Biol.* 48: 633-647, 2002.

37. T. Nakamura, P. Vrinten, M. Saito and M. Konda. Rapid classification of partial waxy wheats using PCR-based markers. *Genome*. 45: 6 (1150-1156) 2000.

38. P. Vrineten, T. Nakamura, and M. Yamamori. Molecular characterization of waxy mutations in wheat. *Mol. Gen. Genet*. 261: 463-471, 1999.

39. M. Chakraborty, K. Matkovic, D. G. Grier, E. L. Jarabek, W.A. Berzonsky , M. S. McMullen, and D. C. Doehlert. Physicochemical and Functional Properties of Tetraploid and Hexaploid Waxy Wheat Starch. *Starch – Stärke*. 56: 8 (339 – 347).

40. D. C. Doehlert, Edwin R. Duke and Leslie J. Smith. Effect of nitrogen supply on expression of some genes controlling storage proteins and carbohydrate synthesis in cultured maize kernels. *Plant Cell, Tissue and Organ Culture*. 47: 2, 1997.

41. K. F. Finney, W. T. Yamazaki, V.L. Youngs and G.L. Rubenthaler. Quality of Hard, Soft and Durum Wheats. In E.G. Heyne (ed.) Wheat and Wheat Improvement, 2nd Ed. Madison, WI: America Society of Agronomy, Crop Science Society of America, Soil Science Society of America, 1987.

42. R. Slingsby and R. Kiser. Sample treatment techniques and methodologies for ion chromatography. *TrAC Trends in Analytical Chemistry*. 20: 6-7 (288-295) 2001.

43. P. R. Griffiths and D. E. Henry Coupled Gas Chromatography and Fourier Transform Infrared Spectrometry. *Progress in Analytical Spectroscopy*. : 455-482, 1986.

44. Y. Pomeranz (a), and O. K. Chung. The lipid composition of a single wheat kernel and its structural parts. *Journal of Chromatography A*. 19: 540-550, 1965. Y. Pomeranz (b). Interaction Between Glycolipids and Wheat Flour Macromolecules in Breadmaking. Advances in Food Research, 20: 153-188, 1973.

45. T. N. Tweeten, D. L. Wetzel, and O. K. Chung. "Physicochemical Characterization of Galactosyldiglycerides and Their Quantitation in Wheat Flour Lipids by High Performance Liquid Chromatography", *J. of Am. Oil Chem. Soc*. 58: 6 (664-672) 1981.

46. M. Zhao. Ph.D. Dissertation, "Selective Supercritical Fluid Extraction of Wheat Flour Glycolipids and Their Determination by Supercritical Fluid Chromatography", Kansas State University, 1997.

47. F. S. Deschamps, K. Gaudin, and A. Baillet. Profiling Wheat digalactosyldiacylglycerol molecular species profiling using porous graphitic carbon stationary phase. *J. of Separation Science*. 27: 15-16 (1313-1322) 2004.

48. L. R. Brewer and D. L. Wetzel. "Phenotypic Expression in Wheat revealed using FT-IR Microspectroscopy" (AES no. 09-179-J Accepted Vibrational Spectroscopy) 2009

49. F. E. Dowell, E. B. Maghirang, and R. A. Graybosch. Selecting and Sorting Waxy Wheat Kernels Using Near-Infrared Spectroscopy. *Cereal Chem*. 86:3 (251-255) 2009.

50. E. N. C. Mills, M.L. Parker and N. Wellner. Chemical imaging: the distribution of ions and molecules in developing and mature wheat grain *J. Cereal Sci.* 41: 2 (193-201) 2005.

51. G. Guella, R. Frassanito, and I. Mancini. A new solution for an old problem: the regiochemical distribution of the acyl chains in galactolipids can be established by electrospray ionization tandem mass spectrometry. *Rapid Comm. In Mass Spec*. 17: 17 (1982-1994) 2003.

52. R. Welti, W. Li, M. Li, Y. Sang, H. Biesiada, H. Zhou, C. B. Rajashekar, T. D. Williams, and X. Wang. Profiling membrane lipids in plant stress responses: Role of phospholipase D{alpha} in freezing-induced lipid changes in Arabidopsis. *J. Biol. Chem*. 277: 31994-32002, 2002.

53. R. Welti, X. Wang, and T. D. Williams. Electrospray ionization tandem mass spectrometry scan modes for plant chloroplast lipids. *Anal. Biochem*. 314: 149-152, 2003.

54. A. M. Monari, M. C. Simeone, M. Urbano, B. Margiotta, and D. Lafiandra. Molecular characterization of new waxy mutants identified in bread and durum wheat. TAG Theor. & Appl. Genet. 110:8 (1481-1489) 2005.

55. D. Lafiandra, F. Sestili, A. Saliola Bucelli, M. Silvestri, and E. De Ambrogio. "Genetic modification of starch composition in wheat". Cereal science and technology for feeding ten billion people: genomics era and beyond. Zaragoza : CIHEAM-IAMZ / IRTA, 2008. p. 267-270.

56. L. R. Brewer and D. L. Wetzel. "FT-IR Microspectroscopic Imaging Provides Objective Chemically Defined Morphological Class Discrimination In Wheat". (In preparation) 2009.

57. N. B. Colthup, L. H Daly, and S.E. Wiberley. Introduction to Infrared and Raman Spectroscopy 3rd ed. 1975 Academic press.

58. R. J. Meier. Vibrational spectroscopy: a 'vanishing' discipline? *Chem. Society Reviews*. 34: 9 (743-752) 2005.

59. Infrared spectroscopy. In: Undergraduate Instrumental Analysis-6th edition. J.W. Robinson, E.M.S. Frame and G.M. Frame II (eds.). Marcel Dekker. 2005. New York, NY. pp 213-310.

60. Infrared microspectroscopy: Theory and Applications. Ed. R. G. Messerschmidt and M. A. Harthcock. Practical spectroscopy series, Vol 6.1998.

61. R. Bhargava and I. W. Levin. 2005. Spectrochemical analysis using infrared multichannel detectors. Blackwell Pub. Ames, IA.

62. D. L. Wetzel, 1995. Microbeam molecular spectroscopy of biological materials. In: Food Flavors: Generation, Analysis and Process Influence. G. Charalambous (ed.), Elsevier. Pgs 2039-2108.

63. D. L. Wetzel, "FT-IR Microscopic Imaging of Plant Material" Chapter 7, In (eds) Salzer, Reiner and Siesler, Heinz, Infrared and Raman Spectroscopy Imaging, Wiley, 2009.

64. Spectrum Spotlight User's Guide, 2001. Perkin Elmer Instruments. Prentice-Hall Inc, pp 1-12.

65. B. Brügger, G. Erben, R. Sandhoff, F. T. Wieland, and W. D. Lehmann. 1997. Quantitative analysis of biological membrane lipids at the low picomole level by nano-electrospray ionization tandem mass spectrometry. Proc. Natl. Acad. Sci. USA. 94, 2339-2344.

66. R. W. Kiser. Introduction to mass spectrometry and its applications. 1965. Prentice Hall, USA, pp 32-65, 140-160.

67. Applied Biosystems. API 4000 manual. http://www3.appliedbiosystems.com/cms/groups/psmsupport/documents/generaldocuments/cms_039341.pdf. Online May 01, 2009.

68. Mass Spectrometry diagrams. http://www.chemguide.co.uk/analysis/masspec/howitworks.html. Online January 15, 2009.

69. J. Bottier, J. Gean, and F. Artzner. Galactosyl headgroup interactions control the molecular packing of wheat lipids in Lahgmuir films and in hydrated liquid-crystalline mesophases. *Biochimica et Biophysica acta-biomembranes*. 1768: 6 (1526-1540) 2007.

70. Gzyl-Malcher, M. Filek, K. Makyla. Differences in surface behaviour of galactolipoids originating from different kind of wheat tissue cultivated in vitro. *Chem. & Phys. of Lipids*. 155: 1 (24-30) 2008.

71. D. L. Wetzel, P. Srivarin, and J. R. Finney. Revealing protein infrared spectral detail in a heterogeneous matrix dominated by starch. *Vibr. Spectrosc*. 31:109-114, 2003.

Appendix A - Genetic Expression in Wheat Revealed Using FT-IR Microspectroscopy

Wheat selected for cultivation through the centuries has a glume that is "soft" instead of "tough" as naturally occurring. In production, this is desirable because it enables mechanical threshing with efficient separation of kernel from the head of each stalk without damaging the kernel. FT-IR microspectroscopy provides chemically based, objective assessment of genetic expression by measuring the extent of specific expression. In the Microbeam Molecular Spectroscopy Laboratory, Manhattan, KS, a PerkinElmer Spectrum Spotlight 300 FT-IR microspectrometer was used to obtain spectral data from nine tough and eleven soft glume samples in a rectangular mapping pattern. With cellulose as the substrate, the extent of lignification is measurable from the ratio of the lignin (1508 cm^{-1}) baseline adjusted band area to the representation cellulousic (1370 cm^{-1}) band area. A distinction between soft and tough glumes is obtained in numerical terms. Using a band ratio minimizes variation due to thickness differences. While mapping microtomed sections of glume, care is taken to avoid tabulation of spectral data from vascular bundles. Inclusion of these data would bias the analysis toward the composition of highly lignified vascular bundles. Spatially resolved focal plane array FT-IR microspectroscopy reveals the extent of glume lignification that is coincident with the toughness trait. This enables breeders to objectively rank the genetic expression and discriminate between soft and tough breeding results.

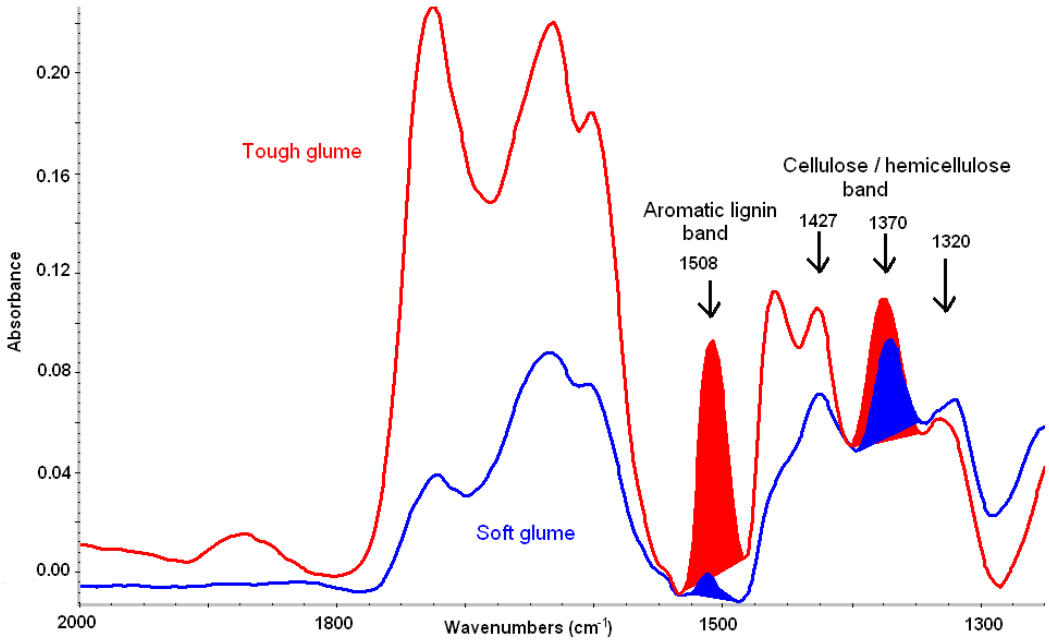

Figure A.1 A: Locating lignin and appropriate ratio band from maps. The ratio used as 1508/1370 cm^{-1}.

Appendix B - Microspectroscopic Imaging Provides Objective Chemically Defined Morphological Class Discrimination In Wheat

In the registry of new wheat varieties, a most important designation is the wheat class to which the new entry belongs. Hard wheat vs. soft wheat is classically assigned on the basis of subjective criteria, visual inspection, and functionality (how it performs for end use). At the time of registry, the pedigree is recorded. In commerce and during grain inspection, the pedigree is usually unknown. Transverse sections of wheat 4μm thick are imaged with an FT-IR MCT array instrument. FT-IR microspectroscopic focal plane array imaging of 4 μm thick transverse sections chemically defines botanical parts within the kernel. The prominence of the subaleurone endosperm in the hard wheat compared to the subaleurone endosperm of the soft wheat is one distinguishing feature. Irregular morphology found in nature complicates distinct measurement. However, the pixilated chemical image allows counting pixels within each row of an x,y map to provide a meaningful average. Also central endosperm multivariate spectroscopic features and chemometric characterization of the subaleurone endosperm are established. Each pixel is subsequently classified from multivariate processing of its spectrum. The kernel morphology is revealed by contrast and dimensions are established by counting the classified pixels. Imaging data is presented to show the utility of this objective approach to wheat classification.

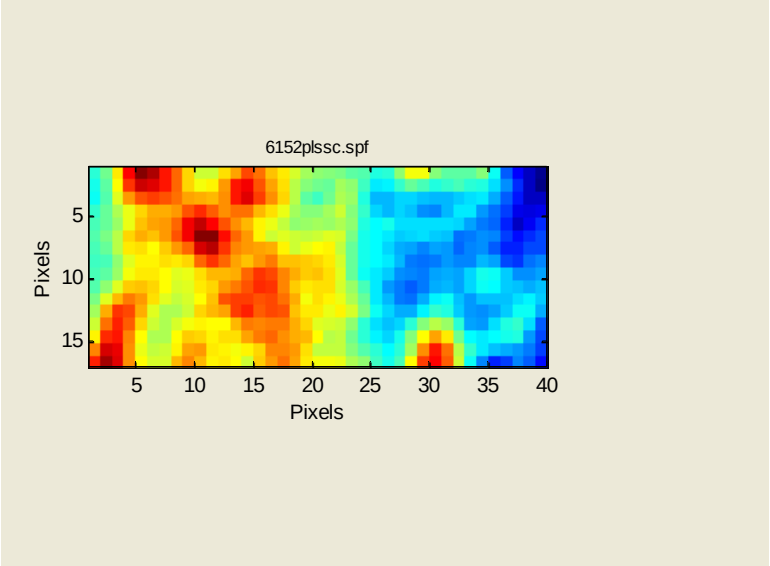

Figure B.2 A: PLS classification image, illustrating pixel counting across the subaleurone layer of a wheat kernel

Appendix C - Data of one microtomed slice

The following tables depict one microtomed slice of N11 waxy central endosperm at a band area ratio of 2927/1025 cm^{-1}, producing thousands of numerical data points. For each sample set, i.e. N11 waxy at 1740/1025 cm^{-1}, at least five slices were used in every *in situ* calculation.

0	-3016.103	-3009.853	-3003.603	-2997.353	-2991.103	-2984.853	-2978.603	-2972.353	-2966.103	-2959.853	-2953.603	-2947.353	-2941.103	-2934.853
-2286.68	1.14E-01	1.25E-01	1.30E-01	1.15E-01	1.12E-01	1.18E-01	1.21E-01	1.20E-01	1.11E-01	1.15E-01	1.14E-01	1.09E-01	1.08E-01	1.08E-01
-2292.93	1.14E-01	1.22E-01	1.31E-01	1.19E-01	1.09E-01	1.15E-01	1.20E-01	1.14E-01	1.12E-01	1.11E-01	1.10E-01	1.01E-01	9.81E-02	1.08E-01
-2299.18	1.16E-01	1.18E-01	1.21E-01	1.19E-01	1.12E-01	1.14E-01	1.14E-01	1.07E-01	1.03E-01	1.06E-01	1.06E-01	1.02E-01	1.09E-01	1.12E-01
-2305.43	1.20E-01	1.20E-01	1.16E-01	1.20E-01	1.17E-01	1.12E-01	1.07E-01	1.06E-01	1.06E-01	1.10E-01	1.11E-01	1.09E-01	1.06E-01	1.15E-01
-2311.68	1.15E-01	1.21E-01	1.13E-01	1.20E-01	1.21E-01	1.17E-01	1.07E-01	1.02E-01	1.05E-01	1.10E-01	1.11E-01	1.13E-01	1.01E-01	1.09E-01
-2317.93	1.16E-01	1.18E-01	1.11E-01	1.16E-01	1.19E-01	1.17E-01	1.08E-01	1.05E-01	1.08E-01	1.08E-01	1.06E-01	1.06E-01	9.60E-02	9.01E-02
-2324.18	1.15E-01	1.14E-01	1.10E-01	1.11E-01	1.14E-01	1.13E-01	1.10E-01	1.10E-01	1.10E-01	1.06E-01	1.05E-01	1.04E-01	9.96E-02	9.69E-02
-2330.43	1.17E-01	1.17E-01	1.12E-01	1.14E-01	1.13E-01	1.16E-01	1.18E-01	1.15E-01	1.13E-01	1.09E-01	1.07E-01	1.08E-01	1.07E-01	1.09E-01
-2342.93	1.12E-01	1.15E-01	1.17E-01	1.19E-01	1.18E-01	1.15E-01	1.12E-01	1.12E-01	1.13E-01	1.16E-01	1.20E-01	1.23E-01	1.20E-01	1.21E-01
-2349.18	1.23E-01	1.24E-01	1.25E-01	1.23E-01	1.21E-01	1.17E-01	1.13E-01	1.13E-01	1.15E-01	1.16E-01	1.18E-01	1.22E-01	1.25E-01	1.19E-01
-2355.43	1.34E-01	1.36E-01	1.33E-01	1.29E-01	1.24E-01	1.21E-01	1.18E-01	1.22E-01	1.19E-01	1.16E-01	1.16E-01	1.16E-01	1.17E-01	1.18E-01
-2361.68	1.38E-01	1.35E-01	1.29E-01	1.27E-01	1.26E-01	1.23E-01	1.28E-01	1.33E-01	1.28E-01	1.11E-01	1.11E-01	1.15E-01	1.16E-01	1.15E-01
-2367.93	1.35E-01	1.29E-01	1.23E-01	1.19E-01	1.17E-01	1.21E-01	1.25E-01	1.28E-01	1.23E-01	1.12E-01	1.09E-01	1.12E-01	1.13E-01	1.14E-01
-2374.18	1.34E-01	1.30E-01	1.25E-01	1.16E-01	1.12E-01	1.14E-01	1.15E-01	1.15E-01	1.11E-01	1.11E-01	1.10E-01	1.12E-01	1.14E-01	1.14E-01
-2386.68	1.24E-01	1.56E-01	1.45E-01	1.29E-01	1.16E-01	1.15E-01	1.15E-01	1.17E-01	1.13E-01	1.12E-01	1.09E-01	1.15E-01	1.14E-01	1.17E-01
-2392.93	7.19E-02	1.07E-01	1.32E-01	1.34E-01	1.28E-01	1.30E-01	1.19E-01	1.20E-01	1.14E-01	1.13E-01	1.14E-01	1.19E-01	1.22E-01	1.24E-01

average	0.107669
stdev	0.015009
max	0.156283
min	0.030803

-2928.603	-2922.353	-2916.103	-2909.853	-2903.603	-2897.353	-2891.103	-2884.853	-2878.603	-2872.353	-2866.103	-2859.853	-2853.603	-2847.353	-2841.103
1.11E-01	1.18E-01	1.16E-01	1.05E-01	1.01E-01	1.01E-01	1.01E-01	1.06E-01	1.09E-01	1.05E-01	1.05E-01	1.08E-01	1.10E-01	1.15E-01	1.17E-01
1.11E-01	1.15E-01	1.17E-01	1.09E-01	1.06E-01	1.01E-01	1.03E-01	1.09E-01	1.08E-01	1.04E-01	1.08E-01	1.10E-01	1.15E-01	1.17E-01	1.17E-01
1.14E-01	1.14E-01	1.04E-01	9.38E-02	9.84E-02	1.02E-01	1.10E-01	1.11E-01	1.12E-01	1.11E-01	1.13E-01	1.11E-01	1.17E-01	1.17E-01	1.20E-01
1.14E-01	1.16E-01	1.03E-01	9.03E-02	9.31E-02	1.03E-01	1.08E-01	1.19E-01	1.15E-01	1.13E-01	1.11E-01	1.13E-01	1.12E-01	1.13E-01	1.09E-01
1.15E-01	1.13E-01	1.07E-01	9.71E-02	9.51E-02	9.87E-02	1.01E-01	1.10E-01	1.15E-01	1.12E-01	1.05E-01	1.06E-01	1.10E-01	1.11E-01	1.07E-01
9.72E-02	1.03E-01	1.05E-01	1.03E-01	1.01E-01	9.23E-02	9.22E-02	1.03E-01	1.09E-01	1.08E-01	1.04E-01	1.05E-01	1.07E-01	1.08E-01	1.09E-01
1.00E-01	1.03E-01	1.06E-01	1.12E-01	1.03E-01	8.91E-02	7.49E-02	7.37E-02	8.00E-02	9.04E-02	1.02E-01	1.04E-01	1.04E-01	1.04E-01	1.11E-01
1.07E-01	1.15E-01	1.17E-01	1.10E-01	1.00E-01	8.50E-02	5.03E-02	3.83E-02	6.07E-02	8.28E-02	9.52E-02	1.07E-01	1.07E-01	1.05E-01	1.09E-01
1.19E-01	1.08E-01	1.00E-01	1.06E-01	1.12E-01	7.81E-02	4.00E-02	3.08E-02	5.62E-02	9.01E-02	1.02E-01	1.10E-01	1.07E-01	1.03E-01	1.01E-01
1.15E-01	1.10E-01	1.09E-01	1.09E-01	1.13E-01	1.08E-01	7.96E-02	5.52E-02	6.25E-02	1.00E-01	1.09E-01	1.13E-01	1.11E-01	1.09E-01	1.06E-01
1.13E-01	1.10E-01	1.11E-01	1.13E-01	1.15E-01	1.12E-01	1.12E-01	9.53E-02	9.28E-02	1.10E-01	1.13E-01	1.12E-01	1.10E-01	1.11E-01	1.11E-01
1.09E-01	1.07E-01	1.10E-01	1.09E-01	1.10E-01	1.18E-01	1.16E-01	1.13E-01	1.07E-01	9.87E-02	1.02E-01	1.07E-01	1.06E-01	1.05E-01	1.06E-01
1.11E-01	1.08E-01	1.04E-01	1.04E-01	1.10E-01	1.11E-01	1.18E-01	1.11E-01	1.06E-01	9.74E-02	1.01E-01	1.06E-01	1.08E-01	1.00E-01	9.89E-02
1.14E-01	1.09E-01	1.07E-01	1.09E-01	1.10E-01	1.12E-01	1.18E-01	1.13E-01	1.08E-01	1.05E-01	1.07E-01	1.02E-01	1.02E-01	9.41E-02	9.27E-02
1.17E-01	1.14E-01	1.12E-01	1.14E-01	1.12E-01	1.15E-01	1.17E-01	1.11E-01	1.09E-01	1.11E-01	1.09E-01	1.09E-01	1.03E-01	9.74E-02	8.94E-02
1.23E-01	1.16E-01	1.13E-01	1.14E-01	1.15E-01	1.17E-01	1.12E-01	1.07E-01	1.09E-01	1.12E-01	1.08E-01	1.06E-01	9.80E-02	9.16E-02	1.09E-01

-2834.853	-2828.603	-2822.353	-2816.103	-2809.853	-2803.603	-2797.353	-2791.103	-2784.853	-2778.603	-2772.353	-2766.103	-2759.853	-2753.603	-2747.353	-2741.103
1.06E-01	7.41E-02	9.79E-02	1.05E-01	1.13E-01	6.00E-02	9.30E-02	1.04E-01	1.10E-01	1.10E-01	1.10E-01	1.11E-01	1.14E-01	1.11E-01	1.14E-01	1.16E-01
1.14E-01	8.76E-02	6.59E-02	9.89E-02	1.14E-01	1.19E-01	8.05E-02	8.60E-02	9.54E-02	1.08E-01	1.15E-01	1.13E-01	1.14E-01	1.11E-01	1.12E-01	1.17E-01
1.20E-01	1.01E-01	6.98E-02	3.68E-02	1.14E-01	3.66E-02	5.40E-02	7.27E-02	8.43E-02	1.06E-01	1.15E-01	1.14E-01	1.14E-01	1.11E-01	1.16E-01	1.20E-01
1.15E-01	1.08E-01	7.84E-02	6.16E-02	5.05E-02	1.15E-01	3.45E-02	5.06E-02	7.95E-02	9.89E-02	1.16E-01	1.18E-01	1.17E-01	1.18E-01	1.16E-01	1.17E-01
1.10E-01	1.08E-01	9.73E-02	8.99E-02	8.34E-02	6.13E-02	4.07E-02	3.54E-02	7.35E-02	1.10E-01	1.23E-01	1.19E-01	1.17E-01	1.16E-01	1.14E-01	1.14E-01
1.08E-01	1.11E-01	1.10E-01	1.04E-01	9.15E-02	7.53E-02	5.99E-02	5.25E-02	7.01E-02	1.03E-01	1.08E-01	1.07E-01	1.11E-01	1.12E-01	1.13E-01	1.14E-01
1.10E-01	1.11E-01	1.14E-01	1.13E-01	9.87E-02	8.79E-02	7.47E-02	7.36E-02	7.61E-02	9.06E-02	9.93E-02	1.02E-01	1.10E-01	1.11E-01	1.13E-01	1.14E-01
1.13E-01	1.12E-01	1.11E-01	1.12E-01	1.15E-01	1.08E-01	9.69E-02	8.66E-02	7.87E-02	7.18E-02	8.69E-02	1.05E-01	1.14E-01	1.17E-01	1.14E-01	1.13E-01
1.00E-01	8.38E-02	8.71E-02	1.03E-01	1.15E-01	1.19E-01	1.11E-01	9.97E-02	9.93E-02	9.61E-02	1.13E-01	1.17E-01	1.18E-01	1.07E-01	1.00E-01	1.02E-01
1.02E-01	9.31E-02	9.13E-02	9.92E-02	1.13E-01	1.18E-01	1.14E-01	1.11E-01	1.13E-01	1.15E-01	1.15E-01	1.16E-01	1.18E-01	1.16E-01	1.05E-01	1.06E-01
1.12E-01	9.95E-02	8.89E-02	8.91E-02	1.05E-01	1.13E-01	1.19E-01	1.16E-01	1.18E-01	1.13E-01	1.16E-01	1.18E-01	1.19E-01	1.21E-01	1.20E-01	1.09E-01
1.08E-01	1.08E-01	8.58E-02	7.97E-02	9.34E-02	1.11E-01	1.21E-01	1.16E-01	1.16E-01	1.14E-01	1.20E-01	1.17E-01	1.20E-01	1.21E-01	1.18E-01	1.13E-01
9.98E-02	1.06E-01	1.04E-01	9.21E-02	8.90E-02	1.03E-01	1.17E-01	1.15E-01	1.13E-01	1.16E-01	1.18E-01	1.18E-01	1.12E-01	1.06E-01	9.99E-02	9.52E-02
9.79E-02	1.02E-01	1.07E-01	1.08E-01	1.02E-01	1.01E-01	1.10E-01	1.14E-01	1.19E-01	1.18E-01	1.18E-01	1.12E-01	1.11E-01	1.03E-01	8.72E-02	7.06E-02
8.46E-02	9.61E-02	1.10E-01	1.14E-01	1.14E-01	1.06E-01	1.05E-01	1.10E-01	1.14E-01	1.17E-01	1.15E-01	1.11E-01	1.14E-01	1.14E-01	1.04E-01	8.54E-02
9.76E-02	1.03E-01	1.13E-01	1.14E-01	1.05E-01	1.02E-01	1.03E-01	1.06E-01	1.12E-01	1.13E-01	1.13E-01	1.10E-01	1.15E-01	1.17E-01	1.17E-01	1.12E-01

Appendix D - Kansas LRC Protocols: Extraction of lipids from animal tissue

Use glass tubes with Teflon-lined screw caps.

To 0.8 parts cells/tissue (homogenized; see below) in aqueous solution, add 1 part chloroform and 2 parts methanol. Shake well, add 1 part chloroform and 1 part water. Shake, centrifuge at low speed for 5-10 min. Remove the lower layer. Add 1 part chloroform, shake, centrifuge, remove the lower layer. Add 1 part chloroform, shake, centrifuge, remove the lower layer. Wash **the combined lower layers** once with a small volume 1 M KCl and once with a small volume of water.

Appendix E - Diacylglycerols Summary (in percent)

DAG 273			N11 wheat		N11 waxy		Svevo		Svevo waxy		Advanced breeding line	
Sample description	**Masses**	**Formula**	**average**	**std**	**average**	**std**	**average**	**std**	**average**	**std**	**Arapahoe**	**Nx05m4499-1**
32:00:00	586.5	**C35H72O5N**	5.50	0.32	9.20	0.73	6.19	0.32	5.24	0.12	14.14	16.03
34:03:00	608.5	**C37H70O5N**	2.34	0.11	2.34	0.38	3.33	0.15	4.78	0.12	2.31	2.53
34:02:00	610.5	**C37H72O5N**	78.41	0.53	77.43	0.59	79.20	0.13	80.84	0.01	63.84	68.87
34:01:00	612.6	**C37H74O5N**	10.12	0.06	8.92	0.65	10.14	0.18	7.99	0.30	10.70	5.99
total 273 DAGS												

DAG 295			n11 wheat		n11 waxy		Svevo		Svevo waxy		advanced breeding line	
Sample description	**Masses**	**Formula**	**average**	**std**	**average**	**std**	**average**	**std**	**average**	**std**	**Arapahoe**	**Nx05m4499-1**
1.4188	608.5	**C37H70O5N**	24.84	0.68	25.14	0.07	30.65	0.31	38.16	2.86	12.92	16.74
1.5035	632.5	**C39H70O5N**	23.27	1.12	23.85	0.93	26.09	1.08	23.01	3.22	25.57	29.21
1.5028	634.5	**C39H72O5N**	49.75	0.55	48.97	0.96	37.32	2.19	34.87	0.25	60.02	52.99
total 295 DAGS												

DAG 297

Sample no.			N11 wheat		N11 waxy		Svevo		Svevo waxy		Advanced breeding line	
Sample description	**Masses**	**Formula**	**average**	**std**	**average**	**std**	**average**	**std**	**average**	**std**	**Arapahoe**	**Nx05m4499-1**
1.4181	610.5	**C37H72O5N**	58.74	0.01	56.03	0.66	57.94	0.31	62.75	0.86	39.48	42.91
1.5028	634.5	**C39H72O5N**	30.52	0.11	33.20	0.47	28.08	0.56	26.59	0.92	43.53	44.81
1.5021	636.6	**C39H74O5N**	7.18	0.10	7.38	0.05	7.58	0.58	5.69	0.11	12.57	7.95
1.5014	638.6	**C39H76O5N**	2.27	0.10	1.75	0.01	4.56	0.40	3.05	0.11	2.66	2.00
total 297 DAGS												

DAG 299			N11 wheat		N11 waxy		Svevo		Svevo waxy		Advanced breeding line	
Sample description	**Masses**	**Formula**	**average**	**std**	**average**	**std**	**average**	**std**	**average**	**std**	**Arapahoe**	**Nx05m4499-1**
1.4174	612.6	**C37H74O5N**	35.21	0.57	31.43	1.81	31.81	1.01	38.15	2.27	22.30	26.01
1.5028	634.5	**C39H72O5N**	10.44	0.24	12.34	0.39	11.23	1.12	12.32	0.29	12.64	18.90
1.5021	636.6	**C39H74O5N**	34.75	0.36	34.21	0.10	32.60	0.40	32.85	0.16	44.38	42.50
1.5014	638.6	**C39H76O5N**	15.56	0.46	18.31	1.20	20.19	0.41	12.82	1.87	17.89	9.87
total 299 DAGS												

DAG 301	N11 wheat	N11 waxy	Svevo	Svevo waxy	Advanced breeding line

Sample description	Masses	Formula	average	std	average	std	average	std	average	std	Arapahoe	Nx05m4499-1
1.334	584.5	**C35H70O5N**	12.23	1.14	9.78	0.72	1.80	1.28	3.92	0.88	0.00	0.00
1.4174	612.6	**C37H74O5N**	13.21	1.47	8.80	0.79	2.13	0.37	3.34	0.56	0.59	0.00
1.5021	636.6	**C39H74O5N**	3.03	0.77	4.02	0.37	3.91	0.54	5.73	0.01	8.64	7.69
1.5014	638.6	**C39H76O5N**	54.59	1.33	58.50	0.38	77.11	0.50	75.98	2.51	70.58	83.87
1.5007	640.6	**C39H78O5N**	14.14	2.57	17.47	0.32	14.14	0.27	10.00	1.25	19.14	6.13
total 301 DAGS												

Appendix F - Triacylglycerols Summary (in percent)

TAG 273			N11 wheat		N11 waxy		Svevo		Svevo waxy		Advanced breeding line	
Sample description	**Masses**	**Formula**	**average**	**std**	**average**	**std**	**average**	**std**	**average**	**std**	**Arapahoe**	**Nx05m4499-1**
50:02:00	848.8	**C53H102O6N**	25.50	0.89	36.38	1.11	26.20	0.89	35.87	0.20	31.00	40.69
50:01:00	850.8	**C53H104O6N**	7.28	0.29	7.97	0.12	7.45	0.72	6.42	0.34	9.00	8.33
52:05:00	870.8	**C55H100O6N**	4.66	0.48	3.38	0.26	5.93	0.05	6.00	0.24	2.88	3.30
52:04:00	872.8	**C55H102O6N**	39.31	1.08	30.56	1.15	39.38	0.31	34.18	0.65	30.48	27.55
52:03:00	874.8	**C55H104O6N**	11.47	0.47	7.85	0.20	10.93	0.79	7.48	0.40	14.41	8.59
52:02:00	876.8	**C55H106O6N**	5.09	0.22	3.82	0.02	5.37	0.22	3.63	0.11	6.91	2.69
TAG total 273												

TAG 295			N11 wheat		N11 waxy		Svevo		Svevo waxy		Advanced breeding line	
Sample description	**Masses**	**Formula**									**Arapahoe**	**Nx05m4499-1**
50:03:00	846.8	**C53H100O6N**	3.88	0.11	6.38	2.80	4.97	0.79	5.58	0.07	5.21	6.56
52:05:00	870.8	**C55H100O6N**	31.20	1.78	32.75	0.13	32.23	0.68	35.66	1.31	23.41	28.31
52:04:00	872.8	**C55H102O6N**	24.11	1.47	26.16	2.99	20.74	0.19	19.58	0.97	23.81	22.60
54:07:00	894.8	**C57H100O6N**	19.65	0.53	18.27	0.02	19.42	1.98	20.35	0.68	23.82	22.93
54:06:00	896.8	**C57H102O6N**	11.99	1.35	9.14	0.77	11.37	0.38	7.95	0.25	12.85	10.44
54:05:00	898.8	**C57H104O6N**	4.83	1.33	4.31	0.70	5.26	0.40	4.61	0.67	7.79	4.63
TOTAL 295 TAG												

TAG 297			N11 wheat		N11 waxy		Svevo		Svevo waxy		Advanced breeding line	
Sample description	**Masses**	**Formula**									**Arapahoe**	**Nx05m4499-1**
50:02:00	848.8	**C53H102O6N**	8.41	0.17	15.95	0.01	7.95	0.04	13.31	0.13	13.11	17.16
52:04:00	872.8	**C55H102O6N**	38.32	1.12	37.90	0.47	35.35	0.58	38.53	1.40	27.85	31.97
52:03:00	874.8	**C55H104O6N**	9.30	0.36	8.22	0.24	9.23	0.07	7.61	0.76	10.98	8.06
54:07:00	894.8	**C57H100O6N**	2.81	0.21	2.53	0.02	4.30	0.02	3.85	0.13	2.79	3.52
54:06:00	896.8	**C57H102O6N**	22.76	0.37	20.72	0.61	22.62	0.55	19.25	0.64	23.70	24.05
54:05:00	898.8	**C57H104O6N**	7.82	0.10	5.88	0.04	8.38	0.04	6.00	0.26	11.69	7.35
54:04:00	900.8	**C57H106O6N**	3.40	0.11	2.43	0.23	4.44	0.26	3.17	0.02	4.58	2.47
TOTAL 297 TAGS												

TAG 299	N11 wheat	N11 waxy	Svevo	Svevo waxy	Advanced breeding line

Sample description	Masses	Formula									Arapahoe	Nx05m4499-1
50:01:00	850.8	**C53H104O6N**	5.61	0.26	10.17	0.17	4.21	0.25	7.24	1.43	6.07	9.13
52:04:00	872.8	**C55H102O6N**	4.73	0.35	4.88	0.54	5.13	0.14	6.48	0.43	3.07	5.69
52:03:00	874.8	**C55H104O6N**	24.78	0.26	26.31	0.02	23.43	0.09	28.35	0.20	22.51	26.42
52:02:00	876.8	**C55H106O6N**	15.97	0.40	15.43	0.30	14.27	0.85	13.11	1.00	16.63	12.14
54:06:00	896.8	**C57H102O6N**	3.49	0.21	3.30	0.06	4.51	0.57	4.74	0.37	3.37	5.02
54:05:00	898.8	**C57H104O6N**	18.46	0.56	16.68	0.40	20.46	0.01	19.07	0.36	23.21	24.49
54:04:00	900.8	**C57H106O6N**	11.14	0.37	8.65	0.52	14.42	0.03	10.22	0.32	15.03	10.15
54:03:00	902.8	**C57H108O6N**	8.88	0.06	9.65	0.57	8.62	0.14	6.39	1.32	6.85	4.06

TOTAL TAGS 299

TAG 301 **N11 wheat** **N11 waxy** **Svevo** **Svevo waxy** **Advanced breeding line**

Sample description	Masses	Formula									Arapahoe	Nx05m4499-1
52:02:00	876.8	**C55H106O6N**	37.58	2.65	42.55	5.31	35.04	0.80	44.88	1.50	37.09	44.38
54:05:00	898.8	**C57H104O6N**	3.22	0.73	1.79	0.89	4.89	0.54	4.90	0.95	2.64	4.13
54:04:00	900.8	**C57H106O6N**	25.47	2.62	30.00	0.23	34.76	2.35	28.23	1.00	39.20	35.71
54:03:00	902.8	**C57H108O6N**	11.89	0.39	8.98	0.01	11.18	1.19	8.39	0.44	13.36	11.38
54:02:00	904.8	**C57H110O6N**	12.73	1.32	11.92	3.88	8.36	3.65	5.13	0.27	5.53	1.45

TOTAL TAGS 301

Appendix G - Neutral Lipids Summary (in percent)

Sample no.			N11 wheat		N11 waxy		Svevo		Svevo waxy		Advanced breeding line	
Sample description	**Masses of ions**	**Chemical formula**	**average**	**std**	**average**	**Std**	**average**	**std**	**average**	**std**	**Arapahoe**	**Nx05m4499-1**
DGDG 34:2	**934.6**	**C49H92O15N**	6.085	0.021	6.417	0.175	6.739	0.084	5.955	0.412	6.113	5.824
DGDG 36:5	**956.6**	**C51H90O15N**	5.2	0.355	6.363	0.013	9.127	0.308	7.779	0.187	5.763	5.268
DGDG 36:4	**958.6**	**C51H92O15N**	34.463	1.112	38.773	0.068	34.075	0.544	29.357	1.558	45.387	37.834
DGDG 36:3	**960.7**	**C51H94O15N**	3.203	0.011	3.336	0.138	3.612	0.162	2.859	0.002	5.464	3.091
***Total DGDG**			***52.424***	***1.614***	***58.514***	***0.179***	***59.74***	***1.056***	***50.469***	***2.14***	***67.21***	***55.716***
MGDG 36:5	**794.6**	**C45H80O10N**	4.155	0.22	3.937	0.078	4.47	0.139	6.885	0.369	2.559	4.309
MGDG 36:4	**796.6**	**C45H82O10N**	32.116	0.585	29.88	0.072	21.785	0.551	28.684	1.924	22.285	32.38
***Total MGDG**			***40.369***	***0.755***	***37.784***	***0.204***	***29.957***	***0.897***	***39.555***	***2.249***	***28.565***	***40.946***
PG 34:2	764.5	**C40H79O10PN**	0.474	0.087	0.629	0.028	0.703	0.021	1.383	0.16	0.211	0.204
***Total PG**			***0.956***	***0.141***	***1.139***	***0.035***	***1.252***	***0.018***	***2.57***	***0.288***	***0.274***	***0.291***
lysoPG 18:3	**505.3**	**C24H42O9P**	0.026	0.004	0.005	0.004	0.033	0.008	0.009	0.013	0	0
***Total lysoPG**			***0.035***	***0.008***	***0.032***	***0.001***	***0.07***	***0.015***	***0.065***	***0.018***	***0***	***0***
LysoPE 16:1	452.3	**C21H43O7PN**	0.004	0.001	0.001	0.001	0.003	0.003	0.002	0.003	0.005	0.001
LysoPE 16:0	454.3	**C21H45O7PN**	0.644	0.059	0.677	0.055	1.119	0.062	0.753	0.035	0.525	0.457
LysoPE 18:3	476.3	**C23H43O7PN**	0.067	0.006	0.028	0.001	0.211	0.013	0.043	0.007	0.05	0.033
LysoPE 18:2	478.3	**C23H45O7PN**	1.826	0.166	0.791	0.007	3.979	0.091	1.239	0.19	1.846	1.133
LysoPE 18:1	480.3	**C23H47O7PN**	0.112	0.009	0.093	0.002	0.229	0.035	0.104	0.033	0.15	0.05
***total LysoPE**			***2.652***	***0.227***	***1.589***	***0.065***	***5.54***	***0.022***	***2.14***	***0.192***	***2.576***	***1.675***
PE 34:3	714.5	**C39H73O8PN**	0.003	0.001	0	0	0.003	0.003	0.006	0.006	0.001	0.001
PE 34:2	716.5	**C39H75O8PN**	0.118	0.007	0.138	0.017	0.193	0.001	0.24	0.073	0.128	0.095
PE 34:1	718.5	**C39H77O8PN**	0.013	0.008	0.004	0.003	0.019	0.004	0.015	0.002	0.005	0.005
PE 36:5	738.5	**C41H73O8PN**	0.01	0.001	0.005	0	0.03	0.004	0.034	0.017	0.02	0.017
PE 36:4	740.5	**C41H75O8PN**	0.184	0.003	0.146	0.003	0.467	0.027	0.435	0.119	0.231	0.215
PE 36:3	742.5	**C41H77O8PN**	0.043	0.002	0.029	0.001	0.106	0.021	0.065	0.018	0.039	0.027
PE 36:2	744.6	**C41H79O8PN**	0.013	0.007	0.006	0.003	0.03	0.009	0.024	0.011	0.012	0.001
PE 40:2	800.6	**C45H87O8PN**	0.017	0.004	0.017	0.003	0.031	0.003	0.029	0.002	0.028	0.01
PE 42:2	828.6	**C47H91O8PN**	0.012	0.004	0.01	0.003	0.021	0.004	0.026	0.001	0.014	0
***total PE**			***0.418***	***0.023***	***0.361***	***0.014***	***0.902***	***0.066***	***0.885***	***0.252***	***0.483***	***0.371***
PI 32:2	824.5	**C41H79O13PN**	0.001	0	0	0	0.001	0	0.002	0.003	0	0
PI 32:1	826.5	**C41H81O13PN**	0.001	0	0	0	0.002	0.001	0.002	0.003	0	0
PI 32:0	828.6	**C41H83O13PN**	0.006	0.002	0.003	0.001	0.006	0.002	0.01	0.006	0.007	0.004
PI 34:4	848.5	**C43H79O13PN**	0	0	0	0	0	0	0.001	0.001	0	0
PI 34:3	850.5	**C43H81O13PN**	0.028	0.004	0.016	0.001	0.066	0.005	0.102	0.07	0.027	0.037
PI 34:2	852.6	**C43H83O13PN**	0.523	0.177	0.331	0.011	1.199	0.131	1.588	1.151	0.45	0.604
PI 34:1	854.6	**C43H85O13PN**	0.125	0.037	0.051	0	0.337	0.033	0.23	0.2	0.072	0.051
PI 36:5	874.5	**C45H81O13PN**	0.015	0.003	0.01	0.002	0.035	0.009	0.068	0.043	0.007	0.018
PI 36:4	876.6	**C45H83O13PN**	0.131	0.033	0.103	0.006	0.393	0.011	0.446	0.279	0.138	0.139
PI 36:3	878.6	**C45H85O13PN**	0.053	0.008	0.023	0.001	0.193	0.018	0.135	0.102	0.059	0.062

PI 36:2	880.6	**C45H87O13PN**	0.04	0.011	0.014	0.002	0.115	0.033	0.108	0.082	0.017	0.01
***total PI**			***0.924***	***0.272***	***0.549***	***0.013***	***2.347***	***0.187***	***2.708***	***1.964***	***0.778***	***0.929***
PS 34:2	760.5	**C40H75O10PN**	0.009	0.005	0.009	0.004	0.015	0.001	0.039	0.011	0.014	0.016
PS 36:4	784.5	**C42H75O10PN**	0.004	0.002	0.002	0.001	0.01	0.002	0.015	0.007	0.005	0.005
PS 36:3	786.5	**C42H77O10PN**	0.002	0.001	0.001	0.001	0.009	0.001	0.011	0.001	0.004	0.002
PS 36:2	788.5	**C42H79O10PN**	0.002	0	0.001	0	0.01	0	0.012	0.005	0.006	0.003
PS 38:2	816.6	**C44H83O10PN**	0.003	0	0.004	0.001	0.007	0.001	0.012	0.008	0.006	0.002
PS 40:3	842.6	**C46H85O10PN**	0.001	0.001	0	0	0.004	0.003	0.01	0.001	0	0.001
PS 40:2	844.6	**C46H87O10PN**	0.028	0.013	0.014	0.011	0.077	0.006	0.098	0.042	0.063	0.039
PS 40:1	846.6	**C46H89O10PN**	0.002	0.002	0	0	0.006	0.005	0.002	0.002	0.01	0
PS 42:3	870.6	**C48H89O10PN**	0.014	0.02	0	0	0	0	0	0	0	0
PS 42:2	872.6	**C48H91O10PN**	0.045	0.063	0	0	0	0	0	0	0	0
PS 42:1	874.7	**C48H93O10PN**	0.004	0.001	0.003	0.001	0.003	0.001	0.003	0.004	0	0
PS 44:3	898.7	**C50H93O10PN**	0	0	0	0	0	0	0	0	0	0
PS 44:2	900.7	**C50H95O10PN**	0	0	0	0	0	0	0	0	0	0
***total PS**			***0.113***	***0.065***	***0.034***	***0.006***	***0.143***	***0.013***	***0.212***	***0.085***	***0.113***	***0.072***
PA 32:0	666.5	**C35H73O8PN**	0.013	0.001	0.021	0.002	0.009	0.004	0.058	0.01	0.005	0
PA 34:3	688.5	**C37H71O8PN**	0.015	0.005	0.025	0.005	0.015	0.004	0.083	0.021	0.013	0.007
PA 34:2	690.5	**C37H73O8PN**	0.621	0.068	0.887	0.033	0.482	0.02	1.819	0.23	0.332	0.142
PA 34:1	692.5	**C37H75O8PN**	0.142	0.002	0.167	0.022	0.119	0.006	0.277	0.1	0.07	0.035
PA 36:5	712.5	**C39H71O8PN**	0.026	0.002	0.023	0.011	0.022	0.003	0.125	0.037	0.022	0.013
PA 36:4	714.5	**C39H73O8PN**	0.557	0.035	0.625	0.04	0.557	0.042	1.554	0.183	0.386	0.228
PA 36:3	716.5	**C39H75O8PN**	0.204	0.008	0.194	0.028	0.221	0.001	0.462	0.105	0.126	0.056
PA 36:2	718.5	**C39H77O8PN**	0.033	0.008	0.031	0.004	0.058	0.007	0.13	0.025	0.024	0.001
***Total PA**			***1.609***	***0.112***	***1.97***	***0.074***	***1.483***	***0.001***	***4.509***	***0.714***	***0.979***	***0.482***